QUALIFICATION OF CORE PHYSICS METHODS FOR BWR DESIGN AND ANALYSIS

WPPSS-FTS-127

March 1990

Principal Engineer

Bill M. Moore

Contributing Engineers

Alan G. Gibbs
James D. Imel
John D. Teachman
Duane H. Thomsen
William C. Wolkenhauer

Approved: David L. Whitcomb Date: 3/29/90

David L. Whitcomb
Manager, Nuclear Fuel

David L. Larkin Date: 4/01/90

David L. Larkin
Manager, Engineering Analysis & Nuclear Fuel

DISCLAIMER

This report was prepared by the Washington Public Power Supply System (the Supply System) for submittal to the Nuclear Regulatory Commission, NRC. The information contained herein is accurate to the best of the Supply System's knowledge. The use of information contained in this document by anyone other than the Supply System, or the NRC, is not authorized and with respect to any unauthorized use, neither the Supply System nor its officers, directors, agents, or employees assume any obligation, responsibility, or liability or makes any warranty or representation concerning the contents of this document or its accuracy or completeness.

ACKNOWLEDGEMENTS

The Supply System acknowledges the effort expended by J. C. Chandler of John Elston Associates for preparation of this report. The Supply System also acknowledges R.J. Cacciapouti of Yankee Atomic Electric Company for his review and comments on this report.

ABSTRACT

This topical report presents benchmark analyses which demonstrate both the validity of the Washington Public Power Supply System steady state core physics model and the qualifications of the Supply System engineering staff to perform calculations in support of the WNP-2 nuclear plant.

The main computer codes in the Supply System's steady state core physics model are the MICBURN gadolinia fuel pin depletion code, the CASMO-2 assembly depletion code and the SIMULATE-E three-dimensional core simulator code.

The lattice physics benchmark presented in this topical report include calculations of uniform lattice criticals and comparisons of local fuel pin power distributions to the results of gamma scan measurements taken at Quad Cities, Unit 1. Extensive core simulation benchmarks are also reported, based on data from four cycles at WNP-2, two cycles at Peach Bottom, Unit 2, and two Cycles of Quad Cities, Unit 1. The data includes hot and cold criticals, neutron TIP data, and assembly gamma scan data.

The benchmark comparisons show good agreement between calculated and measured data, thereby demonstrating the Supply System's qualifications to set up and perform steady state core physics calculations for reload design and licensing applications at the WNP-2 nuclear plant.

TABLE OF CONTENTS

LIST OF TABLES

LIST OF FIGURES

LIST OF FIGURES (Continued)

LIST OF FIGURES (Continued)

LIST OF FIGURES (Continued)

1.0 INTRODUCTION

The Washington Public Power Supply System ("Supply System") operates the WNP-2 nuclear plant near Richland, Washington. WNP-2 is a BWR/5 installation using a nuclear steam supply system designed by the General Electric Company (GE), who also provided the initial core fuel for the reactor. Reload nuclear fuel and associated analyses are currently provided by Advanced Nuclear Fuels Corporation (ANF). Nuclear fuel design and assembly design criteria are provided by the fuel vendors. The core characteristics and core arrangement of WNP-2 are given in Table 1.1 and Figure 1.1, respectively. A typical WNP-2 power-flow operating map is shown in Figure 1.2.

A desire to understand plant performance under conditions both within and outside the normal operating envelope has influenced a number of licensees to develop in-house analytical methods for predicting normal plant operation and responses to off-nominal event initiators. The potential for enhanced cost effectiveness, more rapid analytical response, and greater latitude in evaluation of alternatives relative to analytical dependence on outside agencies has also contributed to the incentive for licensees to develop in-house analytical capabilities.

While specific methods may vary from licensee to licensee, the overall approach to the problem invariably separates the analytical responsibility at the core boundary. Reactor physics analysis provides a detailed, steady-state prediction of neutron flux effects using system performance

as a boundary condition. Systems analysis provides a detailed, transient prediction of plant response based on a simplified core transient model. Inputs for the simplified core transient model used in the systems analysis are derived from the reactor physics analysis.

The Supply System has developed an overall analytical methodology to support the WNP-2 nuclear plant. A simplified overall calculational flow used in this methodology is shown in Figure 1.3. This document covers the segment labeled "Steady State Core Physics Analysis;" the remaining segments are reported separately.

The Supply System's steady state core physics methods are based on the Electric Power Research Institute (EPRI) code package depicted in the flowchart in Figure 1.4. The main computer codes are the CASMO-2 fuel bundle lattice physics depletion code and the SIMULATE-E three-dimensional core simulation code. Both of these codes represent current technology for reactor analysis and are described further in later sections of this report. MICBURN provides a detailed representation of the depletion of a single gadolinia-bearing fuel rod; NORGE-B provides a nuclear cross-section data link from CASMO-2 into SIMULATE-E. CALTIP provides incore instrument responses, plotting, and statistical evaluation.

The Supply System uses these computer programs and associated methodologies for plant operations support applications (such as core follow analyses, development of target control rod patterns, predictions of startup critical rod patterns, and operating strategy evaluations), independent

design verification calculations, reload fuel/core design analyses, and safety analyses. The steady state core physics methods described in this report are also used to develop the necessary neutronics data input to the Supply System's transient analyses.

This report describes the steady state core physics methods used by the Supply System for BWR core analysis and provides qualification of the analytical methodologies that will be used to perform safety-related analyses in support of the WNP-2 operating license. Applications of this methodology are reported separately, as are systems analysis methods and models.

The work reported herein is intended to satisfy the guidelines of Generic Letter 83-11[1], which established that user qualifications are subject to regulatory review consistent with the technology used by the licensee. The major analytical tools used in the Supply System methodology have been used by other BWR licensees and have been reviewed in similar applications[2,3].

The qualification of the Supply System's steady state core physics methods is based on comparisons of calculated core parameters to measured data from WNP-2, Peach Bottom Unit 2, and Quad Cities Unit 1. All of the model preparation and benchmarking calculations represent work performed by the Supply System. The computer codes and the calculations supporting this work are documented, reviewed, and controlled by formal procedures which are encompassed within the Supply System's nuclear quality assurance program.

Subsequent chapters of this report cover the one- and two-dimensional analysis of fuel assembly lattices and the three-dimensional simulation of core-wide phenomena. In each of these chapters, the text describes the computer models and methodologies used for these analyses. Detailed benchmarks provided in both sections show consistently accurate predictions of published and operational data for Quad Cities Unit 1, Peach Bottom Unit 2, and WNP-2.

TABLE 1.1

WNP-2 CORE CHARACTERISTICS

Reactor Type/Configuration	BWR/5 2-loop jet pump recirculation system
Rated Core Power:	3,323 MW thermal
Rated Core Flow:	108.5×10^6 lbm/hr
Reactor Pressure at Rated Conditions:	1035 psia
Number of Fuel Assemblies:	764
Number of Control Rods:	185
Number of Traversing In-Core Probe Locations:	43

Figure 1.1
WNP-2 Core Arrangement

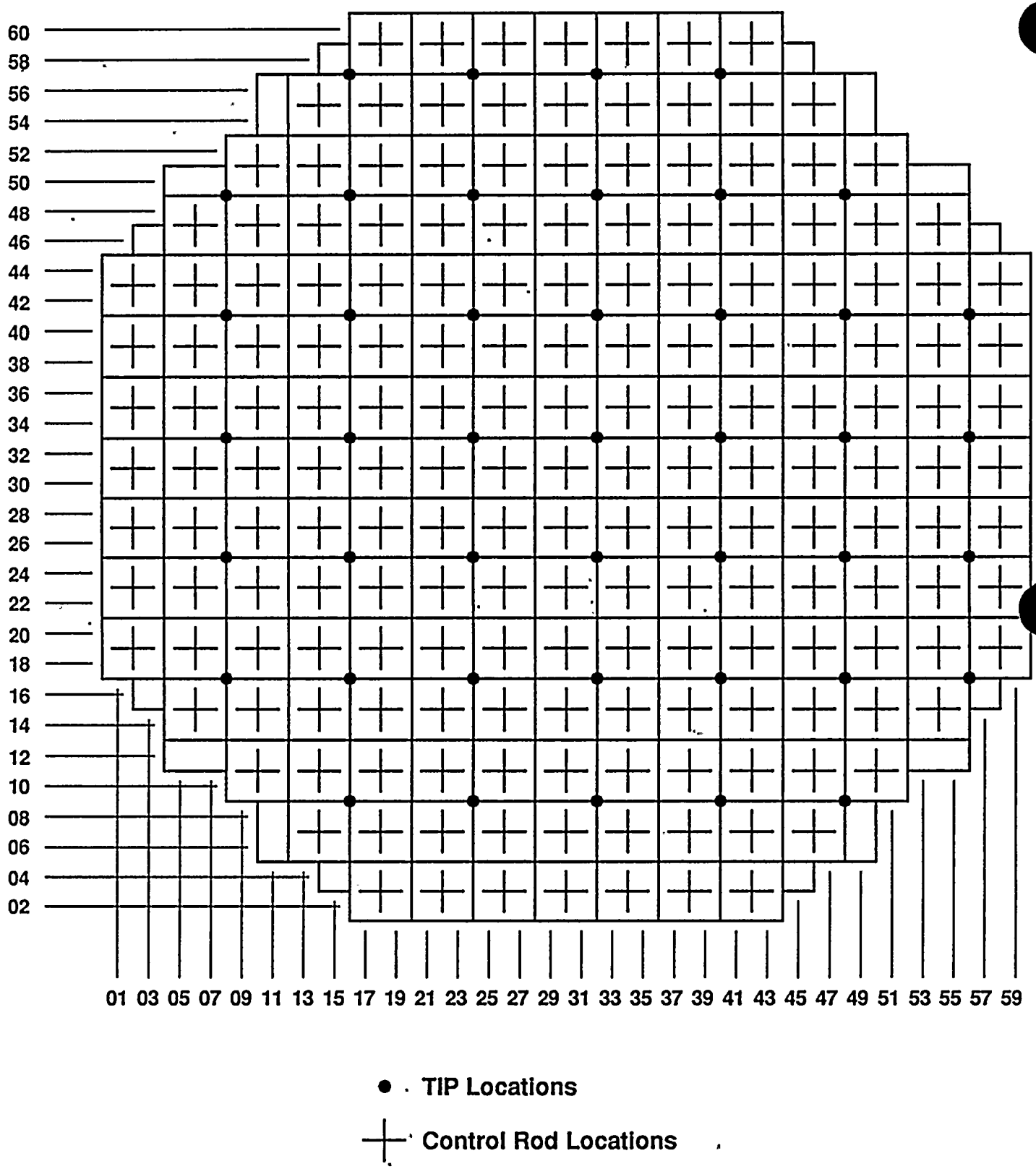

890365.4

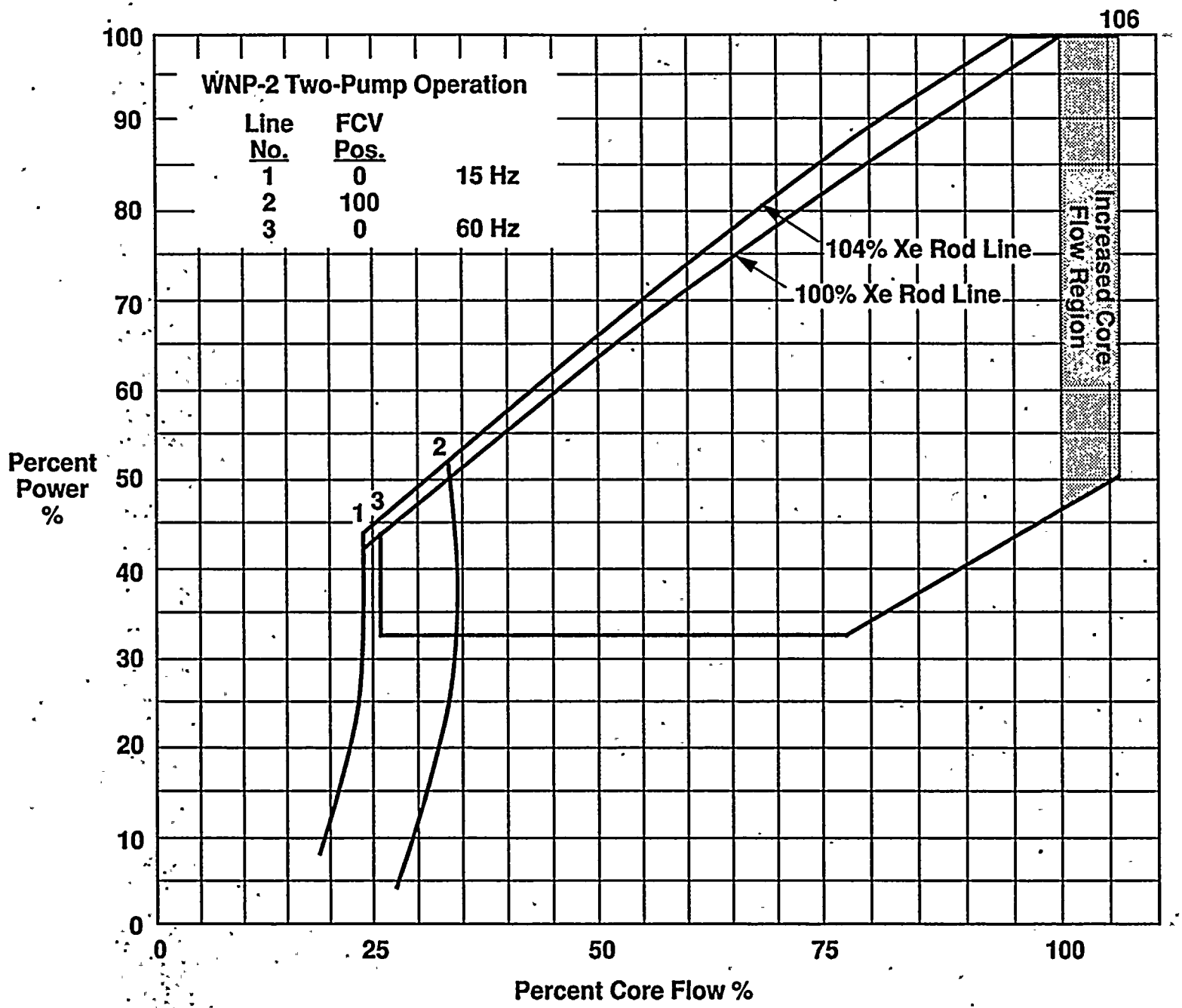

890365.2
Rev. Feb. 1990

Figure 1.2
Typical WNP-2 Power-Flow Operating Map

Figure 1.3
Analytical Methodology for WNP-2

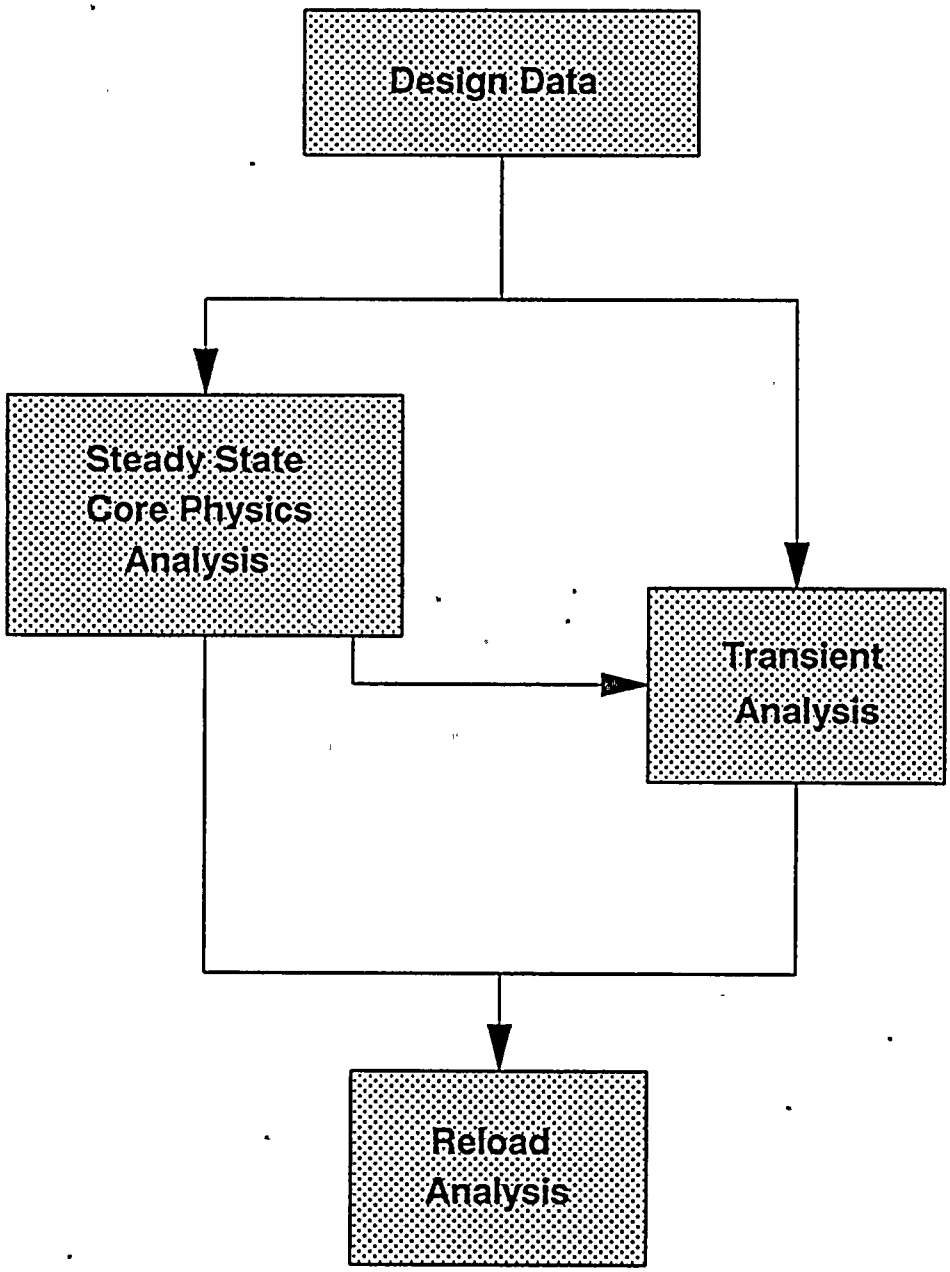

Figure 1.4
Physics Methods Calculational Overview

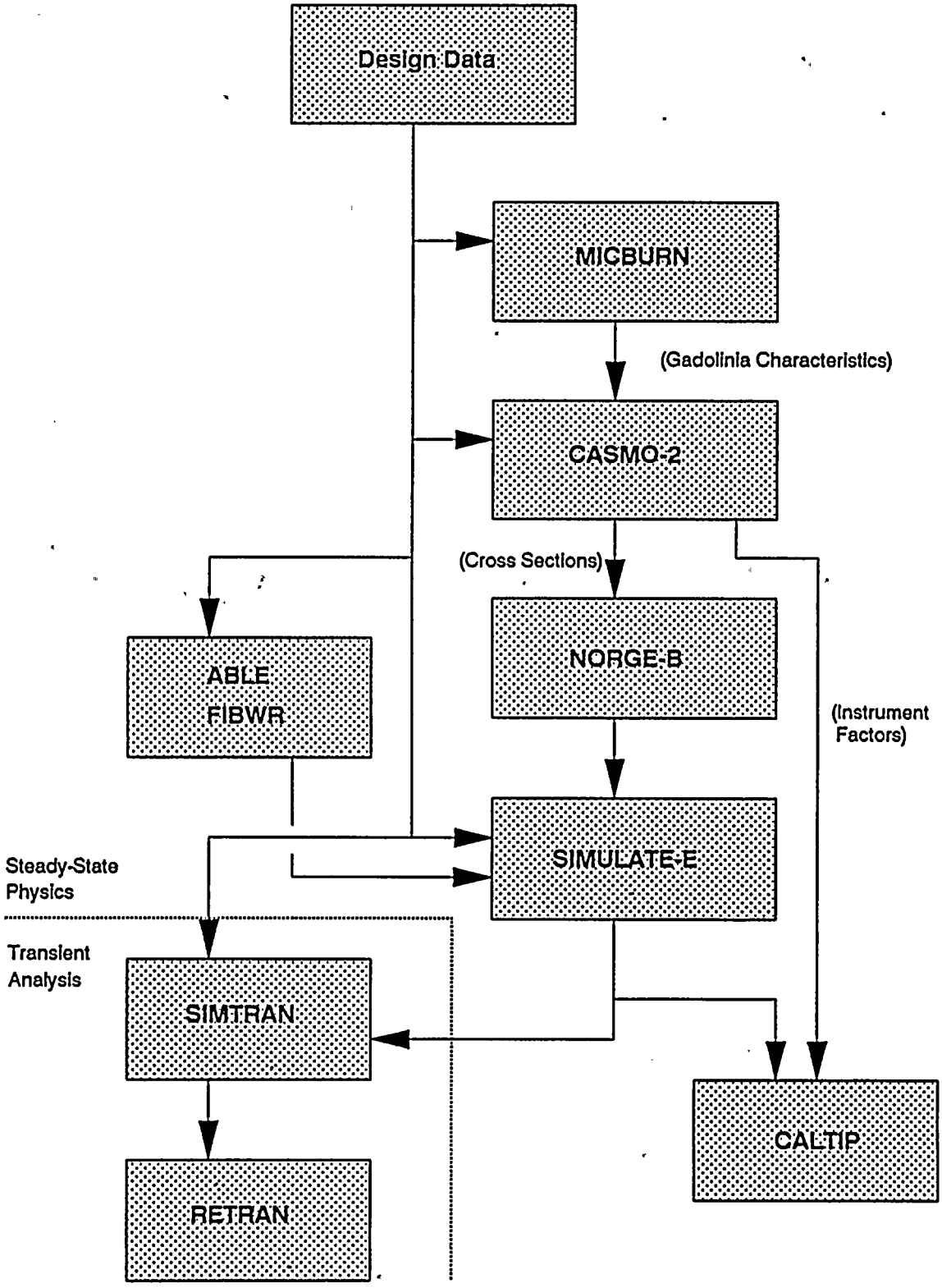

2.0 LATTICE PHYSICS METHODS

The detailed application of reactor theory is contained in the lattice physics analysis. Direct prediction of neutron and nuclide performance within the assembly lattice is accomplished with neutron transport theory and translated into an output form usable by the core analysis programs.

2.1 COMPUTER CODES USED IN THE LATTICE PHYSICS ANALYSIS

This section describes the computer programs used by the Supply System in the analysis of detailed fuel performance characteristics. Each computer code included in this methodology package is subject to qualification in accordance with the Supply System's engineering quality assurance program, which includes verification and validation requirements for computer codes used in design and safety analysis applications.

2.1.1 The MICBURN Burnable Absorber Depletion Program

The homogeneous treatment of the fuel pellet used in CASMO-2 is acceptably accurate for those fuel rods in the core that contain no burnable absorber material. However, BWR fuel assemblies usually contain a number of fuel rods seeded with gadolinia burnable absorber. The gadolinia fuel rods are characterized with the MICBURN computer code[4]. MICBURN provides a one-dimensional neutron transport analysis of the fuel rod and models the consumption of gadolinia in annular rings as burnup accumulates.

The Supply System's methodology for MICBURN uses the same 25-group structure cross-section library as is used for CASMO-2. The gadolinia fueled region is modeled in MICBURN with ten radial rings to provide sufficient detail to calculate the radial flux distribution. These radial rings are expanded to twenty radial regions for the actual gadolinia depletion. The cladding region is modeled with one radial ring, the moderator is modeled with two radial rings and the buffer region with two radial rings. The buffer region's composition is made up of the eight fuel rods and moderator adjacent to the gadolinia fuel rod. The enrichment of the fuel in the buffer region is chosen to correspond to the enrichment of the fuel rod enrichment type of which there is the largest number in the lattice. The results of the MICBURN analysis are used as cross section information by CASMO-2, which in turn assimilates the individual fuel rod performance characteristics into lattice performance factors for use in the core analysis.

As products of the same development agency, MICBURN and CASMO-2 use the same cross section libraries, which are based on a modified version of ENDF/B-III[5].

2.1.2 The CASMO-2 Lattice Depletion Program

Detailed lattice physics analyses for WNP-2 are performed using CASMO-2[5]. This code uses the method of transmission probabilities to solve the neutron transport equation within a two-dimensional representation of a fuel assembly.

The CASMO-2 analysis covers analytical segments which were treated separately in earlier methodologies. Because of the automated link among the segments performed by CASMO-2, no explicit resonance, pin cell, or neutron spectrum calculations are required. From input data which provide a physical description of the fuel rods, the bundle, and the adjacent control rod, CASMO-2 performs in sequence the resonance calculation, a pin cell calculation for each specific fuel rod type in the bundle, a one-dimensional spectrum calculation, and a two-dimensional power distribution and k-infinity calculation. The calculational flow and code input requirements are described in Reference 5.

The Supply System's methodology uses the CASMO-2 25-group energy group cross-section library described in Reference 5. The Supply System uses the defaults specified in CASMO-2 for condensing the 25-group structure down to the 17 energy groups for the one-dimensional pin cell calculation and 7 energy groups for the two-dimensional lattice physics calculation. Specific input provided to the CASMO-2 calculation includes composition data for the fuel

and structure, burnable absorber characteristics calculated by MICBURN, assembly and control dimensions, and internal fuel rod arrangement. CASMO-2 output is retained on magnetic storage for manipulation by NORGE-B into SIMULATE-E compatible input.

In the original qualification of CPM[6], EPRI provided a number of predictions of uniform lattice criticals published in the open literature. To help qualify the k-effective determined by the Supply System using CASMO-2, comparisons were made between CASMO-2 analyses and a number of these uniform lattice criticals. The results of the Supply System's calculations of the uniform lattice critical experiments are described in Section 2.2.1.

To qualify the local power distribution determined by the Supply System using CASMO-2, comparisons were made between the calculated pin powers from CASMO-2 and gamma scan results from EPRI-sponsored testing at the end of second cycle operation at Quad Cities Unit 1. The results of these local power comparisons are given in Section 2.2.2.

2.2 LATTICE PHYSICS BENCHMARKS

Detailed analysis of published data was undertaken to provide assurance that the lattice physics analyses performed in support of the WNP-2 core simulation work will provide quality results. Two aspects of the lattice physics analysis were selected for benchmarking: the calculation of k-effective and the prediction of local power distributions.

2.2.1 Uniform Lattice Critical Benchmarks

Consistent with the qualification performed by EPRI for CPM, the Supply System selected fifteen critical experiments from the TRX and ESADA published data[7,8] for qualification of CASMO-2. These cases comprised eight UO_2 configurations from the TRX series and seven mixed oxide configurations from the ESADA series.

The TRX criticals had fuel pellet densities ranging from 7.52 gm/cm^3 to 10.53 gm/cm^3, and all eight had rod enrichments of 1.3 weight percent U-235. The ESADA criticals all had a compacted powder fuel of density 9.54 gm/cm^3 consisting of 2.0 weight percent PuO_2 in natural UO_2. In five of the ESADA experiments the plutonium was nominally 8% Pu-240; in the remaining two it was nominally 24% Pu-240. The two groups of experiments span a range of

lattice pitches with the equivalent cylindrical cell radii varying from 0.818 cm (TRX-4 and -6) to 1.978 cm (ESADA-7). The corresponding cell radius for WNP-2 is 0.917 cm.

All of the selected criticals were modeled by CASMO-2 as single pin cells, with core leakage accounted for in a fundamental mode approximation using the experimental geometric buckling. The smaller pitch criticals were modeled as three-region, homogenized cells. In the larger pitch criticals, the moderator region was divided into two subregions, and Gaussian integration points were inserted in each of the four resulting regions. For the smallest pitch criticals, which were most typical of WNP-2 geometry, this refinement proved to be unnecessary, exhibiting a negligible effect on the calculated k-effective.

The TRX critical experiments used Lucite spacers. Because Lucite is neutronically similar to the water moderator, no adjustment was necessary to account for the presence of spacers. The ESADA criticals used aluminum spacers, which necessitated some adjustment in the two-dimensional CASMO-2 analysis. ESADA spacer worths were estimated by running CASMO-2 with and without axially homogenized spacers. A two-group perturbation theory analysis was used to correct the axially homogenized spacer worth for the effects of spacer localization. The corrected spacer

worths vary from 6.84 mk for the small-pitch ESADA-1 experiment to 0.11 mk for the large-pitch ESADA-7 experiment.

The results of the uniform lattice critical analyses with CASMO-2 are shown in Table 2.1. The eight TRX urania criticals have a mean k-effective of 0.99616 with a standard deviation of 0.00184. The seven ESADA mixed oxide criticals have a mean k-effective of 1.00872 with a standard deviation of 0.00782. In the ESADA series, the k-effective values are generally higher for the larger pitch criticals while for the smaller pitch criticals, which are similar to WNP-2, k-effective values are in the same range as for the TRX series.

2.2.2 Quad Cities Local Power Benchmarks

Gamma scan data for fuel irradiated during the first two operating cycles at Quad Cities 1 were published by EPRI[9]. Pin-by-pin gamma scans were performed on six assemblies as a part of the EPRI study. The three UO_2 assemblies (GEH002, CX0672, and CX0214) and two mixed oxide assemblies (GEB159 and GEB161) were used for the Supply System benchmark. The first two of these assemblies were located about halfway between the core edge and the core center; the remaining three were located near the core center.

Detailed core modeling based on the first two operating cycles of Quad Cities 1 was undertaken to demonstrate the adequacy of the Supply System's methods. Core design information as published by EPRI[10] was used to model and deplete the core to the end of Cycle 2. The modeling of the depletion of the first two cycles and prediction of nodal power distribution results are described in Chapter 3.0 of this report. Barium-140 inventories at the end of Cycle 2 were predicted explicitly in both the lattice calculations and the core calculations for comparison against the measured La-140 activity levels. The predictions of Ba-140 were based on detailed power shapes from the last six statepoints (125 days) of Cycle 2, using a piecewise linear representation of the power history for this time. Contributions to the end of Cycle 2 Ba-140 inventory from earlier irradiation times were shown to be negligible.

The local power benchmarks required an additional analytical step beyond the normal core analysis. In addition to the lattice physics calculations and the three-dimensional depletions, the benchmark also required a return to the lattice physics analysis for detailed fuel performance characteristics. The SIMULATE-E analysis provided void history, instantaneous void, and nodal exposure values for each node in the core. These values were used to interpolate among the CASMO-2 cases for the lattice types in

question to determine local power distributions, which were then used in the explicit determination of Ba-140 inventories for comparison against the experimental data. Since the purpose of this benchmark is to evaluate the local power distribution, the measured and calculated results were normalized to one on each plane of each pin-scanned assembly. This procedure eliminates uncertainties associated with the SIMULATE-E nodal power distribution. The nodal power uncertainties are evaluated separately by comparisons to TIPs and assembly gamma scans in Chapter 3.0.

In this report, the accuracies of predictions are expressed in terms of various statistical measures. These measures are defined either in terms of the fractional calculational error

$$e_i = \frac{(c_i - m_i)}{m_i} \times 100\% \qquad (1)$$

where: e_i = fractional calculational error in percent
c_i = normalized calculation, and
m_i = normalized measurement.

or in terms of the difference,

$$d_i = c_i - m_i \qquad (2)$$

where d_i = the calculation difference.

The mean values of these quantities are defined by

$$e_m = \frac{\Sigma e_i}{N} \qquad (3)$$

and

$$d_m = \frac{\Sigma d_i}{N} \qquad (4)$$

Here, N denotes the total number of points in the sample. Often, calculated and measured results are normalized to a common value; in such cases, d_m is zero.

The degree of variation of e_i and d_i about their mean values can be characterized by their standard deviations, expressed as a percent of the mean measured value:

$$\sigma_e(\%) = \left(\frac{\Sigma(e_i - e_m)^2}{N - 1} \right)^{1/2} \qquad (5)$$

and

$$\sigma_d(\%) = \left(\frac{\Sigma(d_i - d_m)^2}{N - 1} \right)^{1/2} \times \frac{100\%}{M} \qquad (6)$$

Here, M denotes the mean measured result.

Alternatively, the accuracy of a prediction can be characterized by the root mean square values of e_i or d_i, expressed as a percentage of M:

$$E_{rms}(\%) = \left(\frac{\Sigma e_i^2}{N} \right)^{1/2} \qquad (7)$$

$$D_{rms}(\%) = \left(\frac{\Sigma d_i^2}{N} \right)^{1/2} \times \frac{100\%}{M} \qquad (8)$$

Results of the local power gamma scan benchmarks are summarized in Table 2.2. There, the center of axial node N is located (6N - 3) inches above the bottom of the active fuel. These results show a core-wide standard deviation, σ_d, of 3.20% based on the differences between measured and predicted values and including all data points. If the mixed oxide bundles are excluded from the statistics, this standard deviation becomes 3.11%. Measurement error for this database was published at 1.7%; these results indicate a calculational error approximately the same as the measurement error.

The measured and calculated maximum local peaking factors are compared in Table 2.3. This comparison is important because monitored values for linear heat generation rate (LHGR) and critical power ratio (MCPR) are determined by the maximum local power peaking factor in any given node. Comparison of measurement and calculation for maximum local peaking independent of position within the lattice shows an standard deviation, σ_e, of 2.14%. The measurement error was published at 1.7% for this segment of the database as well.

Selected local power comparisons are given in Figures 2.1 through 2.6. These comparisons illustrate the range of calculations and are typical of the datasets which are not reproduced here.

TABLE 2.1

RESULTS OF UNIFORM LATTICE CRITICAL ANALYSES

CASMO-2 RESULTS FOR TRX CRITICALS

Experiment Identification	Experimental Geometric Buckling*	CASMO-2 K-effective
TRX-1	28.37	0.99421
TRX-2	30.17	0.99749
TRX-3	29.06	0.99733
TRX-4	25.28	0.99404
TRX-5	25.21	0.99361
TRX-6	32.59	0.99785
TRX-7	35.47	0.99753
TRX-8	34.22	0.99722

Average K-effective: 0.99616
Standard Deviation: 0.00184

CASMO-2 RESULTS FOR ESADA CRITICALS

Experiment Identification	Experimental Geometric Buckling*	CASMO-2 K-effective
ESADA-1	69.6	0.99809
ESADA-3	90.0	0.99816
ESADA-4	104.72	1.01647
ESADA-6	98.4	1.01715
ESADA-7	50.3	1.00901
ESADA-12	79.5	1.01109
ESADA-13	73.3	1.01105

Average K-effective: 1.00872
Standard Deviation: 0.00782

* Buckling expressed in m^{-2}.

** CASMO-2 calculated k-effectives for the ESADA criticals have been adjusted to account for spacer worth.

TABLE 2.2

SUMMARY OF LOCAL POWER BENCHMARKS

Assembly Ident	Axial Location (Node)	Nodal Relative Water Density History	Nodal Exposure (MWD/MT)	Standard Deviation σ_d(%)
CX0214	3	0.022	16.117	3.32
	4	0.052	17.642	4.34
	9	0.302	20.270	2.77
	10	0.350	20.248	3.29
	15	0.527	19.747	3.09
	16	0.551	19.402	3.90
	21	0.635	15.148	3.51
	22	0.645	12.906	3.08
CX0672	3	0.018	15.768	4.23
	4	0.044	17.352	4.21
	9	0.282	20.089	3.05
	10	0.335	19.980	3.28
	15	0.520	19.501	2.99
	16	0.545	19.127	3.04
	21	0.631	15.383	2.89
	22	0.642	13.256	3.21
GEB159	3	0.039	10.878	3.33
	4	0.087	11.520	3.69
	9	0.398	10.506	3.67
	10	0.443	10.435	3.51
	15	0.597	10.020	2.92
	16	0.617	9.964	3.04
	21	0.689	7.854	3.26
	22	0.698	6.552	3.31
GEB161	3	0.039	10.878	4.06
	4	0.087	11.520	3.41
	9	0.398	10.506	3.82
	10	0.443	10.435	2.34
	15	0.597	10.020	3.06
	16	0.617	9.964	3.26
	21	0.689	7.854	4.79
	22	0.698	6.552	4.72
GEH002	3	0.040	10.523	2.32
	4	0.089	11.138	2.36
	9	0.399	10.215	2.63
	10	0.443	10.061	2.77
	15	0.592	9.531	3.04
	16	0.612	9.434	3.13
	21	0.684	7.334	2.27
	22	0.692	6.175	2.40

TABLE 2.3

COMPARISON OF MAXIMUM LOCAL PEAKING FACTORS

Assembly Ident	Axial Node	Measured Local Peaking	Calculated Local Peaking	Error e_i(%)
CX0214	3	1.1082	1.0873	-1.892
	4	1.0785	1.0795	0.096
	9	1.0910	1.0751	-1.459
	10	1.0657	1.0729	0.679
	15	1.1262	1.0792	-4.172
	16	1.1232	1.0780	-4.017
	21	1.1314	1.0954	-3.175
	22	1.1142	1.1032	-0.985
CX0672	3	1.1057	1.0869	-1.701
	4	1.0801	1.0821	0.186
	9	1.0965	1.0701	-2.413
	10	1.0983	1.0727	-2.330
	15	1.0956	1.0750	-1.876
	16	1.0706	1.0733	0.250
	21	1.0885	1.0975	0.833
	22	1.1013	1.1046	0.302
GEB159	3	1.1499	1.1904	3.520
	4	1.1153	1.1836	6.122
	9	1.1156	1.1516	3.225
	10	1.0994	1.1397	3.666
	15	1.1030	1.1123	0.846
	16	1.1024	1.1121	0.876
	21	1.1335	1.1562	2.000
	22	1.1593	1.1777	1.584
GEB161	3	1.1147	1.0960	-1.679
	4	1.1102	1.0785	-2.860
	9	1.1071	1.0845	-2.048
	10	1.0887	1.0847	-0.369
	15	1.0944	1.1124	1.651
	16	1.1099	1.1156	0.510
	21	1.1312	1.1462	1.325
	22	1.1720	1.1601	-1.022
GEH002	3	1.1031	1.1174	1.291
	4	1.0986	1.1146	1.455
	9	1.1103	1.1168	0.584
	10	1.1002	1.1120	1.074
	15	1.1180	1.1159	-0.188
	16	1.1187	1.1224	0.328
	21	1.1351	1.1369	0.156
	22	1.1351	1.1405	0.478

Figure 2.1

Local Power Benchmark, Assembly CX0214, Axial Node 4

1.0671 0.9800 -8.1596	1.0132 0.9311 -8.0973		1.0293 0.9738 -5.3874		1.0329 0.9932 -3.8469	0.9024 0.9609 6.4809
0.9681 0.9311 -3.8178	1.0056 0.9601 -4.5238	0.9230 0.9295 0.7028	1.0702 1.0353 -3.2607	1.0590 1.0412 -1.6794	1.0432 1.0355 -0.7455	0.9212 0.9753 5.8807
	0.9126 0.9295 1.8521		0.9727 0.9816 0.9174	0.9747 0.9905 1.6169	0.9991 1.0306 3.1576	
1.0051 0.9738 -3.1081	1.0785 1.0353 -4.0063	0.9972 0.9816 -1.5632			0.9976 0.9954 -0.2200	1.0588 1.0617 0.2733
	1.0678 1.0412 -2.4961	1.0021 0.9905 -1.1605	0.9702 0.9728 0.2759	0.9747 0.9766 0.1905	1.0006 1.0165 1.5858	
1.0636 0.9932 -6.6264	1.0450 1.0355 -0.9111	0.9859 1.0306 4.5403	1.0104 0.9954 -1.4801	0.9123 1.0165 11.4211	0.9502 1.0410 9.5550	1.0435 1.0795 3.4546
0.9417 0.9609 2.0462	0.9627 0.9753 1.3169		1.0479 1.0617 1.3220		1.0495 1.0795 2.8577	0.9407 1.0062 6.9647

Meas. Calc. % Err	E_{rms}, %	4.36%
	Standard Deviation, σ_d(%)	4.34%

Figure 2.2

Local Power Benchmark, Assembly CX0214, Axial Node 15

1.1262 1.0636 -5.5581	1.0304 0.9939 -3.5385		1.0563 1.0149 -3.9142		1.0374 1.0354 -0.1847	1.0228 1.0325 0.9495
1.0046 0.9939 -1.0603	0.9707 0.9793 0.8878	0.9344 0.9433 0.9535	1.0842 1.0223 -5.7117	1.0511 1.0259 -2.3998	1.0219 1.0207 -0.1164	0.9705 1.0085 3.9126
	0.9423 0.9433 0.1083	1.0140 0.9615 -5.1827	0.9908 0.9594 -3.1719	0.9751 0.9631 -1.2261		
1.0654 1.0149 -4.7398	1.0568 1.0223 -3.2669	0.9546 0.9594 0.4977		0.9019 0.9369 3.8886	0.9520 0.9493 -0.2844	1.0079 1.0553 4.7074
	1.0446 1.0259 -1.7889	0.9584 0.9631 0.4932	0.9107 0.9369 2.8745	0.8931 0.9385 5.0920	0.9300 0.9807 5.4591	
1.0066 1.0354 2.8686	1.0203 1.0207 0.0386	0.9693 1.0038 3.5590	0.9621 0.9493 -1.3333	0.9664 0.9807 1.4845	0.9731 1.0106 3.8536	1.0618 1.0792 1.6432
1.0206 1.0325 1.1628	0.9794 1.0085 2.9626		1.0444 1.0553 1.0421		1.0882 1.0792 -0.8257	

Meas. Calc. % Err	E_{rms}, %	3.02%
	Standard Deviation, σ_d(%)	3.09%

Figure 2.3

Local Power Benchmark, Assembly CX0672, Axial Node 10

1.0338 1.0236 -0.9870	0.9555 0.9658 1.0806		0.9913 0.9927 0.1455		1.0099 1.0107 0.0780	0.9522 0.9989 4.8961
0.9412 0.9658 2.6167	0.9714 0.9698 -0.1660	0.9209 0.9395 2.0176	1.0661 1.0264 -3.7317	1.0236 1.0314 0.7563	1.0510 1.0232 -2.6441	0.9518 0.9913 4.1438
	0.9094 0.9395 3.3150	1.0304 0.9933 -3.5997	1.0102 0.9723 -3.7545	1.0040 0.9788 -2.5140	1.0339 1.0165 -1.6869	
1.0284 0.9927 -3.4755	1.0755 1.0264 -4.5730	0.9929 0.9723 -2.0776		0.9785 0.9573 -2.1669	1.0089 0.9715 -3.7068	1.0116 1.0541 4.2050
	1.0749 1.0314 -4.0513	0.9688 0.9788 1.0303	0.9733 0.9573 -1.6425	0.9284 0.9603 3.4345	0.9876 0.9993 1.1837	
1.0147 1.0107 -0.3899	1.0983 1.0232 -6.8405	1.0379 1.0165 -2.0605	0.9831 0.9715 -1.1817	0.9570 0.9993 4.4142	1.0133 1.0241 1.0683	1.0482 1.0727 2.3356
1.0080 0.9989 -0.9095	0.9709 0.9913 2.0982		0.9935 1.0541 6.1023		1.0097 1.0727 6.2354	0.9797 1.0244 4.5646
Meas. Calc. % Err		E_{rms}, %			3.20%	
		Standard Deviation, σ_d(%)			3.28%	

Figure 2.4

Local Power Benchmark, Assembly GEB159, Axial Node 4

1.0004 0.9783 -2.2123	1.0015 0.9882 -1.3203		0.9467 0.9794 3.4558		1.0074 1.0073 -0.0048	1.0154 1.0089 -0.6422
0.9919 0.9882 -0.3667	0.9557 0.9321 -2.4703	1.0165 0.9839 -3.2030	1.1144 1.0619 -4.7150	1.0949 1.0614 -3.0585	1.0097 0.9884 -2.1063	0.9654 0.9649 -0.0491
	1.0327 0.9839 -4.7247	0.9140 0.8394 -8.1598	0.9549 0.9412 -1.4427	0.9569 0.9625 0.5883	0.8894 0.8342 -6.2111	
0.9794 0.9794 0.0047	1.1003 1.0619 -3.4893	0.9515 0.9412 -1.0887		1.0359 1.0568 2.0237	1.0872 1.1207 3.0758	1.0886 1.0784 -0.9386
	1.0782 1.0614 -1.5546	0.9421 0.9625 2.1715	1.0309 1.0568 2.5179	0.6118 0.6375 4.1981	1.1038 1.1836 7.2272	
1.0017 1.0073 0.5583	1.0018 0.9884 -1.3291	0.9014 0.8342 -7.4575	1.0812 1.1207 3.6451	1.1153 1.1836 6.1224	0.8389 0.8100 -3.4514	1.0728 1.1346 5.7611
0.9859 1.0089 2.3350	0.9350 0.9649 3.1997		1.0598 1.0784 1.7567		1.1043 1.1346 2.7401	1.0245 1.0901 6.3970

Meas. Calc. % Err	E_{rms}, %	3.65%
	Standard Deviation, σ_d(%)	3.69%

Figure 2.5

Local Power Benchmark, Assembly GEB161, Axial Node 21

			1.0507 1.0876 3.5145			1.1312 1.1462 1.3252
		1.0548 1.0444 -0.9875	1.0848 1.1084 2.1796			
			0.9537 0.9685 1.5492	0.9512 0.9724 2.2260		
				0.9767 1.0058 2.9707		
			1.0155 1.0058 -0.9628			
					0.7813 0.6609 -15.402	

Meas.
Calc.
% Err

E_{rms}, % 5.52%
Standard Deviation, σ_d(%) 4.79%

Figure 2.6

Local Power Benchmark, Assembly GEH002, Axial Node 15

1.061 1.100 3.658	1.099 1.096 -0.249		1.072 1.061 -0.991	1.071 1.051 -1.814		1.094 1.098 0.323	1.111 1.116 0.407
1.091 1.096 0.478	1.027 1.008 -1.818	1.118 1.067 -4.527	1.064 1.019 -4.201	1.045 1.005 -3.919	1.043 1.019 -2.318	1.086 1.066 -1.773	1.020 1.043 2.304
	1.092 1.067 -2.282	1.003 0.947 -5.573	0.951 0.925 -2.718		0.937 0.924 -1.389	0.990 0.948 -4.252	
1.066 1.061 -0.464	1.053 1.019 -3.253		0.908 0.894 -1.584	0.912 0.902 -1.160	0.914 0.891 -2.475	0.936 0.927 -0.999	1.057 1.050 -0.626
1.032 1.051 1.894	1.004 1.005 0.061	0.913 0.911 -0.137	0.919 0.902 -1.870		0.906 0.899 -0.760	0.910 0.913 0.304	1.011 1.035 2.467
	1.051 1.019 -3.079	0.948 0.924 -2.520	0.902 0.891 -1.235	0.909 0.899 -1.113	0.872 0.891 2.155	0.908 0.926 2.015	
1.089 1.098 0.825	1.064 1.066 0.205	0.961 0.948 -1.313	0.910 0.927 1.830	0.877 0.913 4.016	0.902 0.926 2.663	0.928 0.947 1.979	1.040 1.100 5.828
1.091 1.116 2.311	0.999 1.043 4.391		1.040 1.050 0.987	0.997 1.035 3.866		1.039 1.100 5.924	0.956 1.061 10.999

Meas.
Calc.
% Err

E_{rms}, % 3.01%
Standard Deviation, σ_d(%) 3.04%

3.0 CORE SIMULATION METHODS

The detailed performance characteristics of the fuel lattice are collapsed into nodal performance indicators which are linked in the nodal simulator code. These performance indicators, which take the form of regional macroscopic cross sections, are coupled with modified coarse-mesh diffusion theory[11] (MCMDT) to provide an overall flux and power shape for the reactor core. The core analysis in turn provides nodal performance indices which can be keyed back to the lattice physics analysis to determine detailed fuel performance characteristics at any point in the operating cycle.

This chapter covers the computer codes and methodologies used for representation of cross sections, the calculation of albedo factors, the three-dimensional core simulation; and the calculation of neutron TIP responses.

3.1 COMPUTER CODES USED IN THE CORE ANALYSIS

The computer codes used by the Supply System in modeling the three-dimensional behavior of a BWR's core are shown in Figure 1.4. The codes MICBURN and CASMO-2 have already been described in Section 2.0. This section will describe the remaining codes used in the steady state modeling. These codes are NORGE-B, ABLE, FIBWR, SIMULATE-E and CALTIP.

3.1.1 The NORGE-B Cross-Section Representation Program

Tabulation of cross section information for use by SIMULATE-E is a complex operation. In the Supply System's methodology, CASMO-2 is first run for three void level depletion cases (0%, 40%, and 70% voids) and one controlled depletion at 0% void. For the voided depletions, additional runs are made for instantaneous void branch cases, Doppler cases, controlled cases, and cold cases. For the controlled depletion, branch runs are made for uncontrolled hot and cold cases. The resulting output is read by NORGE-B[12], which arranges the data into a form recognizable by SIMULATE-E.

The SIMULATE-E formulation uses the nine basic cross sections shown in Table 3.1. In the core simulation, these cross sections are made up of linear contributors to the overall cross section value and are termed partial cross sections. Each partial cross section generated by NORGE-B from the CASMO-2 data is the product of a tabulated function of two variables and a polynomial function of a third variable.

NORGE-B corrects a slight difference in k-infinity formulation between CASMO-2 and SIMULATE-E. Under input control, the code can be made to adjust the fast group absorption

cross section to make the two group nodal k-infinities the same for both models. This option is selected for depletion and core follow analyses but bypassed for the calculation of kinetics constants and cross sections for system transient analyses.

Cross sections are formulated separately for hot and cold conditions to economize on computer memory requirements.

The accuracy of the NORGE-B cross section representations is assessed by comparing the results to the original CASMO cross section data.

3.1.2 The ABLE Albedo and Boundary Leakage Evaluation Program

Reflective boundary conditions at the core periphery are calculated from the characteristics of the fuel bundles located along the edge of the core. Specific albedo factors are calculated for each peripheral bundle by the ABLE computer code[13].

ABLE uses core and fuel design information to calculate a set of typical moderator conditions for the fueled and non-fueled regions adjacent to the core periphery. Truly typical conditions are used for the upper and lower core faces, but each exterior fuel bundle vertical surface is provided with its own albedo evaluation.

The albedo calculation uses the lattice physics analysis for the moderator void fraction appropriate for the specific albedo being evaluated. Horizontal albedo boundary conditions are based on assembly-specific cross sections at an averaged void level. Each calculated albedo is associated with a specific exposure distribution; because albedoes do not vary rapidly with exposure, average or typical values are used in the Supply System methodology.

3.1.3 The SIMULATE-E Nodal Simulator Code

The primary analytical tool used in core analysis is SIMULATE-E[14]. Originally designed to allow the analyst to choose from a number of calculational schemes, SIMULATE-E has effectively evolved into an application of MCMDT. The other nuclear analysis options are not used in the Supply System methodology.

Core analyses are performed in three dimensions using cubic nodes, varying dimensionally only in thermal expansion effects. In order to reduce computer costs, these three-dimensional calculations normally use quarter core symmetry for depletion and power distribution calculations, relying on internal unfolding routines to generate full-core distributions when they are needed. This approach generates a small uncertainty in nodal

quantities; however, the benchmark results reported later in this chapter indicate that the magnitude of the errors introduced in this fashion is small.

Input to SIMULATE-E includes cross sections, fuel description, core description, core configuration, and calculation control. Cross sections are provided by NORGE-B on the basis of CASMO-2 analyses. Fuel description information is taken from the appropriate design documents. Core description information is taken from as-built design documents and the results of supporting analyses, such as those provided by ABLE and FIBWR discussed later. Core configuration is determined on a case-specific basis and includes such variables as assembly loading maps, control rod positions, total power, and power-flow state. Calculation control is also determined on a case-specific basis.

The Supply System's SIMULATE-E modeling was qualified through a number of benchmark analyses. Specific analyses selected for SIMULATE-E qualification include critical control rod positions, incore instrument response, and nodal power distribution. The information against which these analyses were benchmarked was obtained from several sources. These sources are core operating data covering the first two cycles of Quad Cities Unit 1, core operating data covering the first two cycles of Peach Bottom Unit 2, and operating data from four cycles of WNP-2. Full

SIMULATE-E depletion analyses were required to support these benchmark programs; the data allowed direct benchmarking of the SIMULATE-E analysis. These benchmark analyses are summarized in Section 3.3, below.

3.1.4 The FIBWR Hydraulic Model

SIMULATE-E contains a sophisticated flow-distribution algorithm that allocates core flow among the fuel assemblies in the core through equalization of assembly pressure drops. This algorithm is an adaptation of the one contained in the FIBWR computer code[15,16], which uses the internally calculated bundle power distribution rather than a zone distribution as in FIBWR. With the exception of power distribution and inlet orifice information, the SIMULATE-E hydraulic input coincides with that specified for FIBWR.

Because of the complexity of the nodal power calculation, FIBWR is used in the Supply System's methodology to develop the hydraulic input for SIMULATE-E. The flow distribution in a SIMULATE-E calculation is determined by the FIBWR model in SIMULATE-E.

FIBWR inputs are calculated from geometric design data. A hydraulic calculation is performed with FIBWR using a representative power distribution and results are compared with plant operating data. Input formulations are adjusted until the FIBWR predictions and plant data agree; the SIMULATE-E input is then based on the adjusted FIBWR input.

3.1.5 The CALTIP Instrument Response Model

The CALTIP computer program was developed by the Supply System to calculate TIP readings and compare them against measured Traversing Incore Probe (TIP) traces. Calculated detector signal rates are based on fuel lattice type, exposure, void, control rod position and power. Detector signal rates are calculated by CASMO-2. The contribution to the detector signal from a given assembly node is determined by linear interpolation on detector signal rate using void and exposure values extracted from a SIMULATE-E restart file. The detector signal rates at each node are converted to TIP traces by applying control rod worth and power dependencies. The TIP signal is found by summing the rates from the four adjacent assembly nodes. The signals are normalized for each TIP string, normalized over the whole core, and reported.

3.2 WNP-2 BENCHMARKS

Three different versions of SIMULATE have been used for core modeling activities at WNP-2. Some preliminary core modeling work was based on SIMULATE-1[17], with cross sections calculated by CPM. The Supply System converted core modeling to SIMULATE-2[18] before startup of Cycle 1, and the project changed again to SIMULATE-E for the third and subsequent cycles. The CPM-based cross sections were used during the first operating cycle, but the core was redepleted with CASMO-2 based cross sections when the lattice physics conversion was implemented. The differences in the SIMULATE versions are largely peripheral, although SIMULATE-E includes the FIBWR hydraulic modeling that was absent in the early versions. Each operating cycle was modeled using the methods described in this report. The results are summarized in this section.

Figure 3.1 shows the performance of the SIMULATE critical eigenvalue as a function of core average exposure. This figure contains data for both hot and cold critical predictions. The trend toward increasing eigenvalue as core average exposure accumulates is consistent with other analysts' experience with CASMO-2 and its internal cross section library based on ENDF/B-III. The consistent bias between hot and cold eigenvalues is also seen in other applications of CASMO-2. The step increase in eigenvalue seen between Cycles 2 and 3 can be attributed mainly to different horizontal albedoes in the two cycles: Cycles 1 and 2 used horizontal albedoes established for Cycle 1 which had natural uranium on the periphery. Cycle 3

albedoes were determined with the use of the ABLE code modeling of the actual fuel residing on the core periphery during Cycle 3. Comparison of Cycle 3 results using the Cycle 1 albedoes to those using the ABLE code for Cycle 3 show a increase corresponding to that seen in Figure 3.1.

Critical rod positions were predicted with SIMULATE-E at a number of cold statepoints during WNP-2 plant operation. The results of these cold critical predictions are given in Table 3.2.

The cold critical eigenvalues exhibit a general increase with increasing exposure. For Cycle 1 the mean k-effective is 0.999268 with a standard deviation of 0.00189, while for Cycle 4 the mean k-effective is 1.00767 with a standard deviation of 0.00163. Within a local range of exposures, cold k-effectives are predicted within a standard deviation of less than 2 mk.

Figures 3.2 through 3.33 show the results of WNP-2 TIP prediction benchmarks. Each reported TIP dataset contains a figure of the radial comparisons, showing how closely the calculated readings agree with the measured readings on a core-normalized basis, and a composite figure showing core average axial readings and individual instrument string results for Instrument Locations 08-17, 56-17, 48-25, and 40-33. The locations chosen for individual reporting were selected at random and include typical peripheral and internal core locations. For individual tip string axial comparisons, calculated and measured results were normalized to one for each string.

Figures 3.2 through 3.9 show the results of the Supply System's core follow program for Cycles 1 and 2 of WNP-2. While these TIP predictions were run with SIMULATE-2, they still demonstrate reasonable accuracy. Cycle 3 results, based on the use of SIMULATE-E, are given in Figures 3.10 through 3.21. Cycle 4 results are shown in Figures 3.22 through 3.33. The analytical accuracy of these instrument predictions is summarized in Table 3.3. The table includes all datasets at which TIP data are available. The "RMS" column in Table 3.3 lists D_{rms} (See Equation 8 in Section 2.2.2) calculated using all data points from all 43 TIP strings with calculated and measured datasets both normalized to one. The range of RMS values shown is typical of that obtained by other licensees[2,3] in comparisons of SIMULATE calculations to neutron TIP data.

3.3 PEACH BOTTOM BENCHMARKS

Transient and stability tests were run at Peach Bottom Unit 2 following the end of Cycle 2 operation[19]. EPRI published core design and operating data[20] for the two cycles leading up to the tests. This allows BWR licensees to determine the core conditions at the start of the tests. An unanticipated benefit of this information was the issuance of data suitable for benchmarking reactor physics models.

The Peach Bottom modeling covers only hot conditions because the published data cover only power operation and test conditions.

The operating data consists of statepoint and configuration data for 24 separate data points during Cycle 1 and thirteen more during Cycle 2. TIP readings were taken at many of these statepoints. The published data indicates that all TIP datasets were taken after 48 hours of equilibrium operation. The published power history data, however, does not clearly support the equilibrium xenon judgment in all cases. Table 3.4 lists all of the Peach Bottom statepoints. Statepoints which could not be clearly judged as equilibrium conditions are labeled as "xenon transient." TIP calculations were not performed at these statepoints.

Quarter core geometry was adequate for the WNP-2 and Quad Cities benchmarks. However, the Peach Bottom Unit 2 core was loaded with sufficient asymmetry that quarter-core averages were not thought to provide an adequate prediction of localized effects. For this segment of the qualification work, the model was exercised in a full core mode.

The performance of the SIMULATE-E critical eigenvalue as a function of core average exposure during the first two operating cycles at Peach Bottom 2 is shown in Figure 3.34. Some fluctuation in the calculated eigenvalue is apparent at the end of the first cycle; this phenomenon can be attributed to significant levels of bypass coolant voiding following plugging of the bypass flow holes near the end of Cycle 1. The introduction of bypass-enhanced fuel at the first refueling outage improved the bypass voiding conditions and the eigenvalue restabilizes at that point.

Table 3.5 shows the rms TIP prediction error for each of the selected benchmark cases. The TIP prediction error is the RMS-averaged error between predicted and measured instrument trace integrals for the whole core, calculated as described in Section 2.2.2, Equation (8). The cycle averages shown in the table are the rms of the individual rms values.

The relative contributions of experimental uncertainty and calculational uncertainty to the rms at each data point can be estimated by analyzing the measured and calculated results for assemblies which are symmetrically located about the SW-NE diagonal. The rms averages of these results show that the overall 11.3% rms for Cycle 1 consists of approximately 4.9% experimental rms and 10.2% calculational rms. Similarly, the 8.4% overall rms for Cycle 2 consists of 5.8% experimental rms and 6.0% calculational rms. The overall rms for Cycle 1 has a greater contribution from calculational error, probably reflecting the modeling difficulties associated with the plugging of the bypass flow holes. The results for Cycle 2 show a lower overall rms containing approximately equal contributions from experimental and calculational uncertainties.

Figure 3.35 shows core average TIP prediction error as a function of core average exposure. Figures 3.36 through 3.47 provide core average and selected individual TIP instrument benchmark comparisons for typical TIP datasets collected during Cycle 1. Figures 3.48 through 3.55 show core average and selected individual TIP instrument benchmark comparisons for typical statepoints during Cycle 2. The instrument response figures are consistent with those shown for WNP-2.

These plots indicate a reasonable prediction of axial and radial power shape trends over the two operating cycles which compose the benchmark.

3.4 QUAD CITIES BENCHMARKS

The Quad Cities Unit 1 core design and operating data[10] includes descriptions of the initial core and reload fuel, operating system parameters for hot and cold state points, and TIP data for the first two cycles. Also, in addition to local power measurements, the Quad Cities gamma scan measurements[9] cover nodal Lanthanum-140 distributions accross the core at the end of Cycle 2.

Quad Cities Unit 1 was modeled in quarter core geometry. As in the Peach Bottom analysis, there were some asymmetries in core loading and control rod patterns, but the severity was not as great. The quarter core analysis did result in some difficulty in predicting instrument responses in the quadrants of the core which were not modeled explicitly. For the second cycle, six reported instrument strings were not predicted because fuel assemblies adjacent to those instruments were loaded asymmetrically from their counterparts in the analyzed quadrant.

The Quad Cities Unit 1 core was depleted from beginning of Cycle 1 to end of Cycle 2 in discrete steps corresponding to the distribution of formal datasets in the literature. The specific statepoints selected for the Quad Cities analysis are shown in Table 3.6. The

general performance of the core model is shown in Figure 3.56, which provides the SIMULATE-E critical eigenvalue as a function of core average exposure. The Quad Cities work shows results similar to the Peach Bottom analysis.

The cold cross section model was used at a number of statepoints throughout the analysis to predict the cold criticals published in the data. The cold critical predictions are summarized in Table 3.7. The two results columns in the table list the actual eigenvalue calculated by SIMULATE-E and the adjusted value obtained by applying a correction for reactor period.

The performance of the Supply System's model in predicting the published TIP data is shown in Table 3.8 and Figure 3.57. The results are again similar to the Peach Bottom results, with the Cycle 2 predictions generally more accurate and stable than those of Cycle 1. Figures 3.58 through 3.67 provide typical Cycle 1 TIP predictions, while Figures 3.68 through 3.75 show typical results for Cycle 2. These results are shown in the manner used to present the WNP-2 and Peach Bottom results, but with the individual instrument strings selected differently. In the Quad Cities benchmarks, individual instrument predictions are reported for Instrument Locations 08-17, 08-25, 56-25, and 48-33 during Cycle 1 and for Instrument Locations 16-17, 32-25, 40-33, and 32-41 during Cycle 2.

The results shown in Table 3.8 yield a Cycle 1 overall rms of 10.7% and a Cycle 2 overall rms of 10.0%. Estimates of the contributions of measurement uncertainty and calculational uncertainty to these overall rms's were obtained by analysis of asymmetry as described in Section 3.3. The results show that for Cycle 1, the experimental rms is 7.6% and the calculational rms is 7.5%, while for Cycle 2 the experimental rms is 6.3% and the calculational rms is 7.7%. The overall uncertainty factors contain approximately equal contributions from experimental and calculational uncertainties.

The nodal power benchmarks also include comparisons of normalized calculated and measured Ba-140 distributions. The Ba-140 concentrations, which are the determining mechanism for the La-140 activity during the gamma scan period, were benchmarked in both radial (x-y) and axial dimensions.

The radial gamma scan benchmarks are based on calculated and measured activities normalized to one over the entire set of 89 scanned assemblies. Normalization of the measured data required some care since assemblies could have either 12 point scans or 24 point scans, and some scan points were displaced 1-2 inches from nodal centers. The measured data for each assembly was fit by a natural cubic spline, and the assembly average activity was defined in terms of the analytical integral of the spline.

Of the 89 fuel assemblies scanned for La-140 activity, 77 were physically located in the west-northwest octant of the core or near the core centerline. Figure 3.76 shows the assembly averaged Ba-140 concentration comparisons for this core region, which contains the bulk of the data. D_{rms} for this comparison is 2.37%. Figures 3.77 through 3.79 provide typical radial power benchmarks at selected axial levels in the core. Figure 3.77 shows the results for Plane 7, which has the largest RMS difference, D_{rms}=4.1%. Figure 3.78 shows Plane 15, which is more typical with D_{rms}=3.1%. Figure 3.79 shows Plane 18, which has the smallest D_{rms}, 1.6%. For these radial comparisons, the calculated and measured results were normalized to one on each axial plane. The normalizations included only those nodes at which measured data exits. The uncertainties in the axial power shape were evaluated separately, as described below. The radial benchmarks for all 24 axial planes are summarized in Table 3.9.

The axial power gamma scan benchmarks are summarized in Table 3.10. This table contains the rms difference between measured and calculated intensity values divided by the axial average measured intensity for the assembly. Measured and calculated results are normalized to one over the entire set of scanned assemblies. Calculated activities at nodes with off-center scan points were obtained by spline interpolation of the calculated nodal center activities. Calculation of rms differences excluded data from the top and bottom six-inch nodes. Figure 3.80 shows the core average axial distribution benchmark. Figures 3.81 through 3.84 provide axial power benchmarks for selected assemblies.

The calculated and measured axial peak-to-average activities for each assembly were also compared and the results are shown in Table 3.11. This table shows the percent differences, e_i, calculated as in Section 2.2.2, Equation (1). The overall E_{rms} for all 89 assemblies, calculated by Equation (7) of the same section, is 1.53%, and the average error is 0.59%.

TABLE 3.1

WNP-2 CROSS SECTION FORMULATION

Cross Section	Independent Variables
Σ_{tr1}	Exposure Instantaneous Void
Σ_{a1}	Exposure Control Instantaneous Void Void History Fuel Temperature Control History
Σ_{r1}	Exposure Control Instantaneous Void Void History
$\nu\Sigma_{f1}$	Exposure Instantaneous Void Void History
$\kappa\Sigma_{f1}$	Exposure Instantaneous Void Void History
Σ_{tr2}	Exposure Instantaneous Void
Σ_{a2}	Exposure Control Instantaneous Void Void History Control History Xenon Number Density Samarium Number Density
$\nu\Sigma_{f2}$	Exposure Control Instantaneous Void Void History Control History Fuel Temperature (Cold model only)
$\kappa\Sigma_{f2}$	Exposure Control Instantaneous Void Void History Control History

TABLE 3.2

SUMMARY OF WNP-2 COLD CRITICAL PREDICTIONS

Core Average Exposure (MWD/MT)	Xenon-Free Critical Eigenvalue
Cycle 1	
0	1.0013
0	1.0008
0	0.9999
57	1.0008
121	1.0014
192	1.0019
268	1.0004
440	0.9998
661	0.9989
1037	0.9989
2337	0.9971
2502	0.9975
3253	0.9973
3799	0.9969
5929	0.9962
Cycle 2	
7065	0.9957
7065	0.9965
7167	0.9961
10209	0.9967
11661	0.9997
Cycle 3	
9650	1.0007
9650	1.0029
12666	1.0058
14022	1.0061
14383	1.0077
Cycle 4	
11052	1.0059
12368	1.0091
14173	1.0081

TABLE 3.3

SUMMARY OF WNP-2 TIP DATASETS

Dataset Number	Core Average Exposure, MWd/MT	TIP Prediction Error, % D_{rms}
	Cycle 1	
44	1372	5.09
57	2205	6.45
64	2590	9.57
93	4579	15.40
	Cycle 2	
4	7342	6.59
10	8248	6.40
17	9297	6.15
26	10360	6.09
34	11339	7.55
40	12102	8.49
	Cycle 3	
1	9903	7.89
7	10836	7.97
8	11034	8.38
15	12245	9.75
20	12903	8.47
27	13974	5.43
	Cycle 4	
1	11245	5.73
11	12903	11.05
17	13563	7.87
23	14428	6.90
30	15473	5.92
37	16531	6.54

TABLE 3.4

PEACH BOTTOM 2 CYCLE 1&2 STATEPOINTS

Dataset Number	Core Average Exposure MWD/t	MWD/MT	Data Evaluation
		Cycle 1 Data	
1	230	253	Xenon transient
2	439	484	Xenon transient
3	648	714	No TIP data
4	741	817	Xenon transient
5	1010	1113	Modeled
6	1585	1747	No TIP data
7	2080	2293	No TIP data
8	2555	2816	Modeled
9	2920	3219	Modeled
10	3724	4105	Xenon transient
11	4525	4988	Xenon transient
12	4697	5178	Modeled
13	5262	5800	Modeled
14	5640	6217	Modeled
15	6106	6731	Modeled
16	6470	7132	Modeled
17	7000	7716	No TIP data
18	7300	8047	No TIP data
19	7712	8501	No TIP data
20	8100	8929	Modeled
21	8430	9292	No TIP data
22	8766	9663	Modeled
23	9520	10494	Xenon transient
24	10100	11133	Modeled
		Cycle 2 Data	
25	8042	8865	Modeled
26	8706	9597	Xenon transient
27	9500	10472	Xenon transient
28	9730	10726	Modeled
29	10050	11078	Modeled
30	10730	11830	Modeled
31	11030	12159	Modeled
32	11260	12412	Xenon transient
33	11420	12588	Xenon transient
34	11570	12754	Modeled
35	11910	13129	Modeled
36	12190	13437	Xenon transient
37	12530	13812	Modeled

TABLE 3.5

PEACH BOTTOM 2 CYCLE 1&2 BENCHMARKS

Dataset Number	TIP Prediction Error % D_{rms}
	Cycle 1 Data
5	6.9
8	12.3
9	15.6
12	13.1
13	9.0
14	7.9
15	8.5
16	9.8
20	19.2
22	7.8
24	7.3
Cycle 1 Overall D_{rms}	11.3%
	Cycle 2 Data
25	9.3
28	8.5
29	8.3
30	8.6
31	8.6
34	8.3
35	7.8
37	7.4
Cycle 2 Overall D_{rms}	8.4%

Table 3.6

Quad Cities 1 Statepoints

Dataset Number	Core Average Exposure MWD/t	MWD/MT	Data Evaluation
		Cycle 1 Data	
1	247	272	Modeled
2	646	712	Modeled
3	800	882	Modeled
4	1334	1470	Modeled
5	2031	2239	Modeled
6	2894	3190	Modeled
7	3480	3836	Modeled
8	3696	4074	Modeled
9	4297	4737	Modeled
10	4809	5301	Modeled
11	5471	6031	Modeled
12	5949	6558	Modeled
13	6175	6807	Modeled
14	6710	7397	Modeled
15	6948	7659	Modeled
16	7239	7980	Modeled
		Cycle 2 Data	
17	6625	7303	Modeled
18	6833	7532	Modeled
19	7225	7964	Modeled
20	7641	8423	Modeled
21	7973	8789	Modeled
22	8293	9141	Modeled
23	9229	10173	Modeled
24	10195	11238	Modeled
25	10827	11935	Modeled
26	11699	12896	Modeled
27	11973	13198	Modeled
28	12348	13611	Modeled
29	12466	13741	Modeled

Table 3.7

Quad Cities Cycle 1&2 Benchmark
Summary of Cold Critical Predictions

Identification	Core Average Exposure (MWd/MT)	SIMULATE-E keffective	kcritical
	Cycle 1 Data		
01	0	1.0000	0.9996
02	0	1.0005	0.9995
03	0	0.9988	0.9980
04	0	0.9998	0.9993
05	0	0.9999	0.9994
06	0	0.9987	0.9976
07	0	0.9997	0.9982
08	0	0.9997	0.9988
09	0	0.9999	0.9991
10	0	1.0027	1.0014
11	0	0.9997	0.9988
12	0	1.0001	0.9995
13	0	1.0003	0.9994
14	0	1.0027	1.0025
15	0	1.0027	1.0024
16	0	1.0027	1.0013
17	0	1.0027	1.0015
18	0	1.0028	1.0014
19	0	1.0030	1.0016
20	0	0.9993	0.9989
21	0	1.0008	1.0004
22	0	0.9989	0.9983
23	2866	0.9960	0.9957
24	2866	0.9961	0.9958
25	3748	1.0003	0.9991
26	3748	1.0001	0.9990
26*	3748	0.9990	1.0001
28	3748	0.9977	0.9966
29	3748	0.9960	0.9958
30	3748	0.9958	0.9953
31	3748	0.9958	0.9953
33	3748	0.9961	0.9957
34	4938	0.9959	0.9946
36	6912	0.9992	0.9985
37	6912	0.9968	0.9966
	Cycle 2 Data		
C5	8276	0.9981	0.9974
C6	9177	0.9991	0.9979
C7	10658	0.9988	0.9982

* Data sheet 26 gives two sets of data.

Table 3.8

Quad Cities 1 Cycle 1&2 Benchmark
Summary of TIP Predictions

Dataset Number	TIP Prediction Error % D_{rms}
	Cycle 1 Data
1	9.6
2	8.9
3	8.6
4	10.2
5	9.3
6	10.3
7	11.1
8	11.8
9	10.0
10	9.4
11	13.0
12	9.9
13	9.6
14	11.5
15	10.9
16	14.6
Cycle 1 Overall D_{rms}	10.7%
	Cycle 2 Data
17	10.4
18	10.3
19	9.6
20	10.6
21	9.4
22	9.8
23	9.9
24	8.3
25	10.1
26	9.0
27	8.4
28	11.0
29	12.1
Cycle 2 Overall D_{rms}	10.0%

Table 3.9

Quad Cities Gamma Scan Benchmark
Summary of Radial Power Benchmarks

Axial Plane	D_{rms} All Bundles
24	4.6%
23	3.0%
22	2.5%
21	2.5%
20	1.9%
19	2.5%
18	1.6%
17	2.5%
16	2.4%
15	3.1%
14	2.3%
13	3.0%
12	3.0%
11	3.3%
10	3.7%
9	3.8%
8	3.9%
7	4.1%
6	3.4%
5	3.9%
4	2.9%
3	3.2%
2	2.1%
1	5.1%

Table 3.10

Quad Cities Gamma Scan Benchmark
Summary of Axial Power Benchmarks

Assembly Ident	% D_{rms}	Assembly Ident	% D_{rms}
CX0546	9.09	CX0719	7.15
CX0191	6.28	GEB162	9.02
CX0494	6.88	CX0286	7.44
GEH008	4.89	CX0398	9.24
CX0412	4.97	CX0490	10.96
CX0174	6.95	CX0617	7.69
CX0100	7.61	CX0024	6.61
CX0553	11.96	CX0332	6.92
GEH029	4.30	GEB123	5.09
CX0662	8.33	CX0150	7.18
CX0440	7.55	CX0015	6.13
CX0378	5.07	CX0186	4.77
CX0682	7.91	CX0611	9.06
CX0351	6.53	GEH023	6.32
CX0396	4.90	CX0093	5.92
CX0316	6.34	CX0723	4.52
GEB149	4.19	CX0631	6.78
CX0399	7.78	CX0397	6.00
CX0231	4.63	CX0161	4.07
CX0297	3.79	CX0414	3.92
CX0523	5.84	CX0198	5.35
GEH022	6.91	CX0393	4.78
GEH002	4.16	CX0672	4.46
GEB132	5.02	CX0585	4.90
CX0281	4.27	GEB105	4.91
CX0643	10.66	CX0044	5.00
CX0327	4.99	CX0362	4.55
CX0306	4.13	CX0660	4.16
CX0287	3.76	CX0498	3.77
CX0310	3.65	CX0575	2.92
CX0214	2.88	CX0683	10.63
CX0520	5.10	CX0137	4.42
CX0420	5.88	CX0106	4.49
CX0394	4.26	CX0057	4.66
CX0052	4.35	CX0162	3.81
CX0717	3.79	CX0225	3.70
CX0453	3.48	CX0165	3.50
CX0482	4.40	GEB161	3.86
GEB159	3.64	CX0588	3.98
GEB158	3.99	GEB160	3.05
CX0318	4.02	CX0401	5.76
CX0096	3.88	CX0445	7.15
CX0384	6.37	CX0359	8.32
CX0124	6.54	CX0711	7.87
CX0622	9.81		

Table 3.11

Quad Cities Gamma Scan Benchmark
Axial Peak-to-Average Comparisons

Assembly Identification	Axial Peak-to-Average Calculated	Measured	e_i(%)
CX0546	1.372	1.354	1.28
CX0719	1.331	1.331	0.00
CX0191	1.302	1.293	0.68
GEB162	1.353	1.355	-0.18
CX0494	1.341	1.352	-0.81
CX0286	1.314	1.324	-0.79
GEH008	1.212	1.212	-0.01
CX0398	1.203	1.194	0.76
CX0412	1.203	1.185	1.53
CX0490	1.344	1.354	-0.70
CX0174	1.324	1.337	-0.92
CX0617	1.287	1.307	-1.51
CX0100	1.222	1.221	0.08
CX0024	1.209	1.188	1.77
CX0553	1.331	1.354	-1.70
CX0332	1.217	1.218	-0.03
GEH029	1.183	1.168	1.31
GEB123	1.183	1.167	1.35
CX0662	1.388	1.378	0.72
CX0150	1.284	1.308	-1.86
CX0440	1.229	1.257	-2.26
CX0015	1.191	1.189	0.18
CX0378	1.210	1.212	-0.16
CX0186	1.225	1.205	1.70
CX0682	1.417	1.416	0.11
CX0611	1.359	1.390	-2.25
CX0351	1.251	1.270	-1.45
GEH023	1.198	1.202	-0.26
CX0396	1.197	1.206	-0.73
CX0093	1.196	1.218	-1.84
CX0316	1.215	1.216	-0.09
CX0723	1.213	1.202	0.95
GEB149	1.199	1.187	0.97
CX0631	1.308	1.323	-1.10
CX0399	1.215	1.244	-2.36
CX0397	1.198	1.210	-1.02
CX0231	1.206	1.218	-1.01
CX0161	1.222	1.223	-0.13
CX0297	1.213	1.198	1.27
CX0414	1.198	1.148	4.36
CX0523	1.343	1.345	-0.13
CX0198	1.295	1.284	0.80
GEH022	1.201	1.196	0.42
CX0393	1.213	1.203	0.82

Table 3.11 (Continued)

Quad Cities Gamma Scan Benchmark
Axial Peak-to-Average Comparisons

Assembly Identification	Axial Peak-to-Average Calculated	Measured	e_i(%)
GEH002	1.179	1.168	0.95
CX0672	1.199	1.198	0.12
GEB132	1.171	1.160	0.99
CX0585	1.192	1.211	-1.57
CX0281	1.190	1.184	0.52
GEB105	1.172	1.167	0.42
CX0643	1.364	1.332	2.38
CX0044	1.257	1.242	1.24
CX0327	1.241	1.227	1.13
CX0362	1.220	1.213	0.58
CX0306	1.205	1.200	0.46
CX0660	1.186	1.186	0.03
CX0287	1.188	1.191	-0.22
CX0498	1.203	1.187	1.30
CX0310	1.210	1.185	2.13
CX0575	1.199	1.196	0.23
CX0214	1.210	1.195	1.21
CX0683	1.361	1.326	2.62
CX0520	1.337	1.308	2.18
CX0137	1.289	1.275	1.08
CX0420	1.261	1.239	1.76
CX0106	1.255	1.233	1.74
CX0394	1.248	1.224	1.96
CX0057	1.231	1.222	0.81
CX0052	1.203	1.196	0.56
CX0162	1.184	1.178	0.55
CX0717	1.176	1.155	1.79
CX0225	1.185	1.185	-0.03
CX0453	1.198	1.200	-0.19
CX0165	1.215	1.191	2.02
CX0482	1.206	1.178	2.46
GEB161	1.148	1.137	1.01
GEB159	1.148	1.141	0.63
CX0588	1.206	1.187	1.62
GEB158	1.148	1.133	1.34
GEB160	1.148	1.138	0.87
CX0318	1.198	1.156	3.66
CX0401	1.198	1.216	-1.50
CX0096	1.251	1.201	4.12
CX0445	1.210	1.201	0.77
CX0384	1.203	1.193	0.81
CX0359	1.203	1.167	3.04
CX0124	1.224	1.215	0.74
CX0711	1.314	1.288	2.06
CX0622	1.364	1.309	4.23

Figure 3.1
WNP-2 Critical Eigenvalue
Calculated by SIMULATE-E

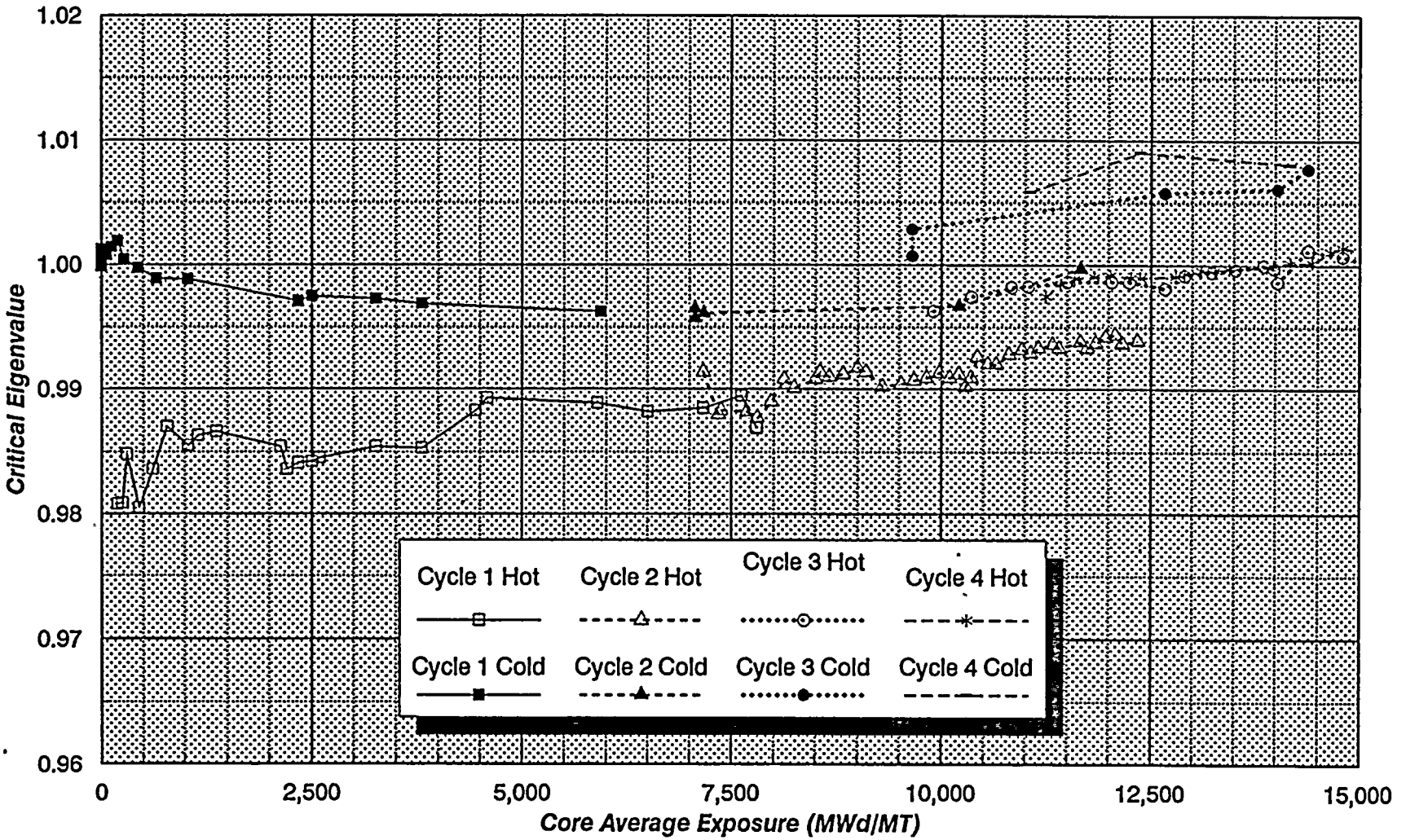

Figure 3.2

WNP-2 Cycle 1 TIP Predictions, 1372 MWd/MT

	16-57	24-57	32-57	40-57		
	0.599	0.852	0.888	0.777		
	0.579	0.856	0.882	0.776		
	-3.252	0.421	-0.670	-0.094		
08-49	16-49	24-49	32-49	40-49	48-49	
0.700	1.021	1.057	1.115	1.047	0.925	
0.652	1.030	1.100	1.113	1.078	0.936	
-6.759	0.938	4.084	-0.130	2.885	1.183	
08-41	16-41	24-41	32-41	40-41	48-41	56-41
0.986	1.083	1.073	1.091	1.044	1.135	0.782
0.998	1.101	1.076	1.071	1.081	1.114	0.737
1.201	1.078	0.301	-1.831	3.499	-1.894	-5.800
08-33	16-33	24-33	32-33	40-33	48-33	56-33
0.963	1.216	1.105	1.096	1.274	1.113	0.815
0.995	1.255	1.139	1.076	1.252	1.136	0.790
3.320	3.214	3.043	-1.813	-1.759	2.098	-3.019
08-25	16-25	24-25	32-25	40-25	48-25	56-25
0.986	1.177	1.082	1.089	1.136	1.133	0.815
1.015	1.152	1.102	1.081	1.143	1.126	0.788
3.007	-2.099	1.898	-0.749	0.619	-0.688	-3.303
08-17	16-17	24-17	32-17	40-17	48-17	56-17
0.937	1.056	1.046	1.078	1.062	1.098	0.619
0.918	1.083	1.063	1.068	1.072	1.090	0.577
-2.063	2.630	1.563	-0.965	0.944	-0.732	-6.789
	16-09	24-09	32-09	40-09	48-09	
	0.933	1.098	1.135	1.048	0.714	
	0.914	1.123	1.147	1.059	0.656	
	-2.026	2.197	1.032	1.033	-8.227	

xx-xx	String Identification
x.xxx	Measured Average Instrument Response
x.xxx	Calculated Average Instrument Response
x.xxx	Percent error

Figure 3.3
WNP-2 Cycle 1 TIP Predictions, 1372 MWd/MT

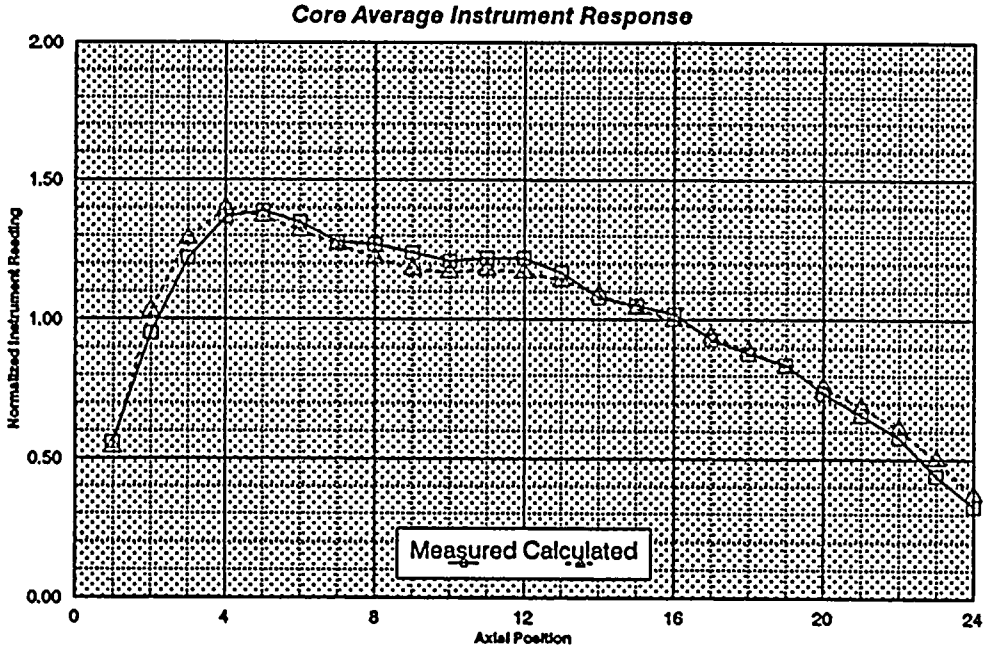

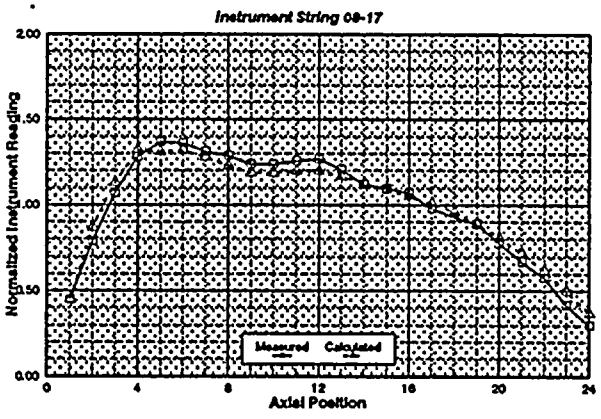

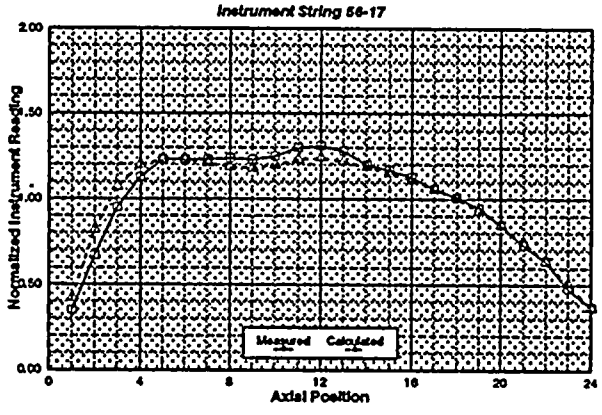

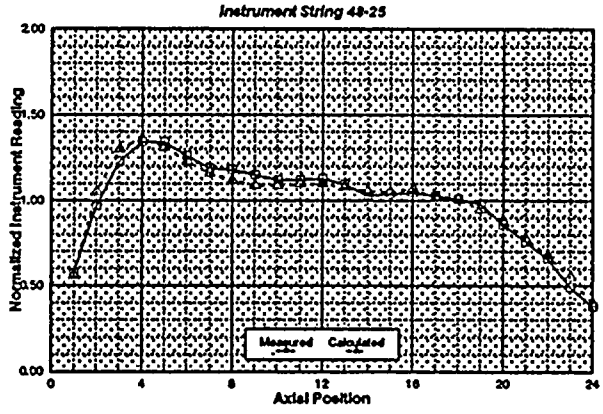

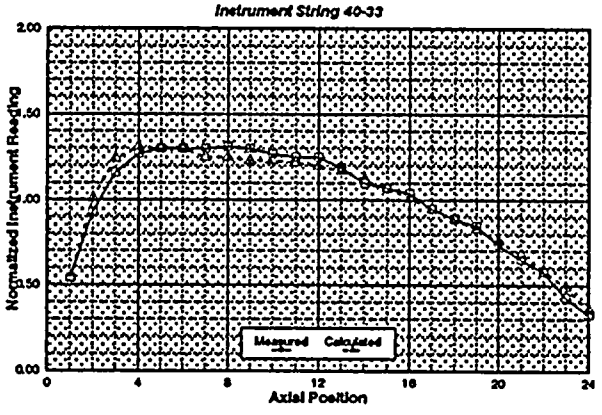

Figure 3.4

WNP-2 Cycle 1 TIP Predictions, 4579 MWd/MT

	16-57	24-57	32-57	40-57		
	0.629	0.701	0.665	0.689		
	0.581	0.707	0.672	0.689		
	-7.492	0.864	1.082	-0.023		
08-49	16-49	24-49	32-49	40-49	48-49	
0.721	1.078	1.093	1.142	1.112	0.929	
0.668	1.075	1.123	1.117	1.122	0.915	
-7.358	-0.235	2.758	-2.140	0.893	-1.494	
08-41	16-41	24-41	32-41	40-41	48-41	56-41
0.999	1.131	1.181	1.186	1.147	1.143	0.677
1.001	1.172	1.182	1.161	1.192	1.121	0.688
0.240	3.565	0.062	-2.101	3.936	-1.975	1.565
08-33	16-33	24-33	32-33	40-33	48-33	56-33
1.003	1.108	1.123	1.181	1.159	1.111	0.666
1.003	1.153	1.162	1.177	1.159	1.117	0.669
0.028	4.029	3.515	-0.390	-0.020	0.489	0.454
08-25	16-25	24-25	32-25	40-25	48-25	56-25
1.003	1.199	1.140	1.148	1.167	1.097	0.700
1.017	1.169	1.178	1.163	1.181	1.122	0.704
1.339	-2.566	3.340	1.333	1.185	2.253	0.559
08-17	16-17	24-17	32-17	40-17	48-17	56-17
0.973	1.117	1.144	1.164	1.136	1.080	0.628
0.919	1.157	1.169	1.155	1.172	1.074	0.580
-5.570	3.583	2.194	-0.715	3.167	-0.508	-7.641
	16-09	24-09	32-09	40-09	48-09	
	0.979	1.023	1.005	1.000	0.723	
	0.920	1.018	1.004	1.003	0.669	
	-5.996	-0.489	-0.057	0.324	-7.530	

xx-xx	String Identification
x.xxx	Measured Average Instrument Response
x.xxx	Calculated Average Instrument Response
x.xxx	Percent error

Figure 3.5
WNP-2 Cycle 1 TIP Predictions, 4579 MWd/MT

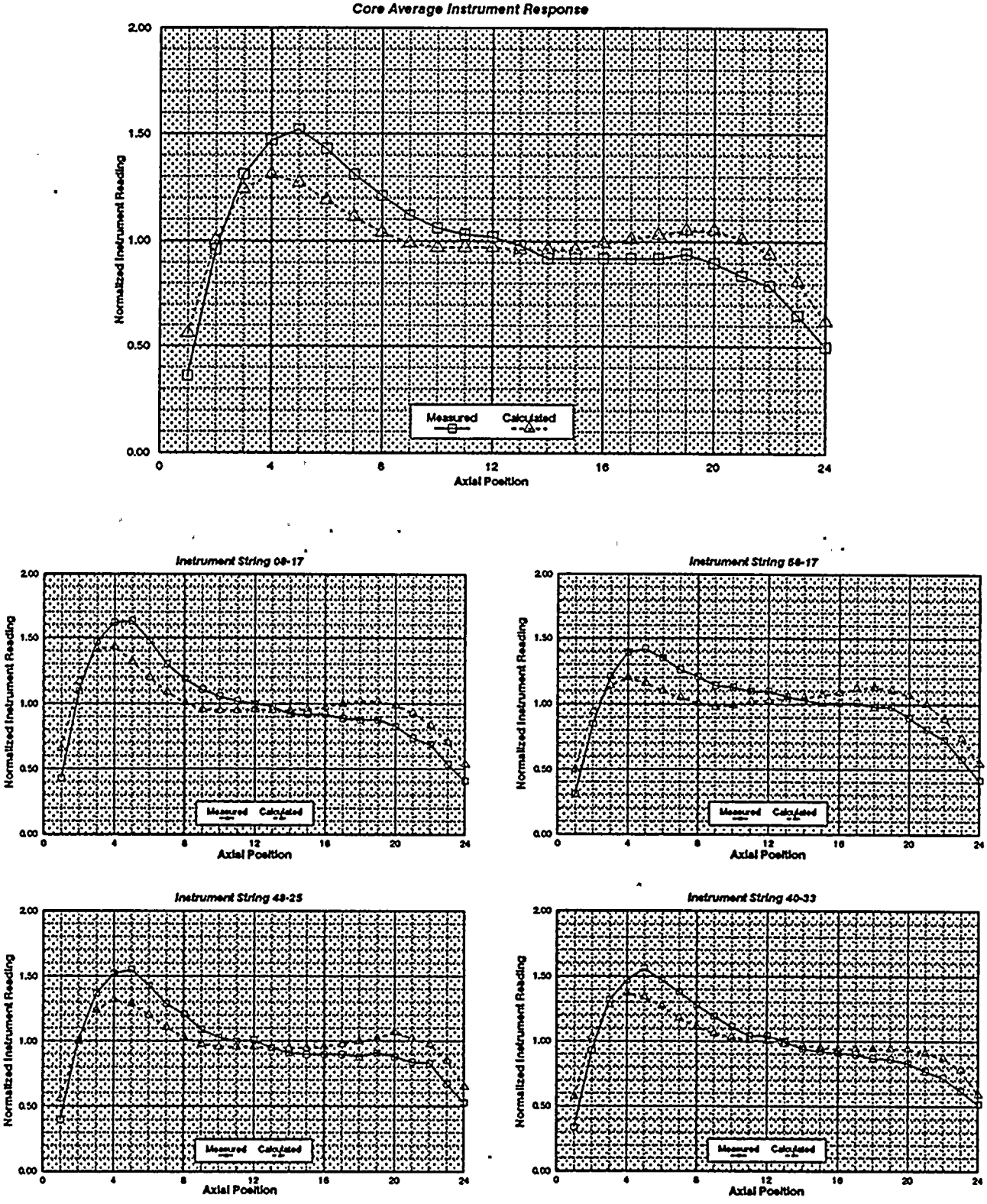

Figure 3.6

WNP-2 Cycle 2 TIP Predictions, 9297 MWd/MT

	16-57	24-57	32-57	40-57		
	0.723	0.962	0.932	0.898		
	0.655	0.876	0.888	0.822		
	-9.295	-8.941	-4.743	-8.509		
08-49	16-49	24-49	32-49	40-49	48-49	
0.788	1.064	1.037	1.031	1.034	1.026	
0.723	1.091	1.076	1.056	1.079	1.006	
-8.293	2.452	3.789	2.404	4.358	-1.971	
08-41	16-41	24-41	32-41	40-41	48-41	56-41
1.060	1.088	1.090	1.050	1.021	1.104	0.940
1.036	1.105	1.105	1.083	1.074	1.086	0.826
-2.188	1.607	1.380	3.184	5.163	-1.648	-12.144
08-33	16-33	24-33	32-33	40-33	48-33	56-33
0.999	1.076	1.038	0.984	1.063	1.091	0.956
1.034	1.104	1.077	1.030	1.087	1.061	0.893
3.499	2.616	3.774	4.720	2.205	-2.816	-6.540
08-25	16-25	24-25	32-25	40-25	48-25	56-25
1.011	1.067	0.998	0.991	1.048	1.080	0.945
1.038	1.088	1.075	1.069	1.105	1.081	0.880
2.655	1.953	7.685	7.838	5.403	0.127	-6.786
08-17	16-17	24-17	32-17	40-17	48-17	56-17
0.970	1.063	1.043	1.052	1.072	1.051	0.741
0.940	1.091	1.084	1.097	1.100	1.089	0.658
-3.077	2.596	3.901	4.325	2.614	3.583	-11.174
	16-09	24-09	32-09	40-09	48-09	
	0.989	0.989	1.000	1.023	0.813	
	0.936	1.027	1.023	1.026	0.721	
	-5.349	3.900	2.246	0.338	-11.352	

xx-xx	String Identification
x.xxx	Measured Average Instrument Response
x.xxx	Calculated Average Instrument Response
x.xxx	Percent error

Figure 3.7
WNP-2 Cycle 2 TIP Predictions, 9297 MWd/MT

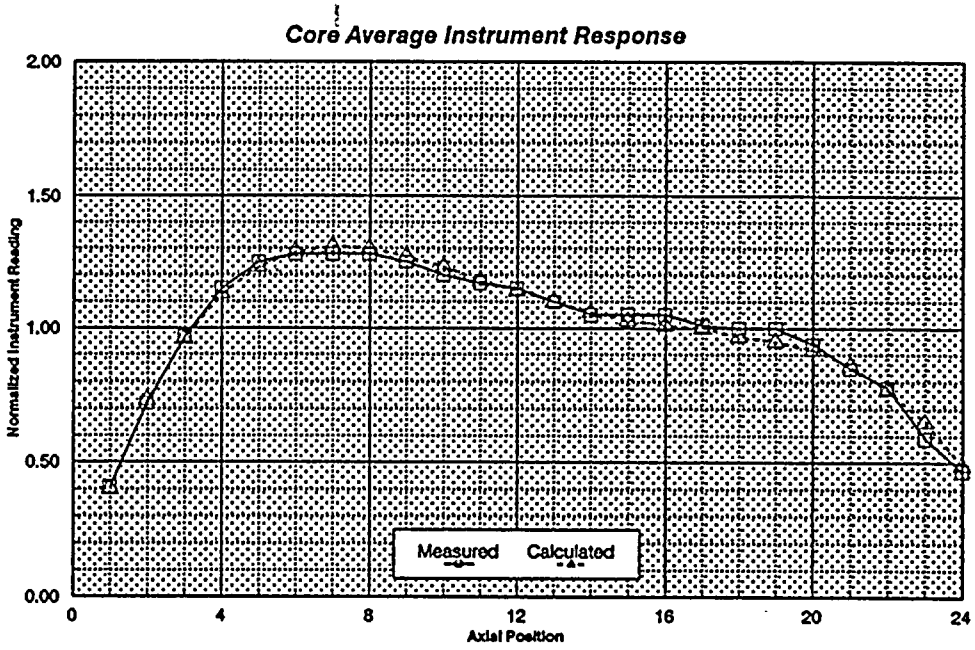

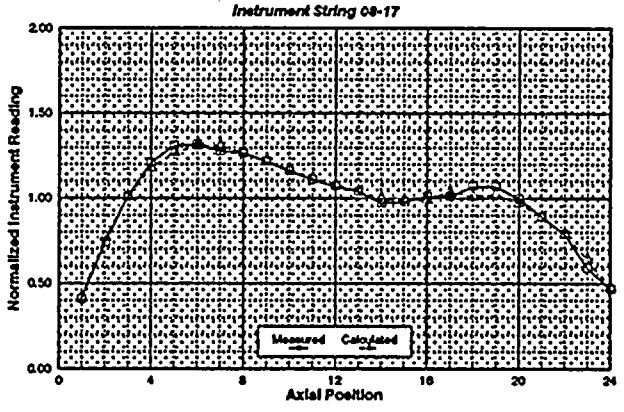

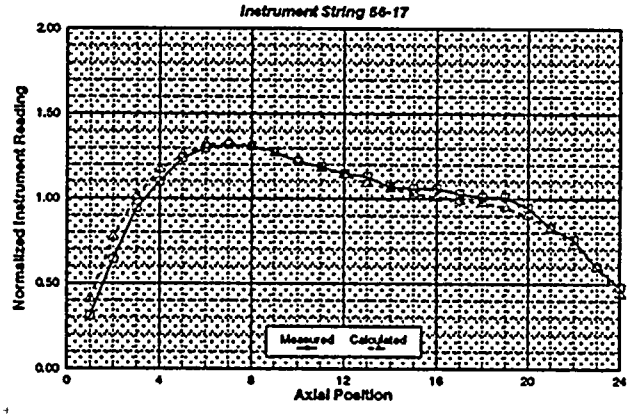

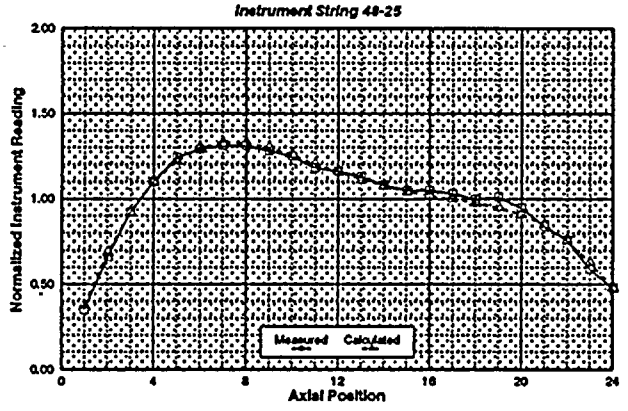

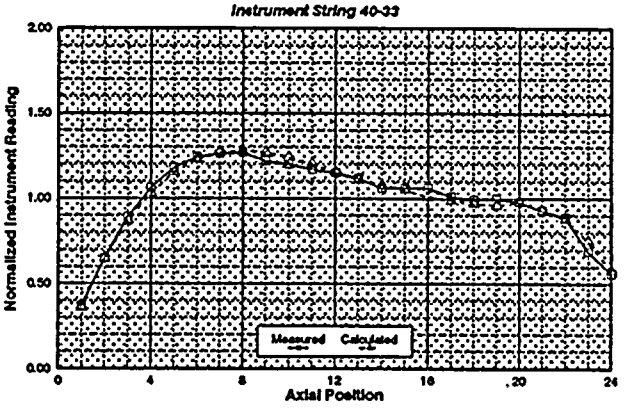

Figure 3.8

WNP-2 Cycle 2 TIP Predictions, 12102 MWd/MT

	16-57 0.697 0.665 -4.593	24-57 0.898 0.830 -7.576	32-57 0.878 0.830 -5.429	40-57 0.879 0.806 -8.319		
08-49 0.738 0.718 -2.615	16-49 1.088 1.104 1.488	24-49 1.030 1.070 3.854	32-49 1.020 1.023 0.287	40-49 1.113 1.101 -1.096	48-49 1.000 0.990 -0.991	
08-41 1.084 1.066 -1.707	16-41 1.031 1.063 3.028	24-41 1.060 1.088 2.662	32-41 1.032 1.078 4.426	40-41 0.950 1.020 7.316	48-41 1.138 1.103 -3.072	56-41 0.871 0.806 -7.448
08-33 0.966 1.002 3.701	16-33 1.001 1.030 2.927	24-33 1.167 1.222 4.706	32-33 1.203 1.263 4.991	40-33 1.040 1.077 3.563	48-33 1.034 1.020 -1.350	56-33 0.890 0.831 -6.719
08-25 1.006 1.035 2.919	16-25 1.001 1.032 3.072	24-25 1.098 1.172 6.723	32-25 1.139 1.219 7.091	40-25 1.021 1.089 6.646	48-25 1.085 1.071 -1.303	56-25 0.897 0.830 -7.422
08-17 0.995 0.982 -1.347	16-17 1.038 1.069 3.055	24-17 0.988 1.031 4.334	32-17 0.997 1.032 3.436	40-17 1.055 1.062 0.680	48-17 1.121 1.104 -1.509	56-17 0.728 0.665 -8.635
	16-09 1.052 0.981 -6.705	24-09 1.006 1.034 2.854	32-09 1.022 1.003 -1.863	40-09 1.132 1.065 -5.924	48-09 0.811 0.718 -11.452	

xx-xx	String Identification
x.xxx	Measured Average Instrument Response
x.xxx	Calculated Average Instrument Response
x.xxx	Percent error

Figure 3.9
WNP-2 Cycle 2 TIP Predictions, 12102 MWd/MT

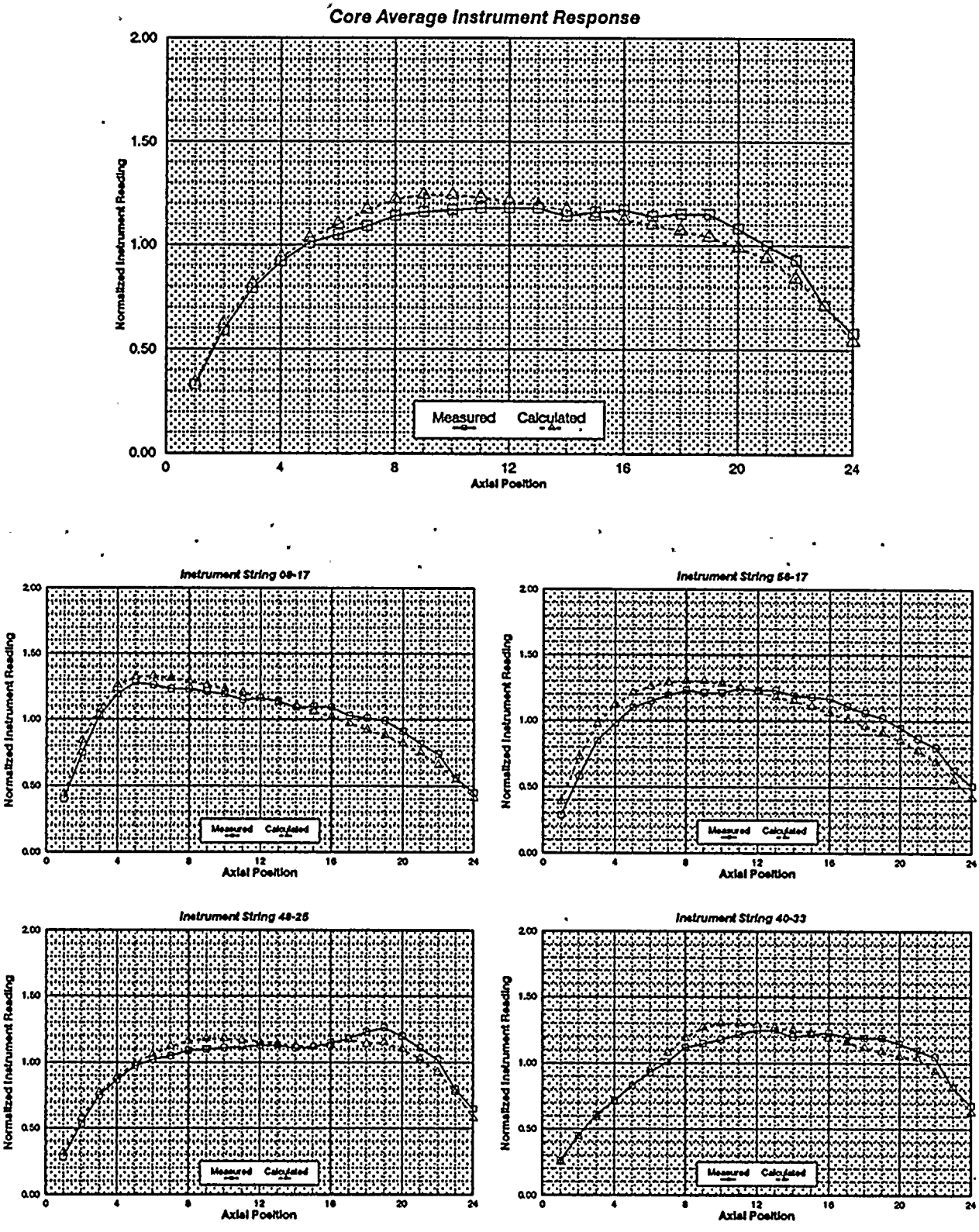

Figure 3.10

WNP-2 Cycle 3 TIP Predictions, 9903 MWd/MT

	16-57 0.701 0.715 2.013	24-57 0.917 0.914 -0.304	32-57 0.837 0.859 2.558	40-57 0.895 0.881 -1.552		
08-49 0.768 0.746 -2.887	16-49 1.024 1.080 5.489	24-49 1.048 1.109 5.839	32-49 1.015 1.016 0.151	40-49 1.096 1.106 0.821	48-49 0.944 0.948 0.342	
08-41 1.122 1.116 -0.530	16-41 1.081 1.112 2.821	24-41 1.053 1.073 1.902	32-41 1.006 0.984 -2.155	40-41 1.077 1.083 0.582	48-41 1.127 1.105 -1.913	56-41 0.922 0.879 -4.698
08-33 1.037 1.036 -0.132	16-33 0.984 1.032 4.822	24-33 0.972 0.997 2.513	32-33 0.961 0.958 -0.323	40-33 1.017 0.984 -3.178	48-33 1.001 1.014 1.358	56-33 0.889 0.856 -3.783
08-25 1.118 1.107 -0.939	16-25 1.042 1.060 1.679	24-25 1.011 1.021 1.006	32-25 0.976 0.997 2.204	40-25 1.056 1.074 1.733	48-25 1.063 1.107 4.102	56-25 0.919 0.910 -0.971
08-17 1.078 1.014 -5.974	16-17 1.129 1.091 -3.354	24-17 1.102 1.059 -3.938	32-17 0.995 1.033 3.799	40-17 1.121 1.109 -1.114	48-17 1.079 1.079 -0.010	56-17 0.736 0.714 -2.909
	16-09 1.036 1.013 -2.198	24-09 1.097 1.110 1.124	32-09 1.025 1.039 1.325	40-09 1.130 1.116 -1.265	48-09 0.792 0.746 -5.806	

xx-xx	String Identification
x.xxx	Measured Average Instrument Response
x.xxx	Calculated Average Instrument Response
x.xxx	Percent error

Figure 3.11
WNP-2 Cycle 3 TIP Predictions, 9903 MWd/MT

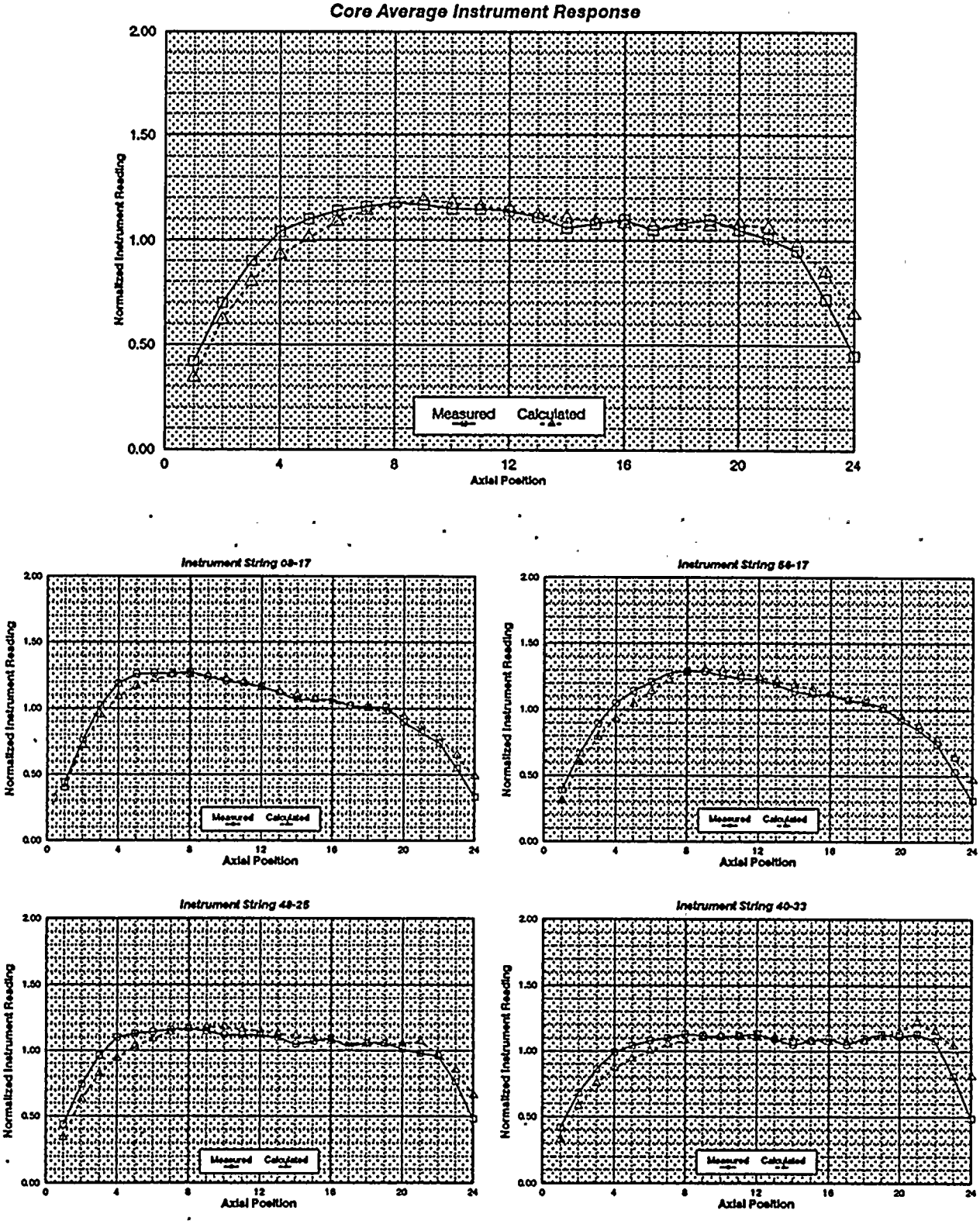

Figure 3.12

WNP-2 Cycle 3 TIP Predictions, 10836 MWd/MT

	16-57 0.713 0.729 2.328	24-57 0.911 0.903 -0.908	32-57 0.836 0.852 1.888	40-57 0.889 0.879 -1.114		
08-49 0.839 0.823 -1.921	16-49 1.136 1.190 4.700	24-49 1.019 1.080 5.973	32-49 1.014 1.004 -0.954	40-49 1.121 1.121 0.003	48-49 1.081 1.093 1.042	
08-41 1.126 1.125 -0.111	16-41 1.070 1.110 3.750	24-41 1.016 1.019 0.302	32-41 0.976 0.942 -3.509	40-41 1.063 1.049 -1.297	48-41 1.142 1.121 -1.878	56-41 0.920 0.877 -4.618
08-33 1.031 1.022 -0.856	16-33 0.960 1.001 4.229	24-33 0.915 0.936 2.219	32-33 0.906 0.894 -1.336	40-33 0.986 0.942 -4.483	48-33 0.989 1.002 1.294	56-33 0.883 0.849 -3.882
08-25 1.093 1.089 -0.322	16-25 0.996 1.018 2.259	24-25 0.949 0.960 1.177	32-25 0.932 0.936 0.429	40-25 0.999 1.021 2.147	48-25 1.033 1.078 4.418	56-25 0.901 0.899 -0.208
08-17 1.115 1.073 -3.766	16-17 1.213 1.180 -2.699	24-17 1.056 1.017 -3.724	32-17 0.968 1.002 3.476	40-17 1.105 1.108 0.250	48-17 1.170 1.189 1.601	56-17 0.740 0.729 -1.489
	16-09 1.097 1.072 -2.229	24-09 1.077 1.092 1.322	32-09 1.018 1.025 0.690	40-09 1.136 1.125 -0.943	48-09 0.857 0.824 -3.944	

xx-xx	String Identification
x.xxx	Measured Average Instrument Response
x.xxx	Calculated Average Instrument Response
x.xxx	Percent error

Figure 3.13
WNP-2 Cycle 3 TIP Predictions, 10836 MWd/MT

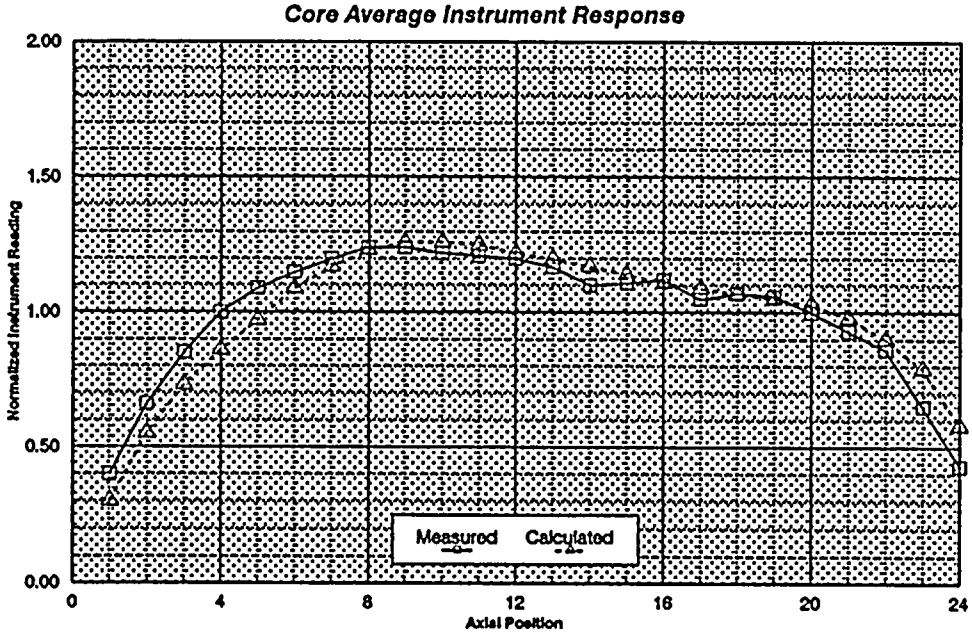

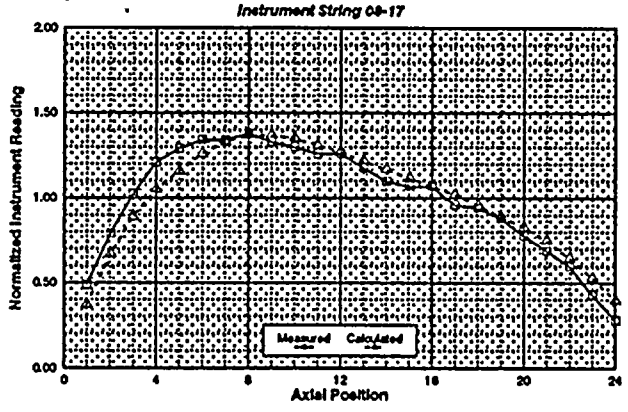

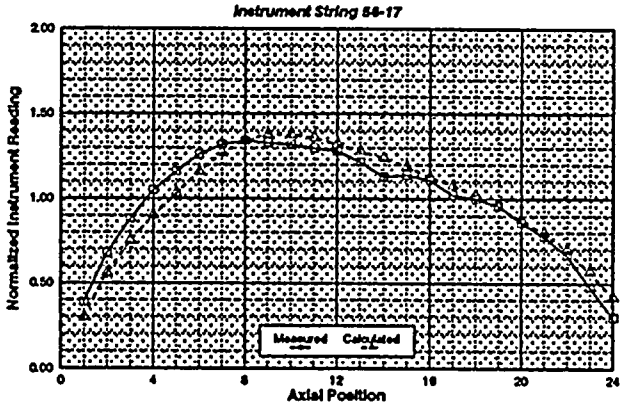

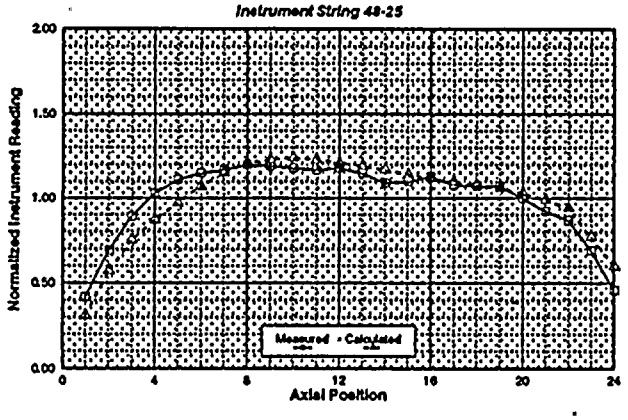

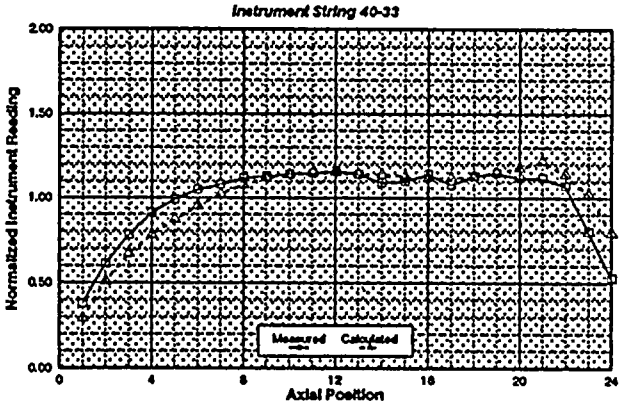

Figure 3.14

WNP-2 Cycle 3 TIP Predictions, 11034 MWd/MT

	16-57	24-57	32-57	40-57		
	0.703	0.965	0.967	0.917		
	0.719	0.975	1.000	0.906		
	2.265	0.961	3.422	-1.142		
08-49	16-49	24-49	32-49	40-49	48-49	
0.807	1.030	1.030	1.028	1.081	1.045	
0.774	1.074	1.093	1.051	1.087	1.024	
-4.018	4.202	6.141	2.195	0.538	-1.957	
08-41	16-41	24-41	32-41	40-41	48-41	56-41
0.986	1.032	1.015	0.978	1.048	1.092	0.871
0.988	1.049	1.030	0.977	1.041	1.044	0.809
0.240	1.642	1.497	-0.060	-0.710	-4.416	-7.092
08-33	16-33	24-33	32-33	40-33	48-33	56-33
0.989	0.970	1.118	1.122	1.063	0.977	0.952
0.986	1.015	1.127	1.120	1.046	0.984	0.894
-0.235	4.557	0.804	-0.171	-1.557	0.761	-6.014
08-25	16-25	24-25	32-25	40-25	48-25	56-25
0.971	1.006	1.024	1.002	1.048	0.999	0.891
0.983	1.023	1.055	1.047	1.059	1.017	0.864
1.193	1.644	3.007	4.540	0.994	1.803	-3.037
08-17	16-17	24-17	32-17	40-17	48-17	56-17
1.052	1.079	1.061	0.957	1.074	1.126	0.698
0.988	1.066	1.026	1.003	1.055	1.100	0.672
-6.064	-1.178	-3.312	4.784	-1.744	-2.268	-3.739
	16-09	24-09	32-09	40-09	48-09	
	1.042	1.120	1.109	1.133	0.825	
	1.026	1.151	1.142	1.126	0.784	
	-1.537	2.802	2.990	-0.564	-4.938	

xx-xx	String Identification
x.xxx	Measured Average Instrument Response
x.xxx	Calculated Average Instrument Response
x.xxx	Percent error

Figure 3.15
WNP-2 Cycle 3 TIP Predictions, 11034 MWd/MT

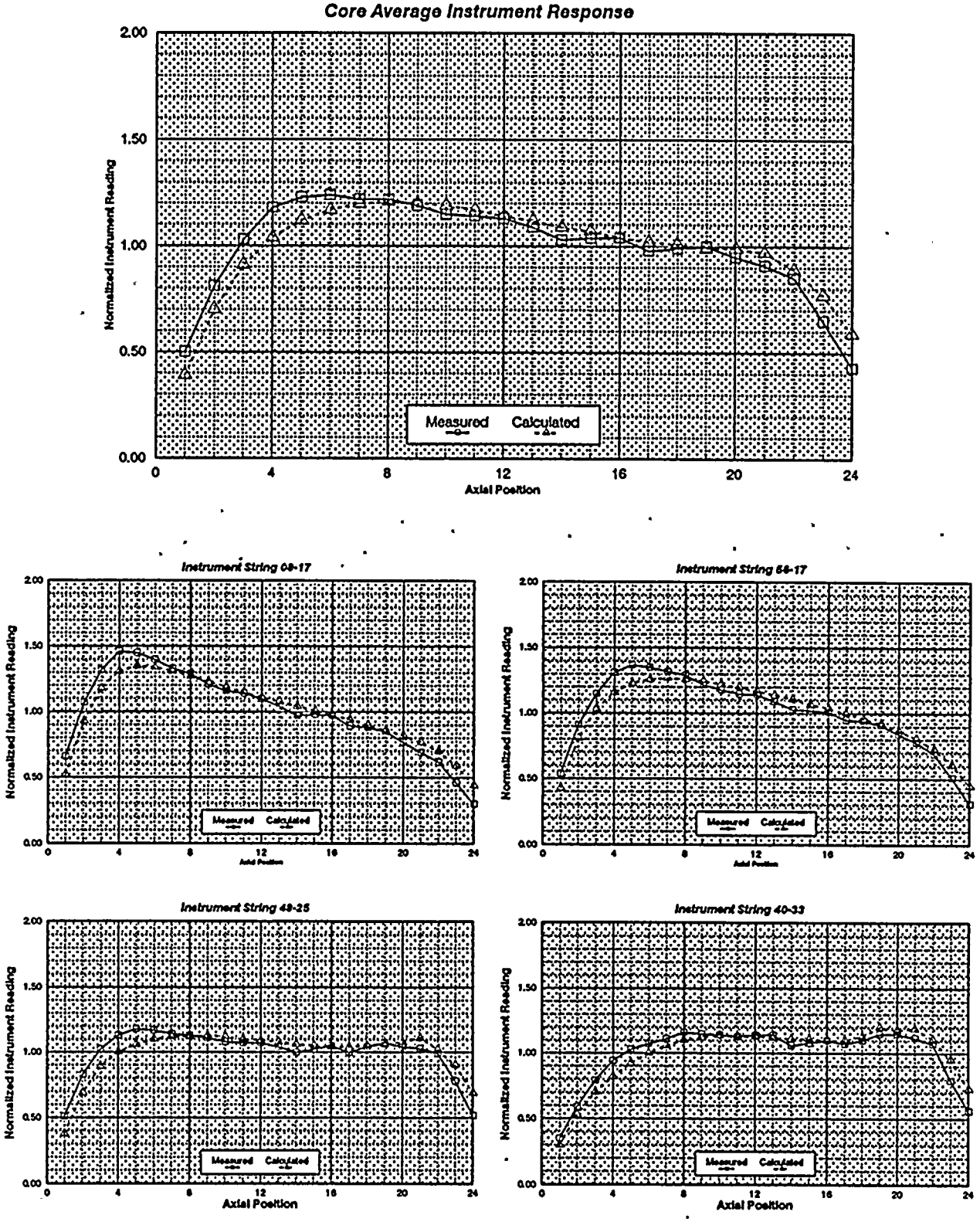

Figure 3.16

WNP-2 Cycle 3 TIP Predictions, 12245 MWd/MT

	16-57 0.642 0.643 0.033	24-57 0.895 0.866 -3.237	32-57 0.919 0.902 -1.774	40-57 0.834 0.807 -3.261		
08-49 0.786 0.749 -4.796	16-49 1.032 1.059 2.665	24-49 1.008 1.054 4.573	32-49 1.008 1.018 0.984	40-49 1.062 1.047 -1.358	48-49 1.022 1.002 -2.009	
08-41 1.001 0.992 -0.835	16-41 1.069 1.109 3.706	24-41 1.176 1.203 2.273	32-41 1.181 1.185 0.280	40-41 1.117 1.135 1.664	48-41 1.094 1.049 -4.070	56-41 0.869 0.806 -7.193
08-33 0.962 0.969 0.719	16-33 1.111 1.178 5.991	24-33 1.022 1.054 3.086	32-33 0.900 0.917 1.898	40-33 1.217 1.186 -2.550	48-33 0.995 1.017 2.189	56-33 0.959 0.900 -6.126
08-25 0.956 0.972 1.675	16-25 1.157 1.156 -0.134	24-25 1.073 1.111 3.477	32-25 1.002 1.058 5.562	40-25 1.200 1.205 0.385	48-25 1.019 1.056 3.635	56-25 0.887 0.865 -2.543
08-17 0.970 0.934 -3.736	16-17 1.060 1.055 -0.555	24-17 1.203 1.152 -4.250	32-17 1.139 1.177 3.375	40-17 1.104 1.104 -0.017	48-17 1.047 1.057 0.960	56-17 0.669 0.643 -3.858
	16-09 0.932 0.933 0.110	24-09 0.944 0.969 2.677	32-09 0.951 0.967 1.678	40-09 1.000 0.988 -1.183	48-09 0.802 0.750 -6.548	

xx-xx	String Identification
x.xxx	Measured Average Instrument Response
x.xxx	Calculated Average Instrument Response
x.xxx	Percent error

Figure 3.17
WNP-2 Cycle 3 TIP Predictions, 12245 MWd/MT

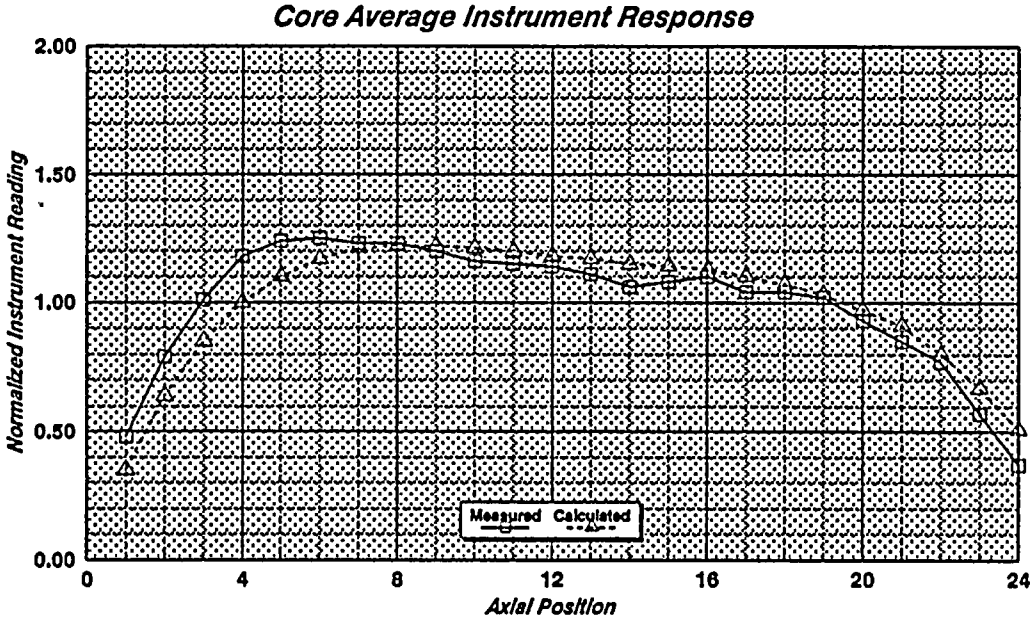

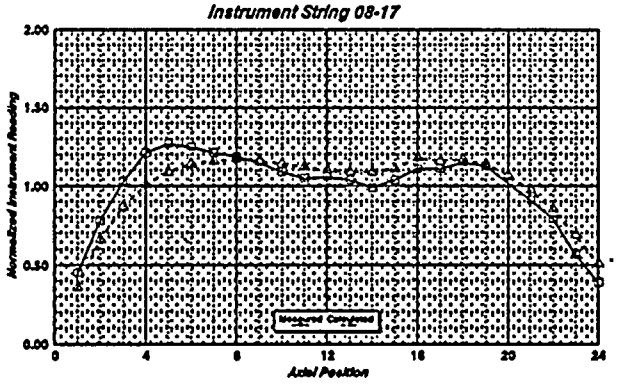

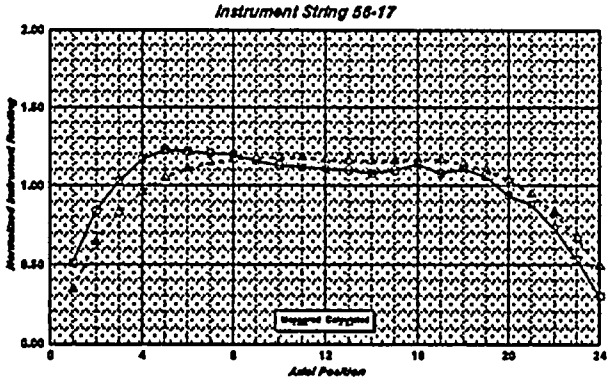

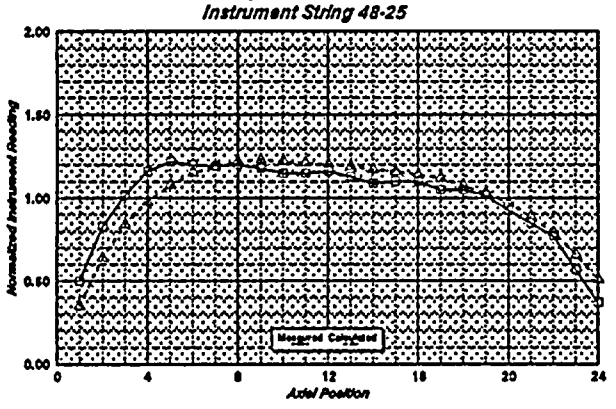

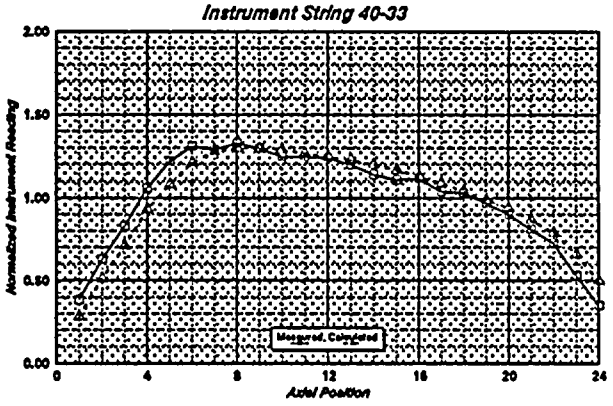

Figure 3.18

WNP-2 Cycle 3 TIP Predictions, 12903 MWd/MT

	16-57	24-57	32-57	40-57		
	0.643	0.906	0.936	0.831		
	0.641	0.876	0.921	0.808		
	-0.397	-3.335	-1.572	-2.755		
08-49	16-49	24-49	32-49	40-49	48-49	
0.792	1.025	1.007	1.017	1.058	1.013	
0.748	1.053	1.058	1.037	1.040	0.999	
-5.588	2.757	5.074	1.980	-1.708	-1.404	
08-41	16-41	24-41	32-41	40-41	48-41	56-41
1.001	1.063	1.153	1.171	1.098	1.088	0.879
0.994	1.097	1.183	1.178	1.116	1.042	0.808
-0.693	3.204	2.630	0.640	1.694	-4.274	-8.043
08-33	16-33	24-33	32-33	40-33	48-33	56-33
1.000	1.103	1.020	0.908	1.205	1.016	0.976
0.998	1.168	1.051	0.919	1.178	1.036	0.922
-0.124	5.905	3.050	1.196	-2.229	1.999	-5.548
08-25	16-25	24-25	32-25	40-25	48-25	56-25
0.968	1.150	1.061	1.007	1.178	1.024	0.896
0.988	1.141	1.101	1.055	1.184	1.060	0.876
2.098	-0.819	3.771	4.785	0.537	3.568	-2.305
08-17	16-17	24-17	32-17	40-17	48-17	56-17
0.968	1.050	1.185	1.129	1.092	1.038	0.672
0.934	1.047	1.139	1.169	1.092	1.051	0.641
-3.505	-0.248	-3.915	3.469	0.048	1.274	-4.581
	16-09	24-09	32-09	40-09	48-09	
	0.930	0.961	0.981	1.001	0.804	
	0.933	0.984	0.995	0.990	0.749	
	0.361	2.492	1.480	-1.136	-6.838	

xx-xx	String Identification
x.xxx	Measured Average Instrument Response
x.xxx	Calculated Average Instrument Response
x.xxx	Percent error

Figure 3.19
WNP-2 Cycle 3 TIP Predictions, 12903 MWd/MT

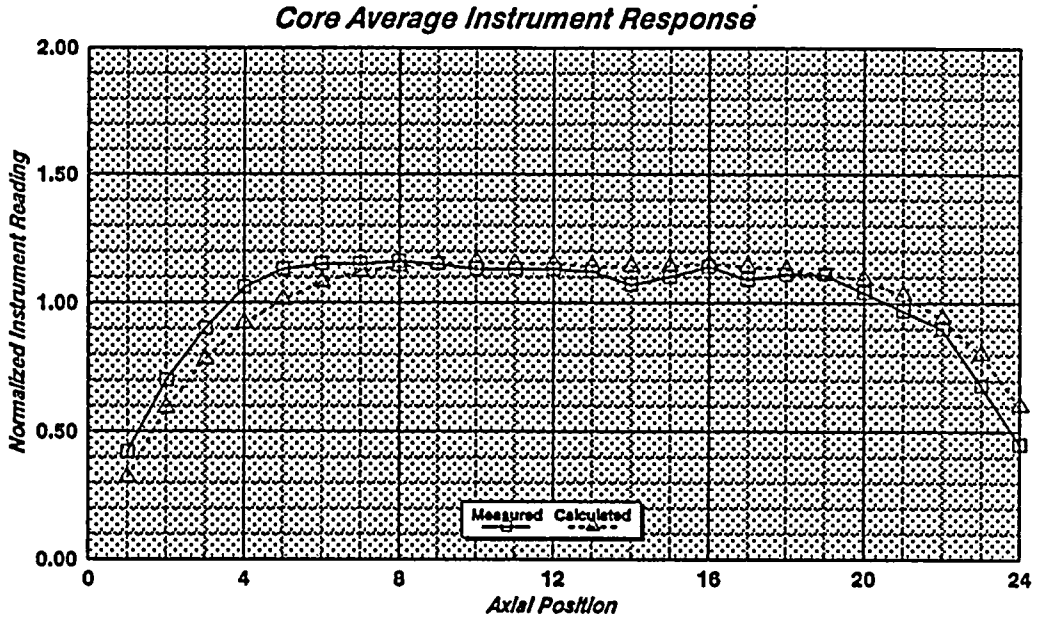

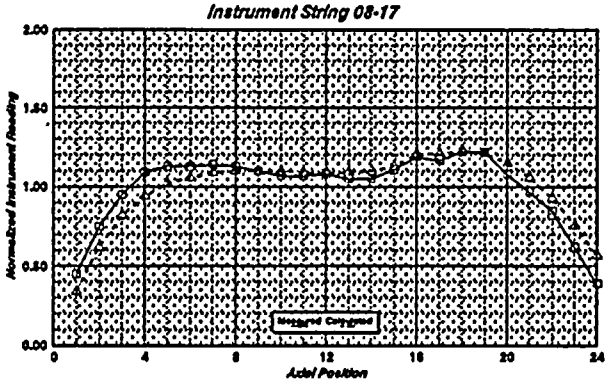

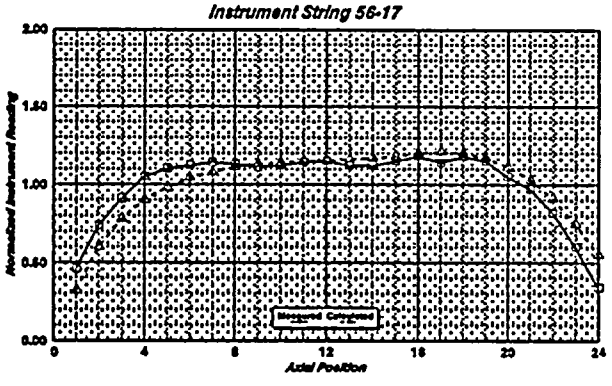

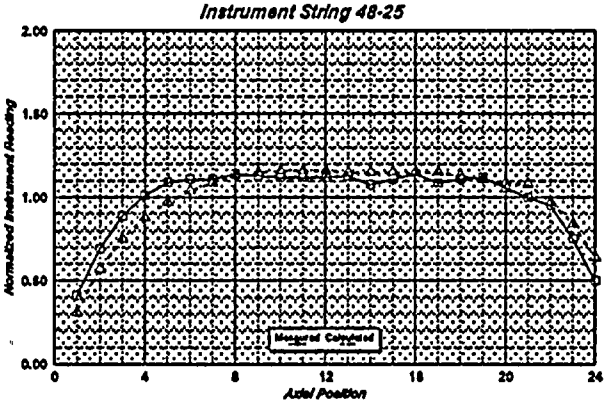

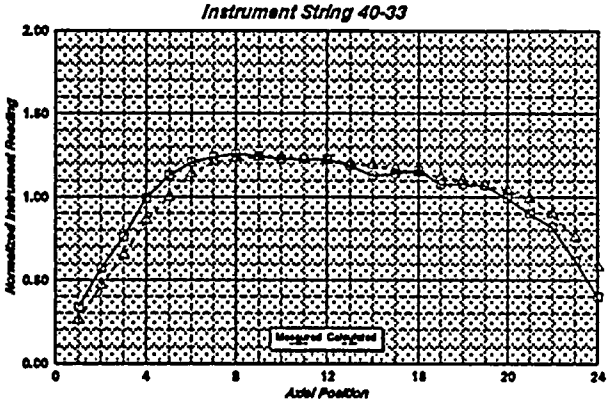

Figure 3.20

WNP-2 Cycle 3 TIP Predictions, 13974 MWd/MT

	16-57 0.624 0.630 0.912	24-57 0.886 0.861 -2.836	32-57 0.946 0.950 0.449	40-57 0.798 0.774 -3.005		
08-49 0.789 0.764 -3.160	16-49 1.071 1.073 0.192	24-49 1.004 1.064 6.000	32-49 1.142 1.138 -0.389	40-49 1.028 1.024 -0.370	48-49 1.004 1.010 0.627	
08-41 1.061 1.029 -2.978	16-41 1.082 1.111 2.615	24-41 1.141 1.170 2.526	32-41 1.188 1.196 0.687	40-41 1.128 1.126 -0.121	48-41 1.098 1.074 -2.199	56-41 0.850 0.790 -7.054
08-33 0.996 0.983 -1.229	16-33 1.069 1.109 3.661	24-33 0.952 0.981 3.097	32-33 1.024 1.026 0.145	40-33 1.014 1.007 -0.712	48-33 1.102 1.114 1.040	56-33 0.829 0.789 -4.904
08-25 0.988 1.000 1.180	16-25 1.109 1.104 -0.482	24-25 1.018 1.053 3.412	32-25 1.091 1.124 2.983	40-25 1.028 1.065 3.625	48-25 1.103 1.113 0.896	56-25 0.776 0.775 -0.061
08-17 1.033 0.982 -4.903	16-17 1.077 1.085 0.740	24-17 1.182 1.146 -3.086	32-17 1.142 1.198 4.879	40-17 1.158 1.128 -2.560	48-17 1.045 1.066 2.055	56-17 0.679 0.653 -3.800
	16-09 0.965 0.948 -1.734	24-09 0.947 0.984 3.895	32-09 1.086 1.089 0.326	40-09 0.942 0.940 -0.149	48-09 0.806 0.755 -6.343	

xx-xx	String Identification
x.xxx	Measured Average Instrument Response
x.xxx	Calculated Average Instrument Response
x.xxx	Percent error

Figure 3.21
WNP-2 Cycle 3 TIP Predictions, 13974 MWd/MT

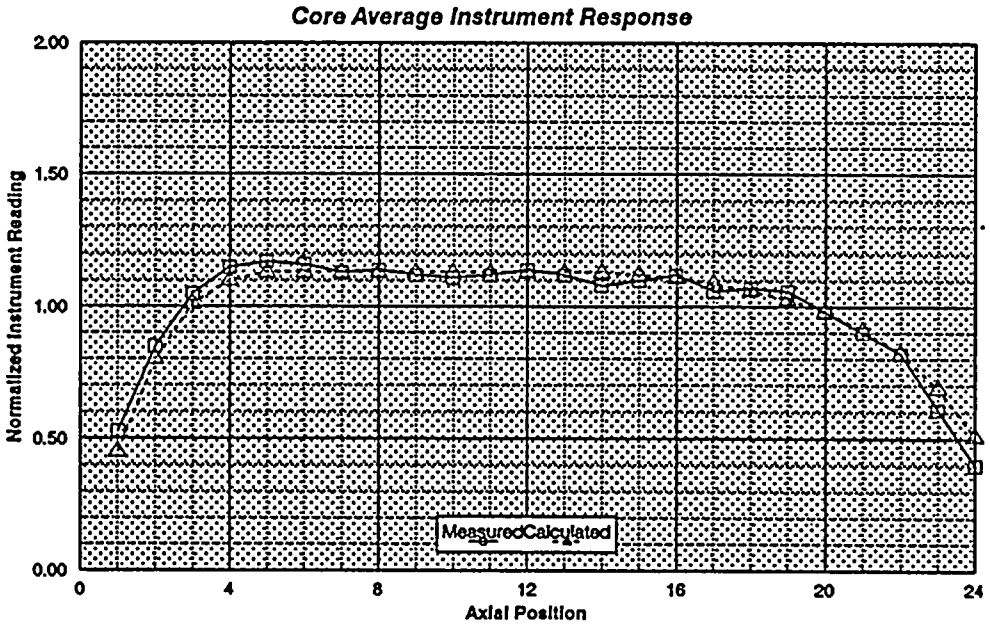

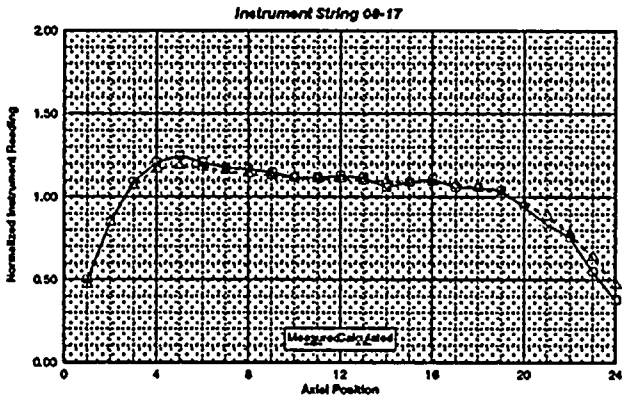

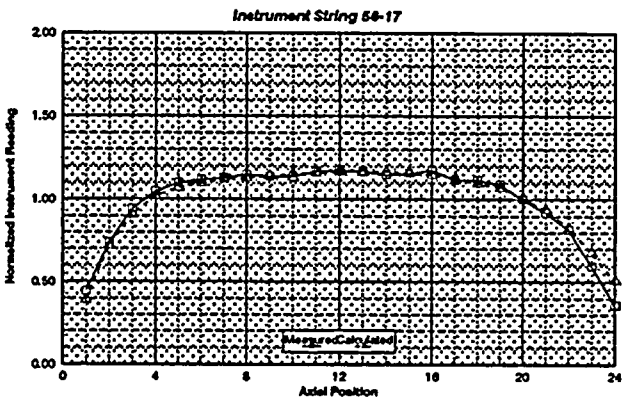

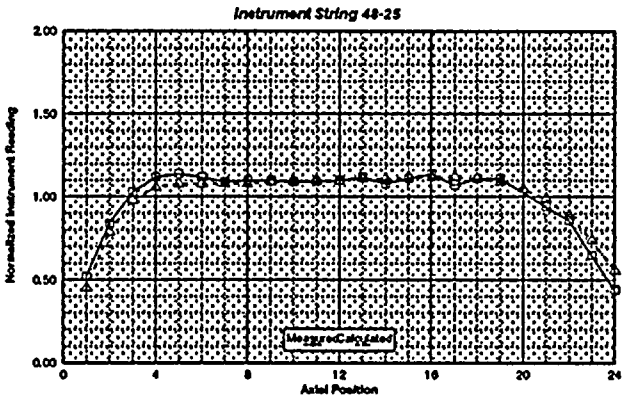

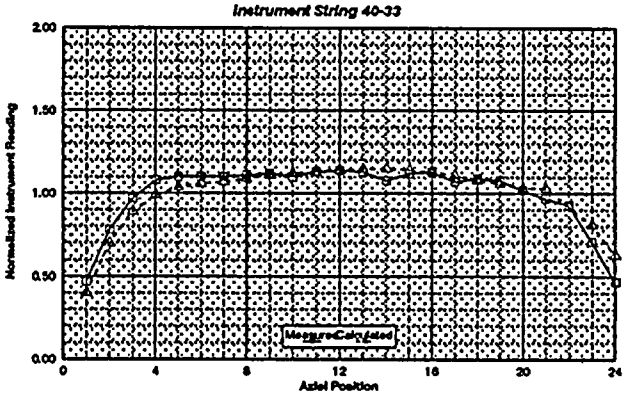

Figure 3.22

WNP-2 Cycle 4 TIP Predictions, 11245 MWd/MT

	16-57	24-57	32-57	40-57		
	0.663	0.919	0.932	0.828		
	0.680	0.937	0.970	0.856		
	2.629	1.921	4.054	3.351		
08-49	16-49	24-49	32-49	40-49	48-49	
0.789	1.111	1.033	1.011	1.019	1.089	
0.801	1.121	1.055	1.063	1.064	1.052	
1.451	0.850	2.087	5.090	4.396	-3.427	
08-41	16-41	24-41	32-41	40-41	48-41	56-41
1.094	1.058	1.029	0.995	0.982	1.045	0.881
1.094	1.009	0.979	0.972	0.974	1.067	0.857
0.001	-4.634	-4.817	-2.305	-0.799	2.068	-2.757
08-33	16-33	24-33	32-33	40-33	48-33	56-33
1.133	0.990	1.029	1.121	0.986	1.048	0.942
1.144	0.988	1.022	1.113	0.973	1.061	0.972
1.025	-0.171	-0.721	-0.762	-1.330	1.232	3.199
08-25	16-25	24-25	32-25	40-25	48-25	56-25
1.135	0.980	1.015	1.020	0.987	1.056	0.916
1.125	0.976	1.008	1.022	0.981	1.057	0.939
-0.811	-0.383	-0.648	0.256	-0.630	0.109	2.419
08-17	16-17	24-17	32-17	40-17	48-17	56-17
1.052	1.092	0.983	1.036	1.027	1.132	0.690
1.021	1.097	0.973	0.986	1.006	1.123	0.681
-2.926	0.494	-1.015	-4.816	-2.030	-0.790	-1.308
	16-09	24-09	32-09	40-09	48-09	
	1.042	1.082	1.137	1.091	0.799	
	1.020	1.124	1.144	1.092	0.800	
	-2.135	3.936	0.644	0.130	0.116	

xx-xx	String Identification
x.xxx	Measured Average Instrument Response
x.xxx	Calculated Average Instrument Response
x.xxx	Percent error

Figure 3.23
WNP-2 Cycle 4 TIP Predictions, 11245 MWd/MT

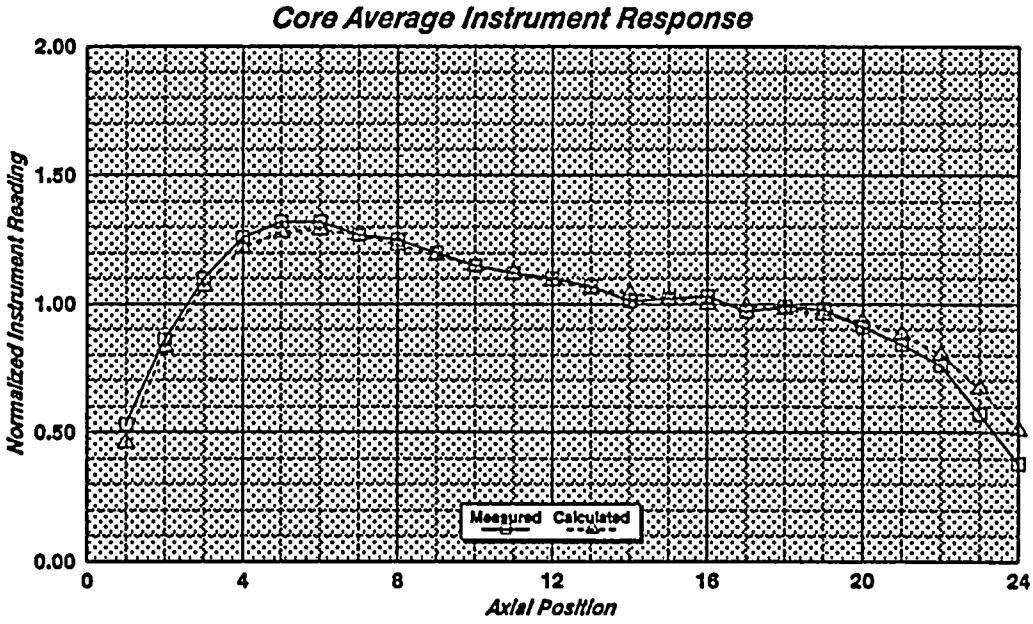

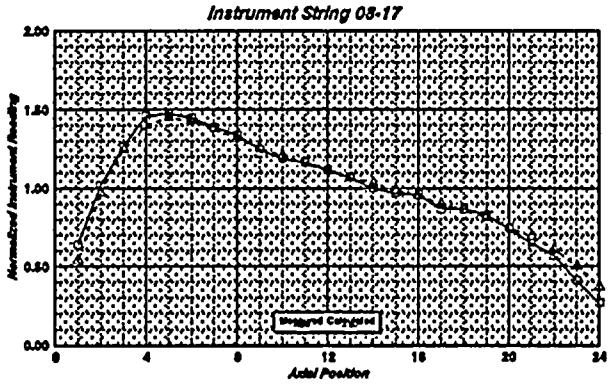

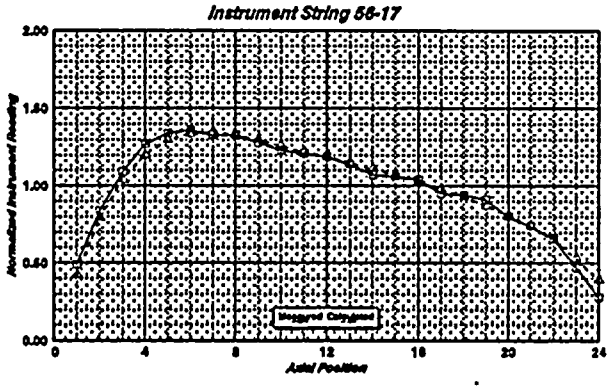

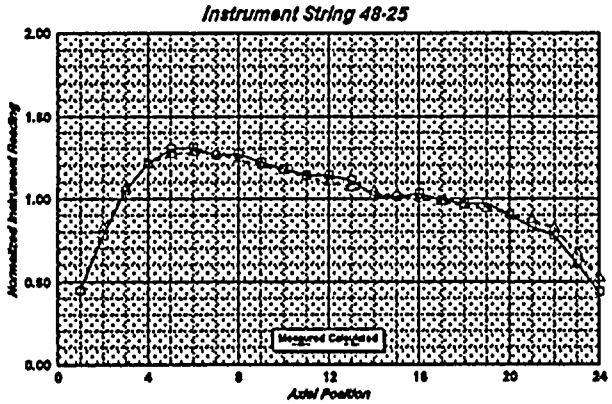

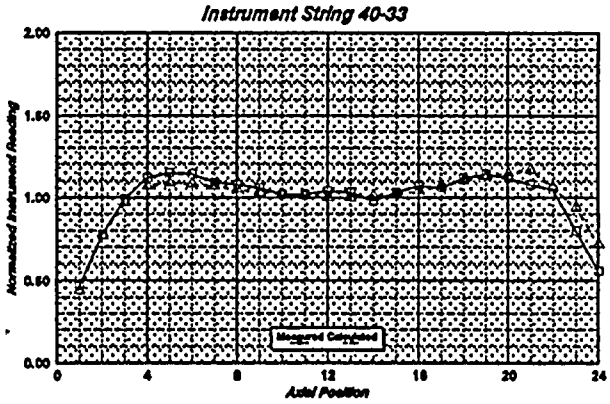

Figure 3.24

WNP-2 Cycle 4 TIP Predictions, 12903 MWd/MT

	16-57	24-57	32-57	40-57		
	0.656	0.912	0.919	0.843		
	0.672	0.931	0.950	0.862		
	2.397	2.160	3.332	2.244		
08-49	16-49	24-49	32-49	40-49	48-49	
0.752	1.047	1.066	1.013	1.044	1.061	
0.772	1.079	1.070	1.050	1.083	1.029	
2.708	3.017	0.376	3.637	3.769	-3.049	
08-41	16-41	24-41	32-41	40-41	48-41	56-41
1.115	1.090	0.996	0.978	0.950	1.142	0.900
1.130	1.033	0.954	0.957	0.962	1.159	0.871
1.347	-5.227	-4.168	-2.155	1.249	1.467	-3.249
08-33	16-33	24-33	32-33	40-33	48-33	56-33
1.042	0.987	1.114	1.119	1.033	1.050	0.922
1.055	0.992	1.088	1.128	1.013	1.050	0.917
1.270	0.460	-2.392	0.871	-1.958	-0.033	-0.621
08-25	16-25	24-25	32-25	40-25	48-25	56-25
1.132	1.011	0.998	1.005	0.960	1.139	0.923
1.126	1.021	1.007	1.010	0.965	1.127	0.925
-0.600	1.019	0.916	0.532	0.496	-1.058	0.237
08-17	16-17	24-17	32-17	40-17	48-17	56-17
1.046	1.054	1.000	1.016	1.035	1.141	0.689
1.030	1.074	0.993	0.964	1.007	1.139	0.683
-1.449	1.859	-0.617	-5.109	-2.659	-0.200	-0.865
	16-09	24-09	32-09	40-09	48-09	
	1.023	1.075	1.125	1.102	0.772	
	1.000	1.129	1.121	1.101	0.768	
	-2.233	4.957	-0.358	-0.053	-0.458	

xx-xx	String Identification
x.xxx	Measured Average Instrument Response
x.xxx	Calculated Average Instrument Response
x.xxx	Percent error

Figure 3.25
WNP-2 Cycle 4 TIP Predictions, 12903 MWd/MT

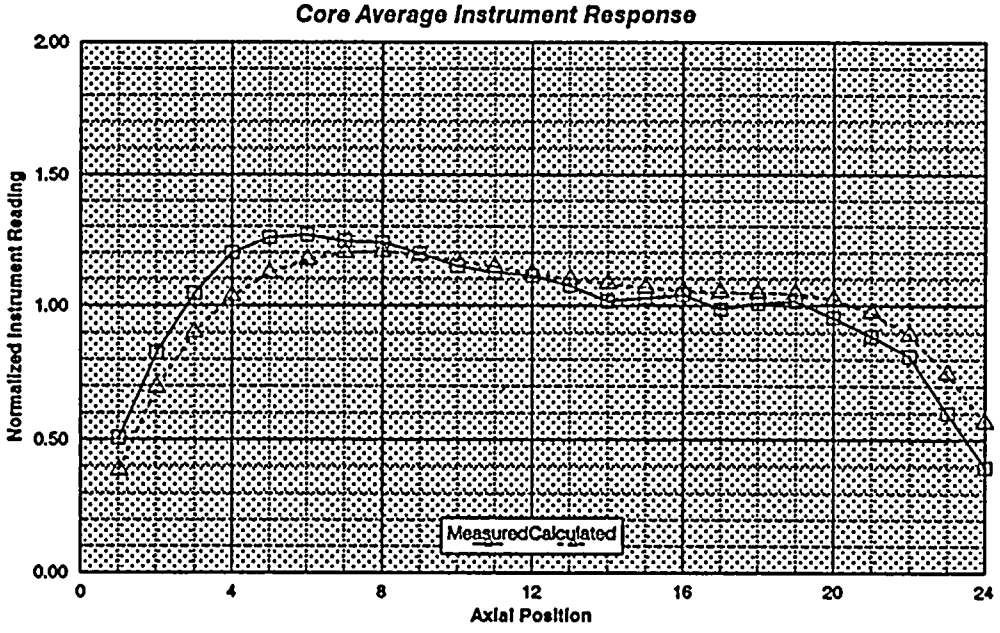

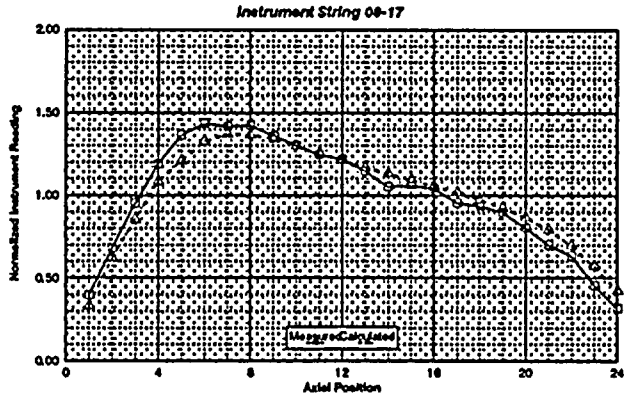

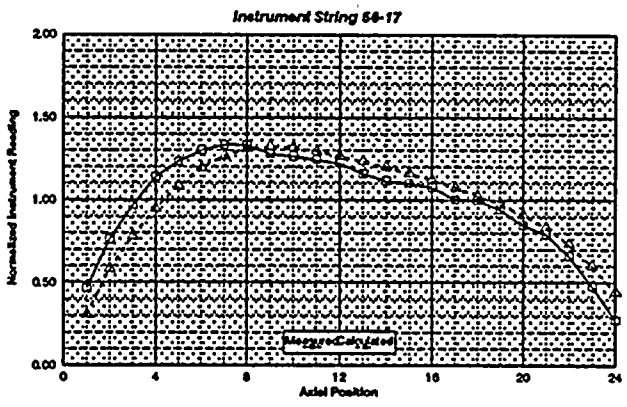

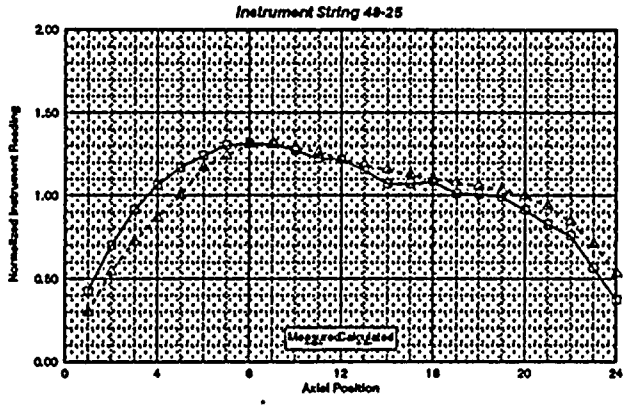

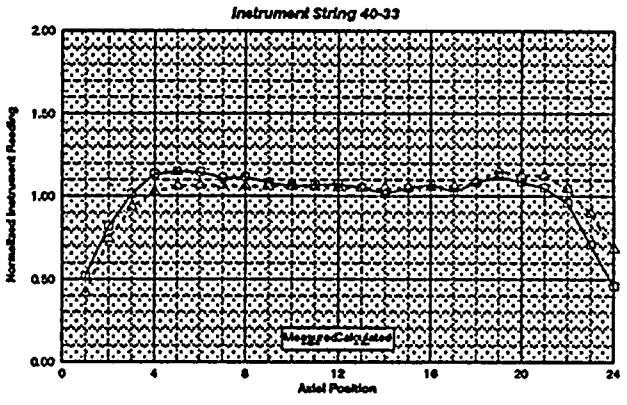

Figure 3.26

WNP-2 Cycle 4 TIP Predictions, 13563 MWd/MT

	16-57	24-57	32-57	40-57		
	0.640	0.855	0.834	0.808		
	0.649	0.842	0.829	0.814		
	1.359	-1.552	-0.549	0.781		
08-49	16-49	24-49	32-49	40-49	48-49	
0.757	1.118	1.054	0.965	1.108	1.099	
0.767	1.132	1.063	0.991	1.124	1.048	
1.276	1.269	0.864	2.637	1.441	-4.687	
08-41	16-41	24-41	32-41	40-41	48-41	56-41
1.055	1.160	1.189	1.162	1.079	1.119	0.841
1.059	1.107	1.133	1.133	1.103	1.127	0.816
0.392	-4.540	-4.704	-2.537	2.158	0.721	-2.936
08-33	16-33	24-33	32-33	40-33	48-33	56-33
0.923	1.132	1.023	0.929	1.161	0.984	0.836
0.934	1.124	1.029	0.959	1.137	0.995	0.835
1.136	-0.691	0.620	3.302	-2.040	1.142	-0.189
08-25	16-25	24-25	32-25	40-25	48-25	56-25
0.990	1.133	1.041	1.014	1.124	1.064	0.843
0.992	1.137	1.076	1.028	1.134	1.067	0.845
0.181	0.356	3.394	1.326	0.869	0.289	0.301
08-17	16-17	24-17	32-17	40-17	48-17	56-17
1.007	1.070	1.143	1.172	1.104	1.127	0.665
0.997	1.109	1.131	1.114	1.100	1.132	0.649
-0.968	3.631	-1.114	-4.916	-0.328	0.481	-2.431
	16-09	24-09	32-09	40-09	48-09	
	1.005	0.919	0.929	1.050	0.768	
	0.997	0.989	0.928	1.057	0.767	
	-0.750	7.602	-0.128	0.717	-0.190	

xx-xx	String Identification
x.xxx	Measured Average Instrument Response
x.xxx	Calculated Average Instrument Response
x.xxx	Percent error

Figure 3.27
WNP-2 Cycle 4 TIP Predictions, 13563 MWd/MT

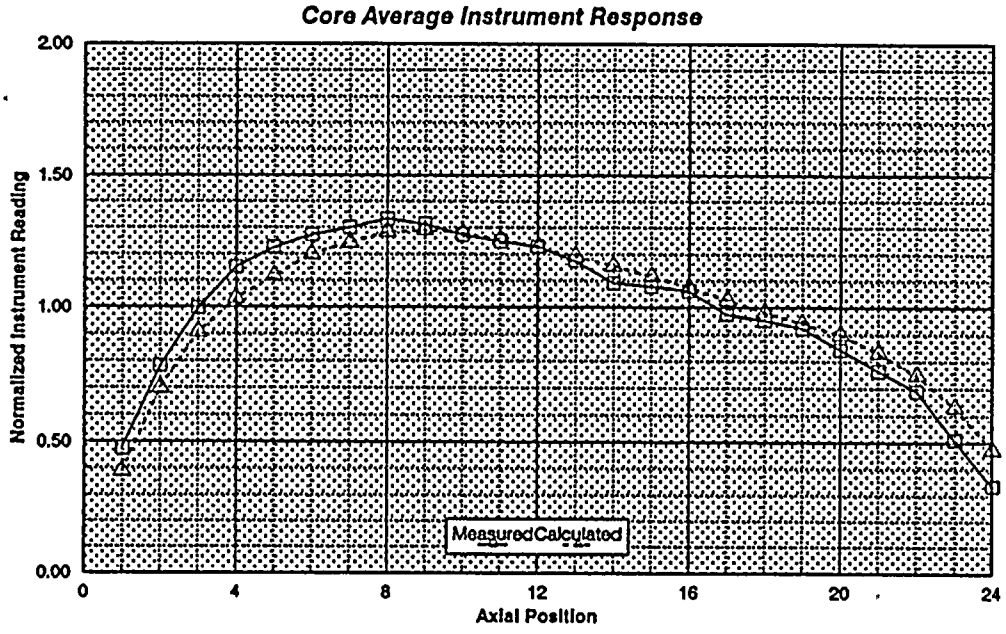

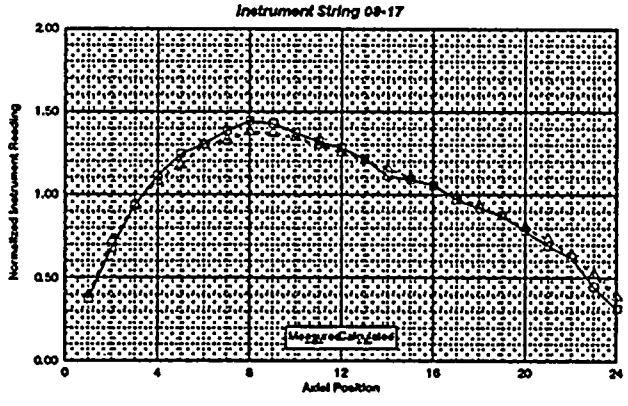

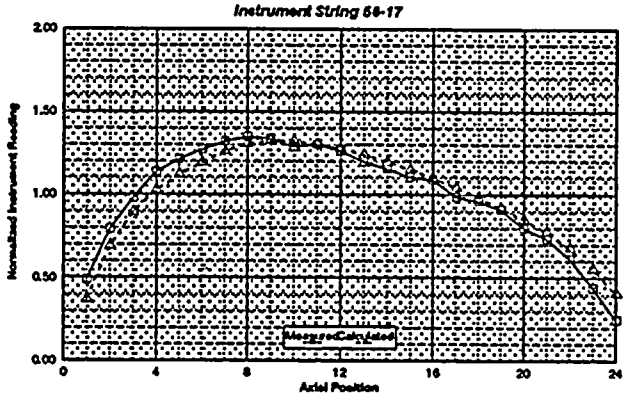

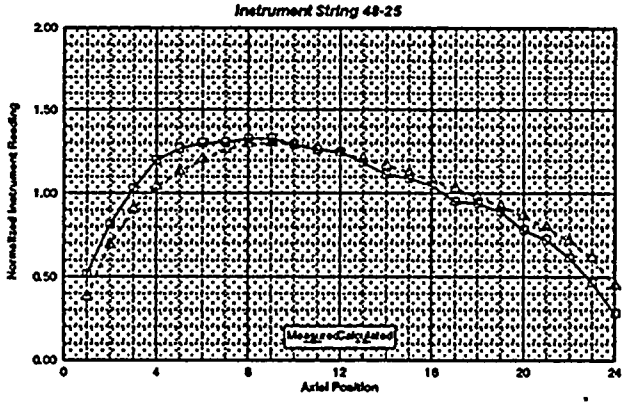

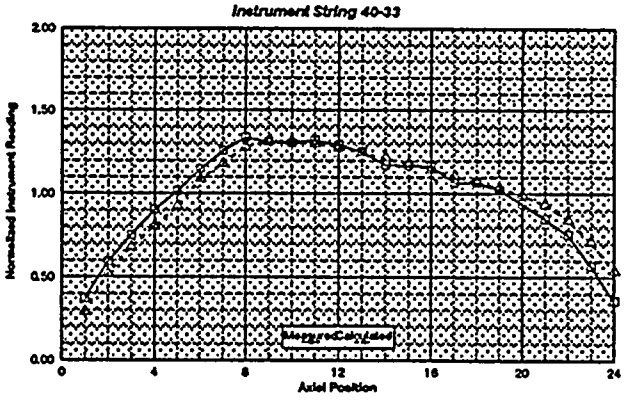

Figure 3.28

WNP-2 Cycle 4 TIP Predictions, 14428 MWd/MT

	16-57	24-57	32-57	40-57		
	0.635	0.855	0.831	0.806		
	0.640	0.841	0.826	0.810		
	0.762	-1.640	-0.601	0.520		
08-49	16-49	24-49	32-49	40-49	48-49	
0.736	1.103	1.060	0.973	1.102	1.078	
0.747	1.121	1.074	0.999	1.123	1.029	
1.395	1.655	1.312	2.683	1.911	-4.572	
08-41	16-41	24-41	32-41	40-41	48-41	56-41
1.045	1.159	1.190	1.169	1.100	1.117	0.841
1.053	1.115	1.144	1.137	1.120	1.124	0.811
0.775	-3.812	-3.880	-2.730	1.797	0.656	-3.646
08-33	16-33	24-33	32-33	40-33	48-33	56-33
0.929	1.125	1.036	0.932	1.161	0.991	0.834
0.937	1.128	1.031	0.955	1.140	1.000	0.830
0.846	0.194	-0.485	2.523	-1:854	0.957	-0.450
08-25	16-25	24-25	32-25	40-25	48-25	56-25
0.996	1.151	1.052	1.024	1.127	1.066	0.843
0.996	1.148	1.082	1.031	1.146	1.076	0.842
0.029	-0.225	2.874	0.699	1.617	0.880	-0.007
08-17	16-17	24-17	32-17	40-17	48-17	56-17
0.999	1.069	1.156	1.179	1.106	1.115	0.654
0.986	1.107	1.144	1.121	1.111	1.120	0.640
-1.342	3.515	-1.052	-4.907	0.499	0.383	-2.270
	16-09	24-09	32-09	40-09	48-09	
	0.993	0.927	0.940	1.044	0.749	
	0.987	0.995	0.933	1.054	0.747	
	-0.598	7.336	-0.792	0.919	-0.167	

xx-xx	String Identification
x.xxx	Measured Average Instrument Response
x.xxx	Calculated Average Instrument Response
x.xxx	Percent error

Figure 3.29

WNP-2 Cycle 4 TIP Predictions, 14428 MWd/MT

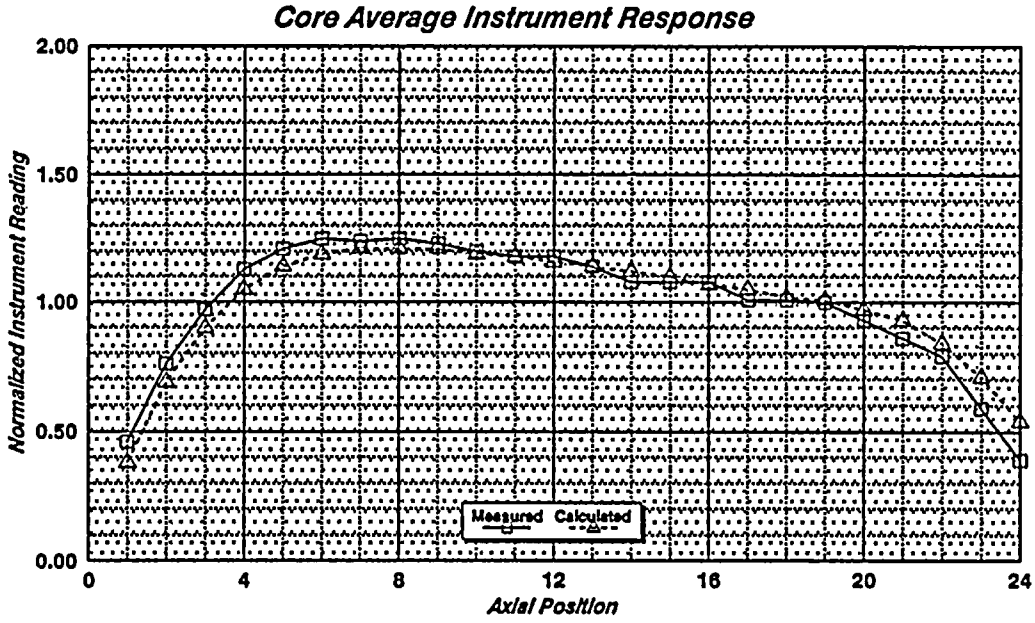

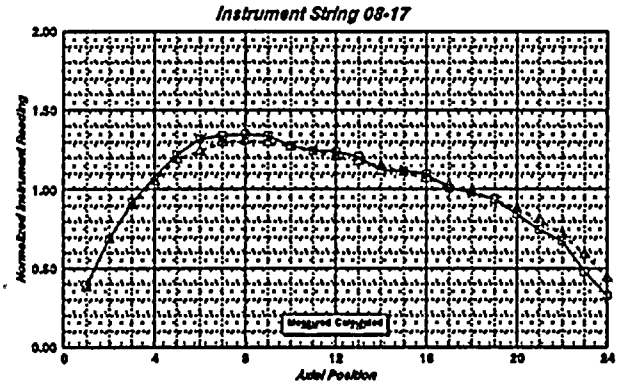

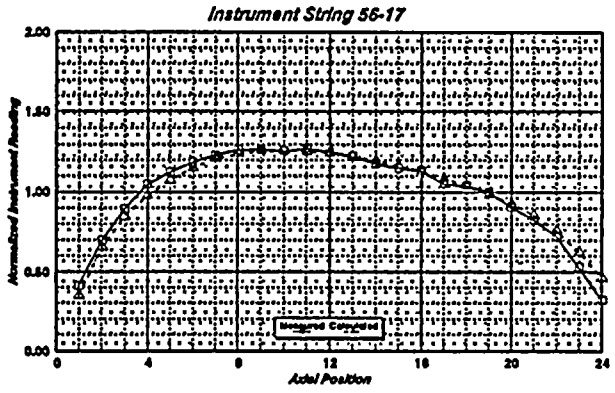

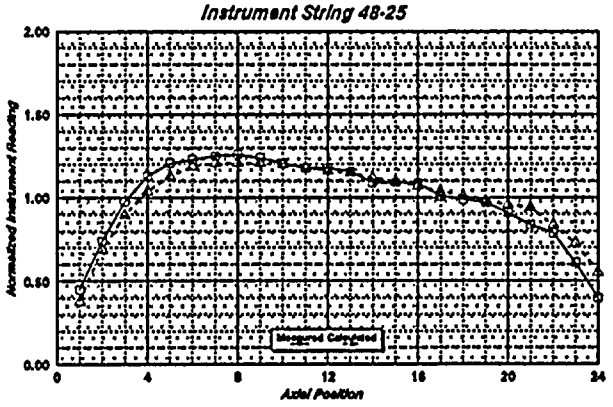

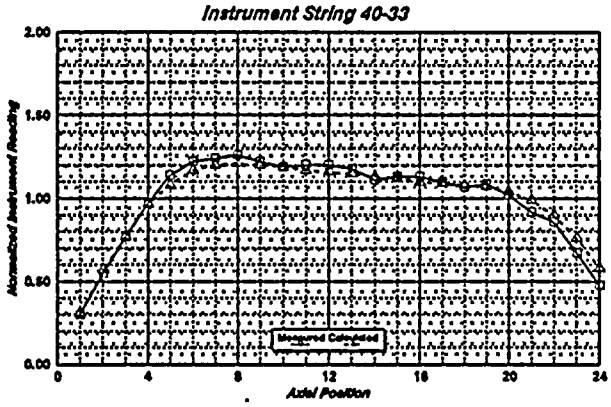

Figure 3.30

WNP-2 Cycle 4 TIP Predictions, 15473 MWd/MT

	16-57 0.640 0.663 3.561	24-57 0.889 0.900 1.293	32-57 0.872 0.893 2.441	40-57 0.811 0.844 4.095		
08-49 0.753 0.763 1.376	16-49 1.118 1.105 -1.356	24-49 1.020 1.014 -0.581	32-49 0.945 0.964 2.004	40-49 1.017 1.062 4.369	48-49 1.080 1.026 -4.974	
08-41 1.149 1.134 -1.294	16-41 1.097 1.019 -7.095	24-41 1.034 1.011 -2.260	32-41 1.035 1.000 -3.380	40-41 1.018 1.024 0.662	48-41 1.064 1.081 1.637	56-41 0.940 0.909 -3.242
08-33 1.155 1.160 0.481	16-33 0.984 1.024 4.063	24-33 1.162 1.121 -3.504	32-33 0.975 0.991 1.711	40-33 1.162 1.139 -1.917	48-33 1.028 1.050 2.166	56-33 0.963 1.005 4.290
08-25 1.177 1.175 -0.159	16-25 1.047 1.056 0.807	24-25 1.122 1.098 -2.134	32-25 0.978 0.996 1.824	40-25 1.119 1.117 -0.105	48-25 1.068 1.082 1.358	56-25 0.953 0.993 4.194
08-17 1.068 1.019 -4.581	16-17 1.028 1.045 1.630	24-17 0.994 0.994 -0.094	32-17 1.045 0.977 -6.520	40-17 1.030 1.002 -2.762	48-17 1.070 1.065 -0.493	56-17 0.693 0.685 -1.116
	16-09 1.004 1.002 -0.199	24-09 0.977 1.026 4.983	32-09 0.969 0.971 0.187	40-09 0.996 1.038 4.161	48-09 0.751 0.757 0.775	

xx-xx	String Identification
x.xxx	Measured Average Instrument Response
x.xxx	Calculated Average Instrument Response
x.xxx	Percent error

Figure 3.31
WNP-2 Cycle 4 TIP Predictions, 15473 MWd/MT

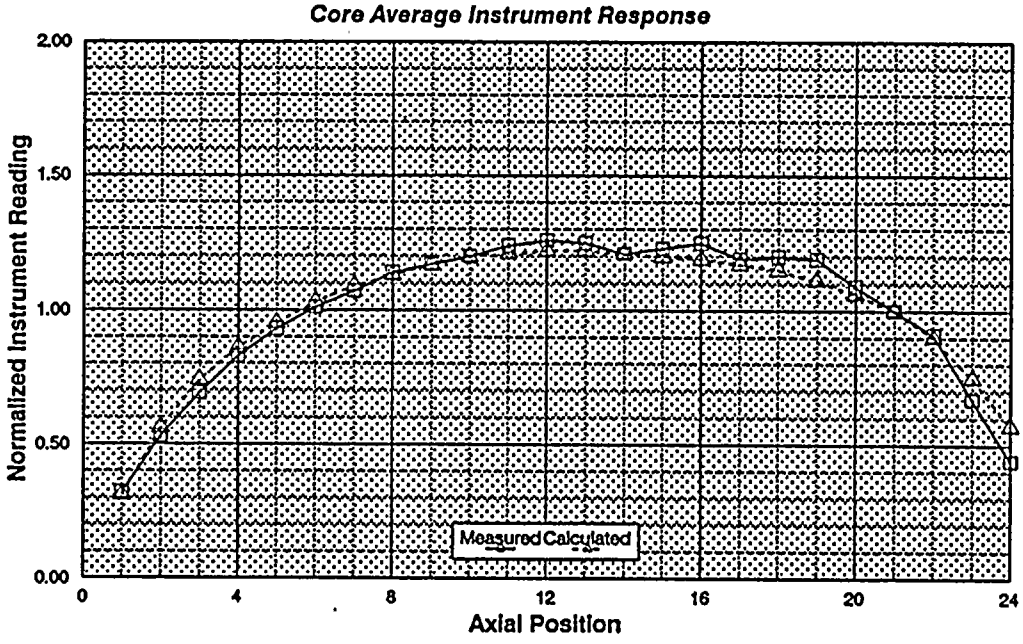

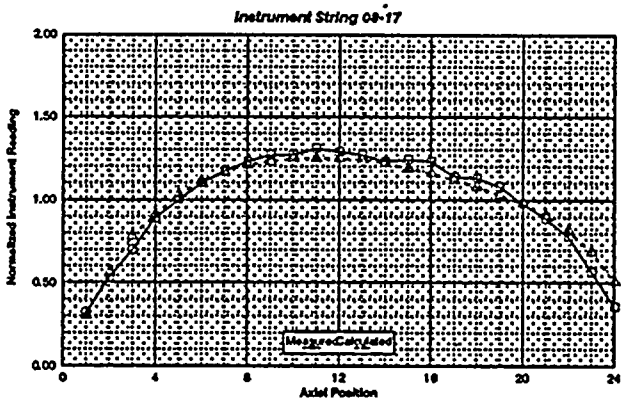

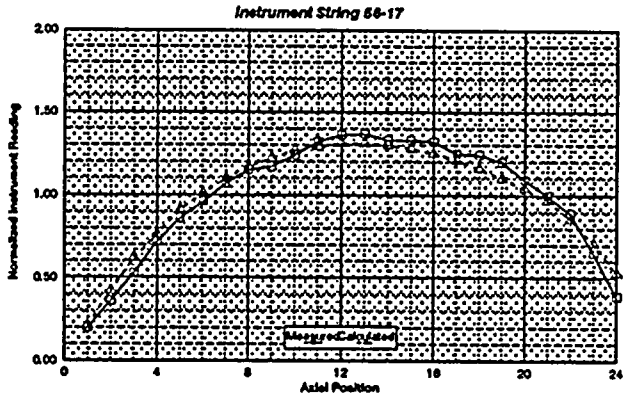

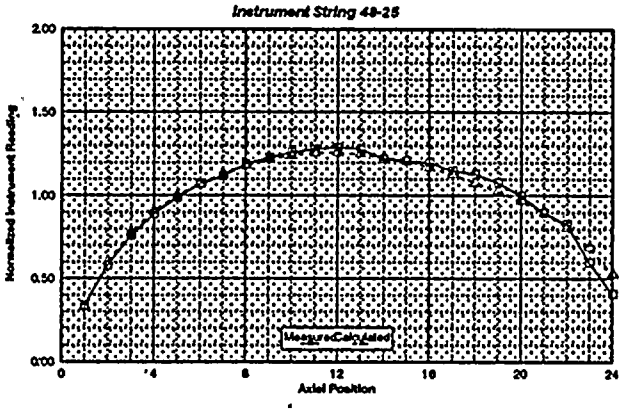

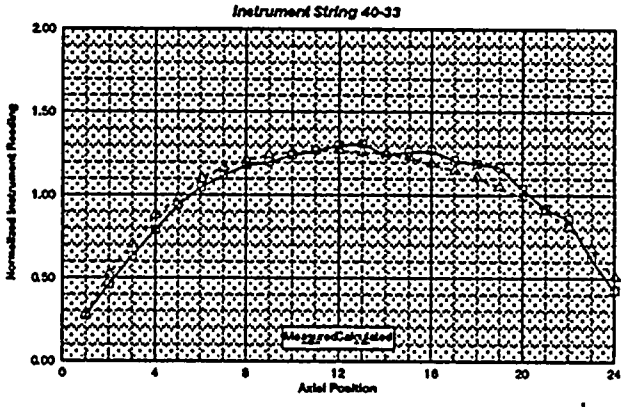

Figure 3.32

WNP-2 Cycle 4 TIP Predictions, 16531 MWd/MT

	16-57	24-57	32-57	40-57		
	0.619	0.886	0.867	0.810		
	0.640	0.901	0.891	0.838		
	3.281	1.660	2.837	3.379		
08-49	16-49	24-49	32-49	40-49	48-49	
0.709	1.116	1.140	0.976	1.130	1.064	
0.727	1.137	1.129	1.004	1.167	1.014	
2.559	1.865	-0.918	2.839	3.278	-4.740	
08-41	16-41	24-41	32-41	40-41	48-41	56-41
1.095	1.212	1.008	1.058	0.977	1.151	0.843
1.096	1.129	0.989	1.007	1.020	1.166	0.836
0.108	-6.846	-1.801	-4.828	4.401	1.273	-0.828
08-33	16-33	24-33	32-33	40-33	48-33	56-33
1.069	0.951	1.043	1.043	1.045	0.969	0.886
1.056	0.972	1.027	1.057	1.002	1.003	0.892
-1.221	2.209	-1.486	1.312	-4.138	3.559	0.706
08-25	16-25	24-25	32-25	40-25	48-25	56-25
1.132	1.076	0.937	1.047	0.941	1.149	0.890
1.110	1.076	0.972	1.035	0.987	1.129	0.900
-1.957	0.038	3.733	-1.110	4.919	-1.763	1.179
08-17	16-17	24-17	32-17	40-17	48-17	56-17
1.011	1.148	1.099	0.988	1.170	1.150	0.653
0.990	1.166	1.076	0.970	1.130	1.135	0.638
-2.037	1.533	-2.115	-1.878	-3.431	-1.273	-2.308
	16-09	24-09	32-09	40-09	48-09	
	1.000	1.045	1.083	1.084	0.728	
	0.992	1.111	1.056	1.098	0.727	
	-0.786	6.248	-2.500	1.280	-0.106	

xx-xx	String Identification
x.xxx	Measured Average Instrument Response
x.xxx	Calculated Average Instrument Response
x.xxx	Percent error

Figure 3.33
WNP-2 Cycle 4 TIP Predictions, 16531 MWd/MT

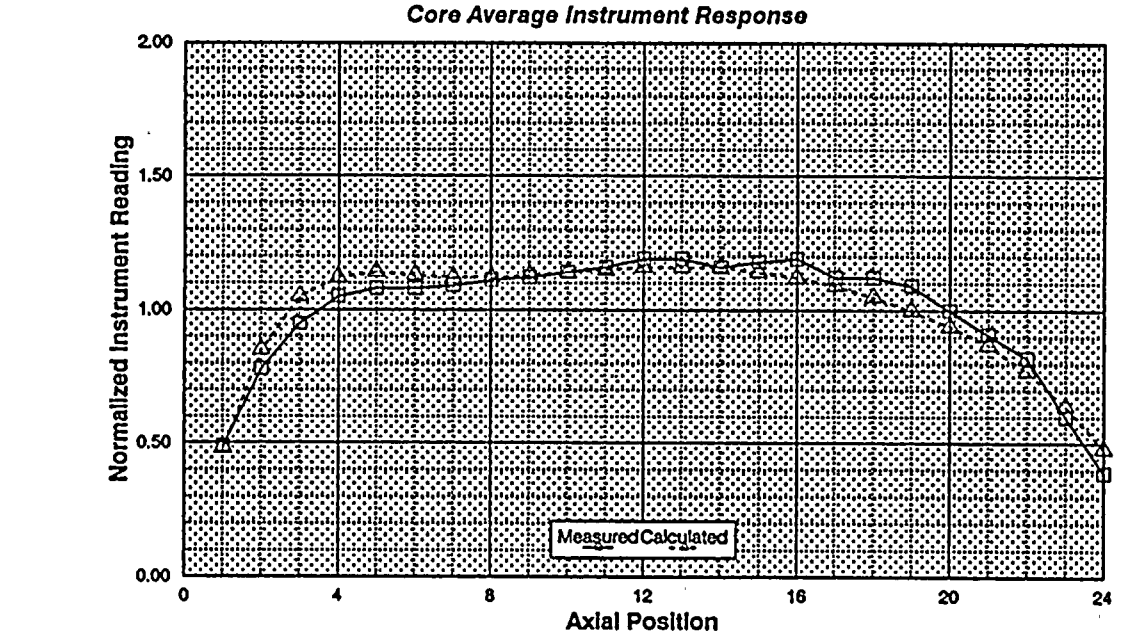

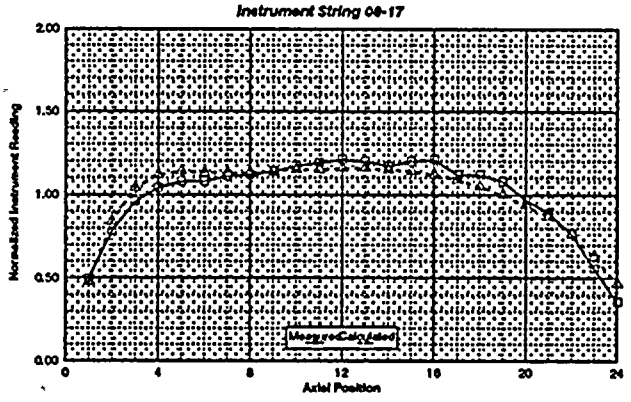

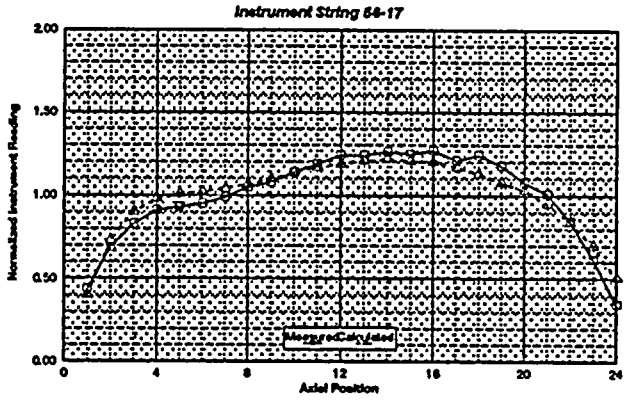

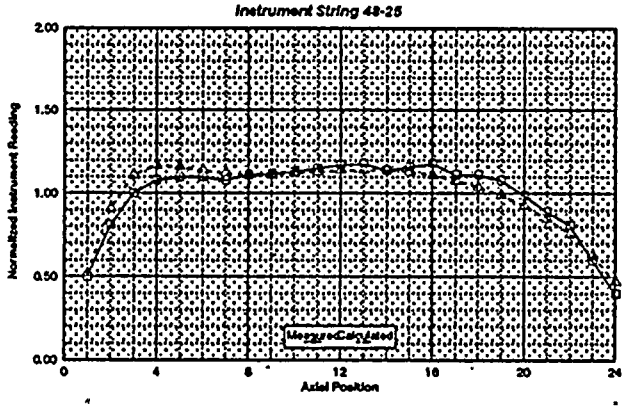

Figure 3.34
Peach Bottom Unit 2 Critical Eigenvalue Calculated by SIMULATE-E

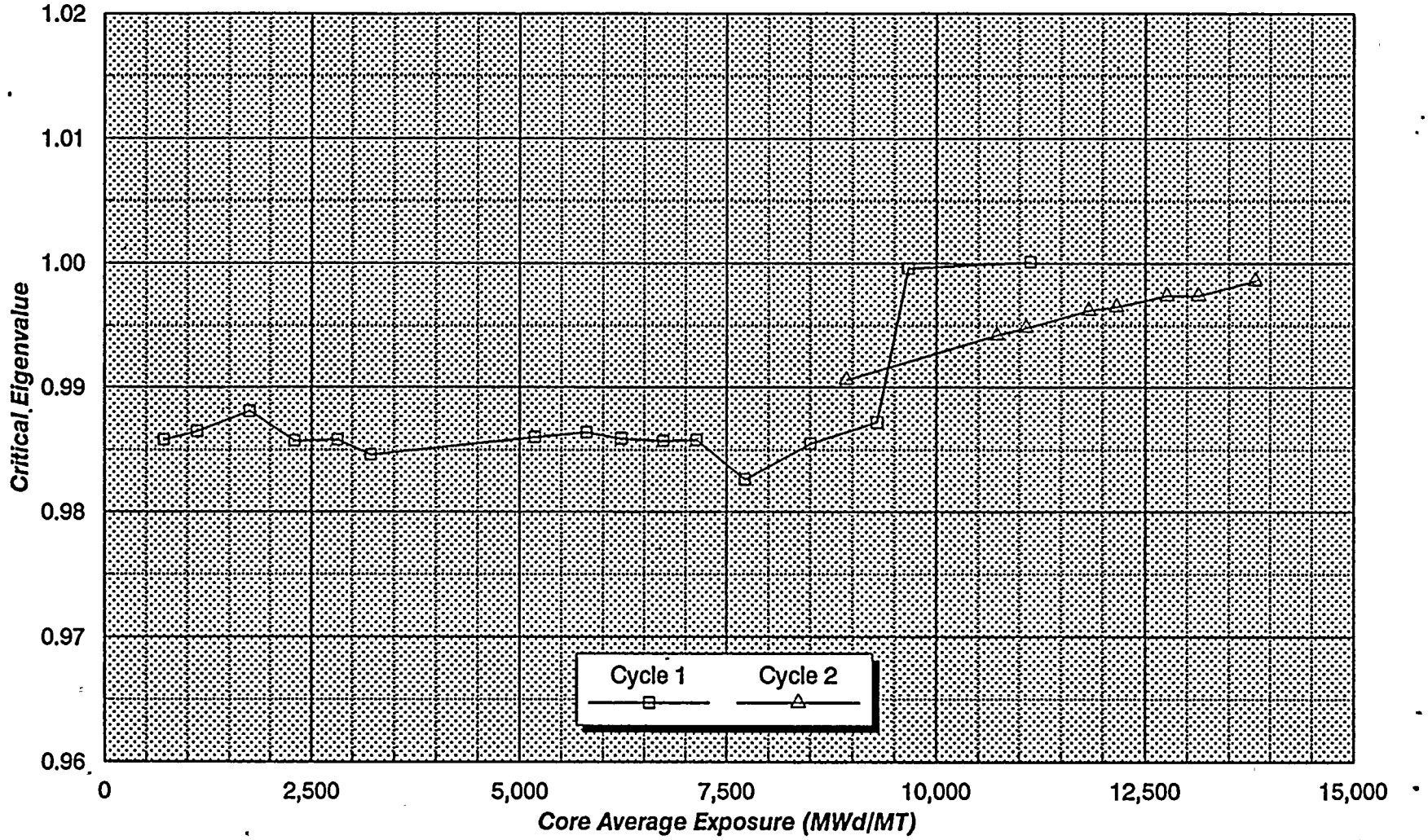

Figure 3.35
Summary of TIP Predictions
Peach Bottom Benchmark

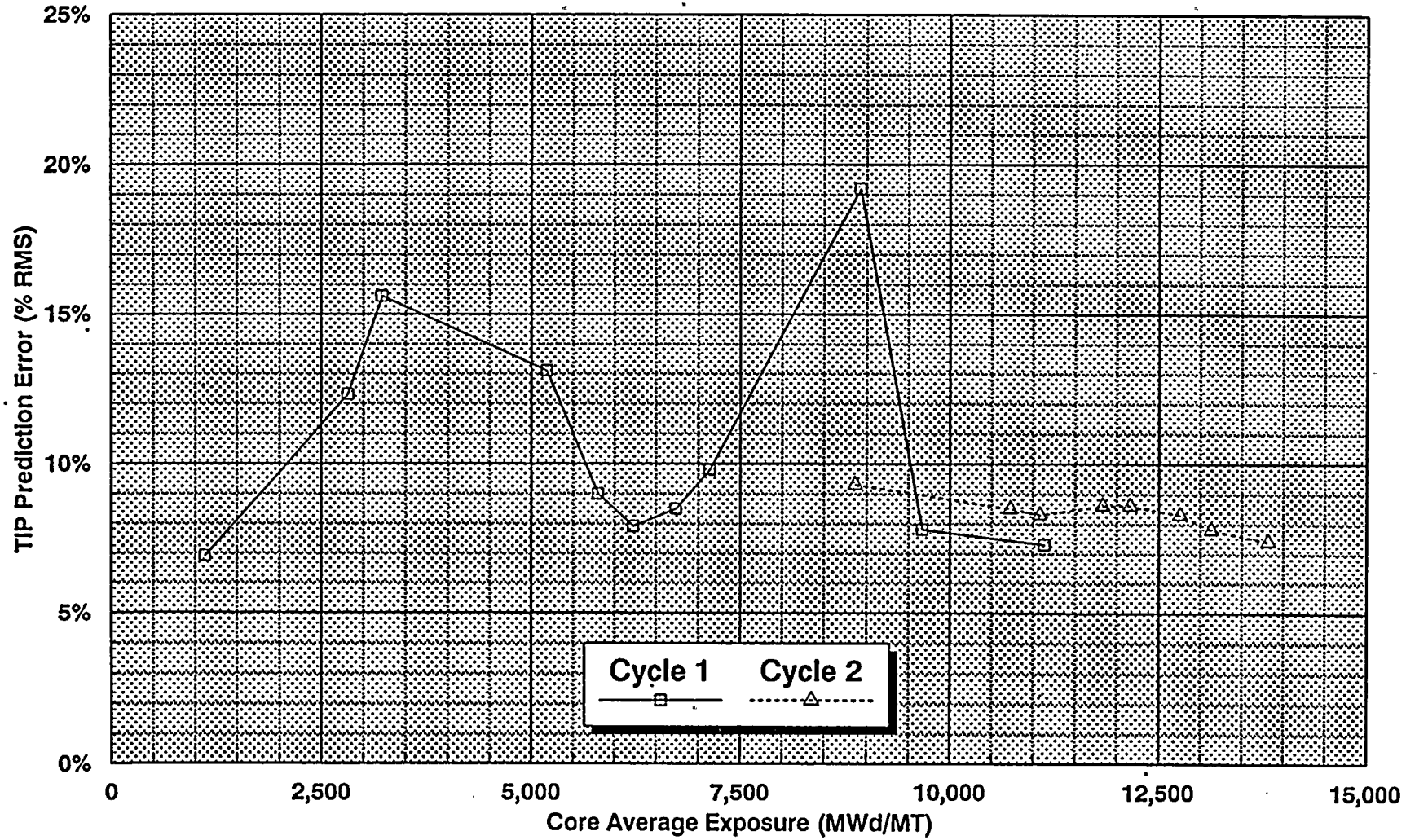

Figure 3.36

Peach Bottom 2 Cycle 1 TIP Predictions, 1113 MWd/MT

	16-57	24-57	32-57	40-57		
	0.597	0.792	0.887	0.787		
	0.625	0.860	0.916	0.804		
	4.683	8.692	3.291	2.260		
08-49	16-49	24-49	32-49	40-49	48-49	
0.697	1.044	1.071	1.096	1.155	0.931	
0.730	1.059	1.083	1.101	1.090	0.942	
4.727	1.439	1.135	0.490	-5.614	1.228	
08-41	16-41	24-41	32-41	40-41	48-41	56-41
1.045	1.139	0.983	1.108	1.080	1.084	0.758
1.051	1.108	1.033	1.076	1.039	1.067	0.800
0.580	-2.744	5.149	-2.965	-3.827	-1.534	5.510
08-33	16-33	24-33	32-33	40-33	48-33	56-33
1.125	1.070	1.101	1.072	1.127	1.098	0.879
1.123	1.104	1.055	1.025	1.072	1.092	0.913
-0.105	3.174	-4.142	-4.394	-4.896	-0.574	3.836
08-25	16-25	24-25	32-25	40-25	48-25	56-25
1.086	1.097	1.111	1.136	1.071	1.117	0.864
1.083	1.083	1.027	1.054	1.040	1.103	0.861
-0.255	-1.288	-7.594	-7.209	-2.849	-1.271	-0.352
08-17	16-17	24-17	32-17	40-17	48-17	56-17
0.944	1.080	1.134	1.086	1.118	1.044	0.622
0.947	1.101	1.105	1.098	1.091	1.066	0.627
0.274	2.033	-2.596	1.182	-2.468	2.144	0.811
	16-09	24-09	32-09	40-09	48-09	
	0.860	1.043	1.109	1.038	0.715	
	0.953	1.095	1.122	1.043	0.730	
	10.921	4.983	1.183	0.476	2.058	

xx-xx	String Identification
x.xxx	Measured Average Instrument Response
x.xxx	Calculated Average Instrument Response
x.xxx	Percent error

Figure 3.37
Peach Bottom 2 Cycle 1 TIP Predictions
1113 MWd/MT

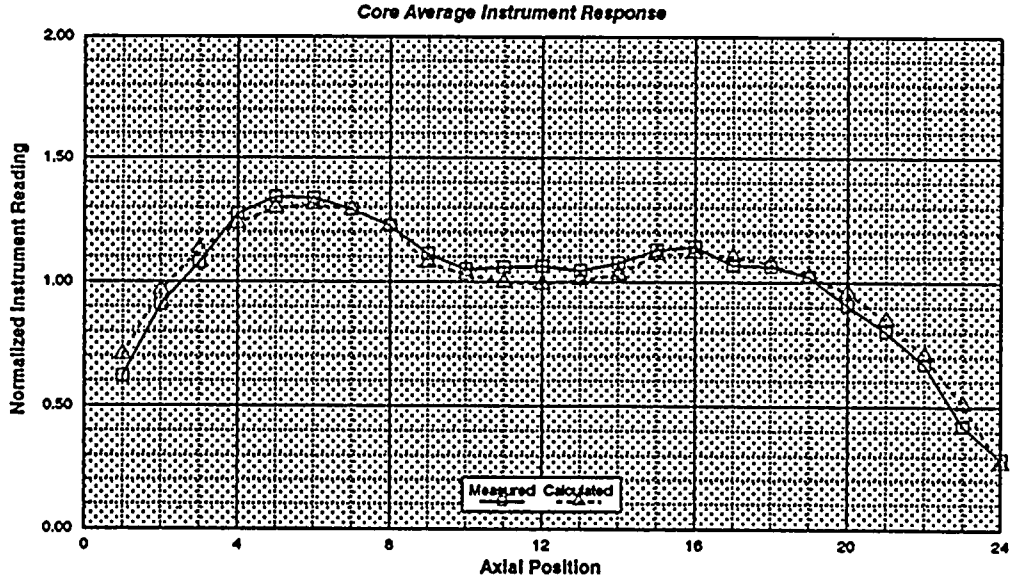

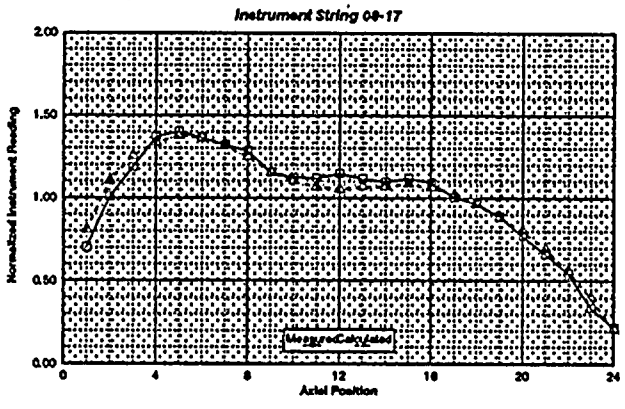

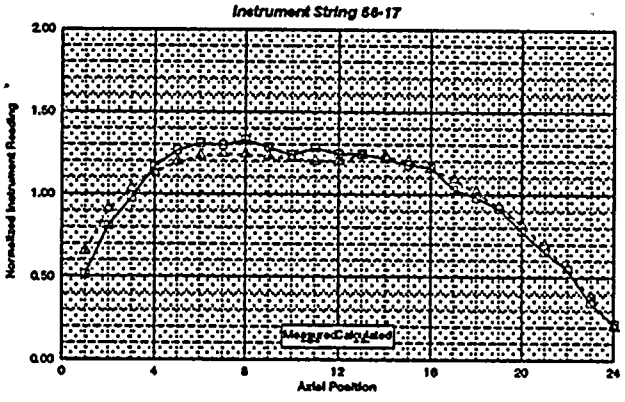

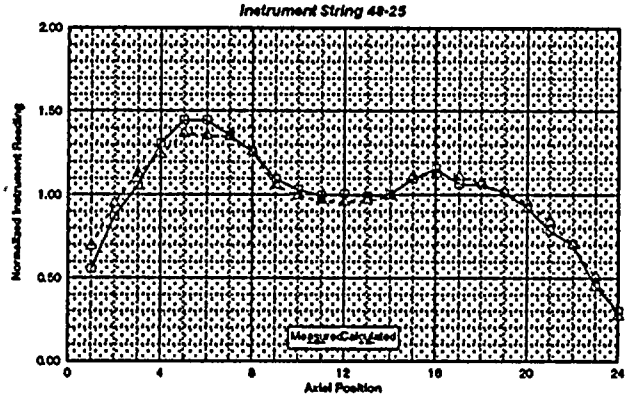

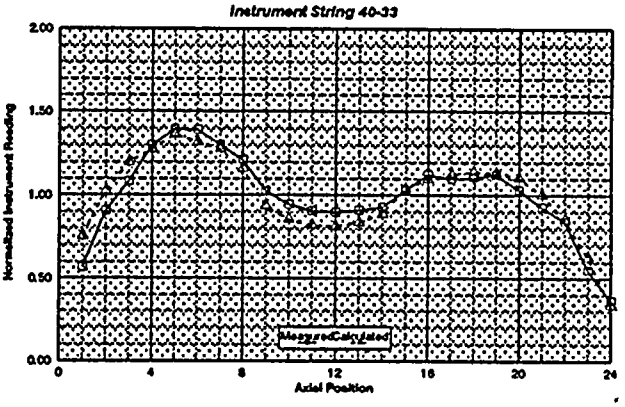

Figure 3.38

Peach Bottom 2 Cycle 1 TIP Predictions, 2816 MWd/MT

	16-57	24-57	32-57	40-57		
	0.625	0.790	0.830	0.844		
	0.677	0.886	0.902	0.876		
	8.330	12.126	8.782	3.767		
08-49	16-49	24-49	32-49	40-49	48-49	
0.703	1.064	1.020	1.018	1.126	0.933	
0.766	1.064	1.025	1.009	1.065	0.972	
9.000	0.034	0.531	-0.912	-5.437	4.086	
08-41	16-41	24-41	32-41	40-41	48-41	56-41
1.090	1.047	1.022	1.109	1.063	1.092	0.830
1.109	1.019	1.036	1.056	0.994	1.066	0.903
1.722	-2.682	1.379	-4.795	-6.432	-2.400	8.819
08-33	16-33	24-33	32-33	40-33	48-33	56-33
1.063	1.108	1.059	1.046	1.140	1.075	0.890
1.106	1.095	0.999	0.971	1.055	1.065	0.963
4.102	-1.159	-5.590	-7.124	-7.500	-0.913	8.182
08-25	16-25	24-25	32-25	40-25	48-25	56-25
1.120	1.069	1.166	1.148	1.088	1.108	0.914
1.130	1.037	1.033	1.044	1.010	1.075	0.947
0.911	-2.980	-11.426	-9.088	-7.136	-2.932	3.662
08-17	16-17	24-17	32-17	40-17	48-17	56-17
0.989	1.042	1.045	1.033	1.106	1.060	0.667
1.000	1.055	1.023	1.020	1.048	1.073	0.693
1.196	1.290	-2.099	-1.228	-5.281	1.226	3.863
	16-09	24-09	32-09	40-09	48-09	
	0.880	1.027	1.057	1.113	0.783	
	1.010	1.111	1.103	1.118	0.788	
	14.816	8.142	4.390	0.490	0.650	

xx-xx	String Identification
x.xxx	Measured Average Instrument Response
x.xxx	Calculated Average Instrument Response
x.xxx	Percent error

Figure 3.39
Peach Bottom 2 Cycle 1 TIP Predictions
2816 MWd/MT

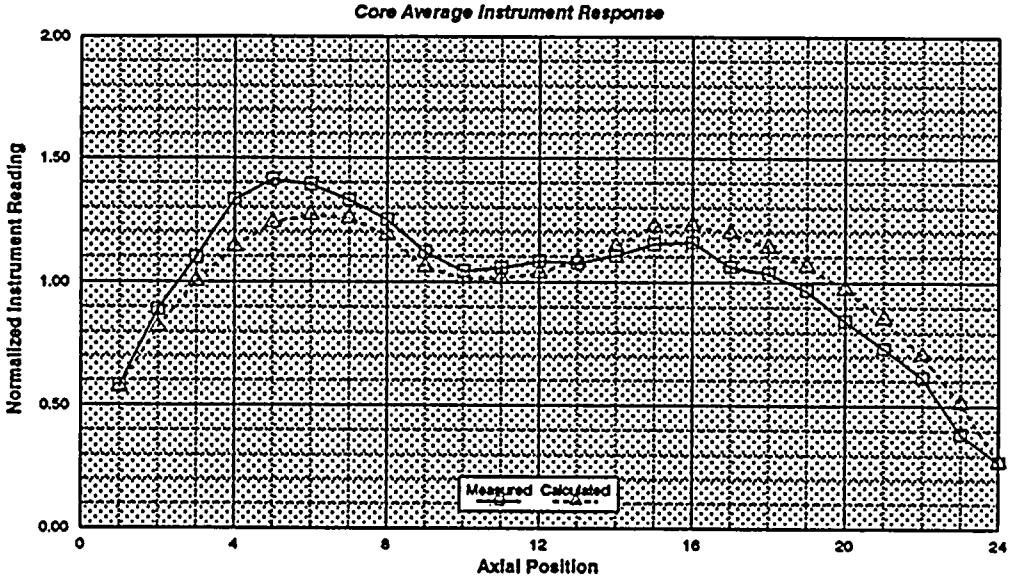

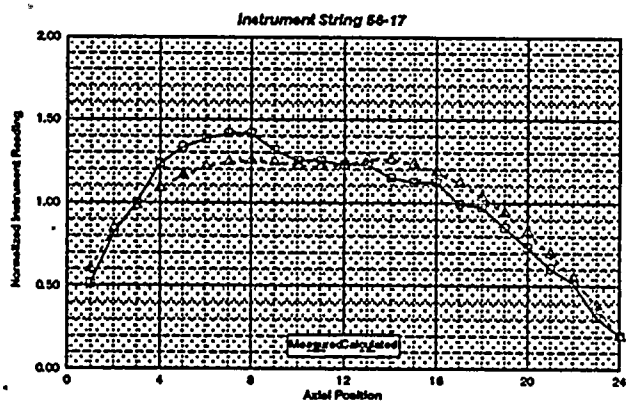

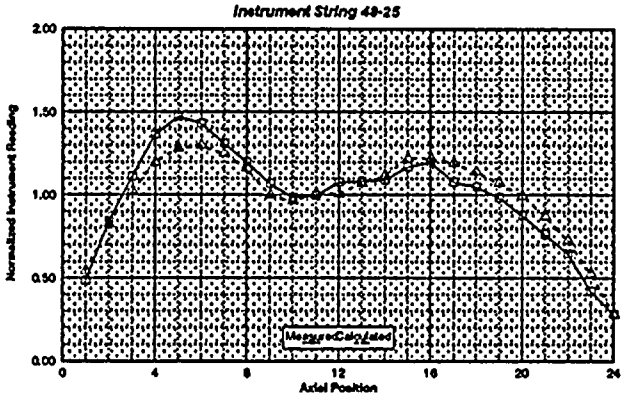

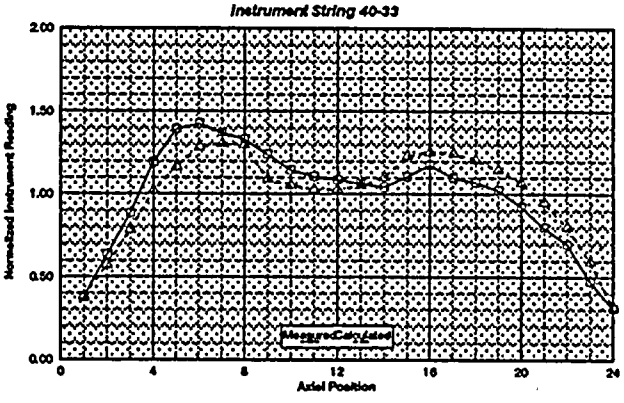

Figure 3.40

Peach Bottom 2 Cycle 1 TIP Predictions, 5178 MWd/MT

	16-57	24-57	32-57	40-57		
	0.656	0.784	0.802	0.832		
	0.705	0.881	0.884	0.877		
	7.347	12.470	10.281	5.484		
08-49	16-49	24-49	32-49	40-49	48-49	
0.758	1.042	1.051	1.067	1.144	0.867	
0.808	1.058	1.070	1.051	1.066	0.946	
6.586	1.481	1.752	-1.536	-6.757	9.062	
08-41	16-41	24-41	32-41	40-41	48-41	56-41
1.106	1.086	1.009	1.077	1.084	1.088	0.799
1.125	1.049	1.007	1.010	1.008	1.067	0.878
1.678	-3.382	-0.236	-6.251	-7.024	-1.987	9.898
08-33	16-33	24-33	32-33	40-33	48-33	56-33
1.085	1.023	1.060	1.097	1.083	1.097	0.795
1.117	1.037	1.014	1.016	1.013	1.052	0.887
2.909	1.315	-4.343	-7.417	-6.464	-4.074	11.541
08-25	16-25	24-25	32-25	40-25	48-25	56-25
1.144	1.069	1.143	1.117	1.092	1.101	0.851
1.139	1.047	1.005	1.012	1.008	1.070	0.883
-0.436	-2.001	-12.058	-9.398	-7.678	-2.754	3.758
08-17	16-17	24-17	32-17	40-17	48-17	56-17
1.007	1.048	1.086	1.075	1.107	1.059	0.691
1.041	1.060	1.046	1.033	1.048	1.058	0.705
3.388	1.173	-3.698	-3.894	-5.373	-0.114	1.929
	16-09	24-09	32-09	40-09	48-09	
	0.882	1.048	1.077	1.111	0.800	
	1.040	1.138	1.114	1.122	0.807	
	17.956	8.597	3.436	1.041	0.815	

xx-xx	String Identification
x.xxx	Measured Average Instrument Response
x.xxx	Calculated Average Instrument Response
x.xxx	Percent error

Figure 3.41
Peach Bottom 2 Cycle 1 TIP Predictions
5178 MWd/MT

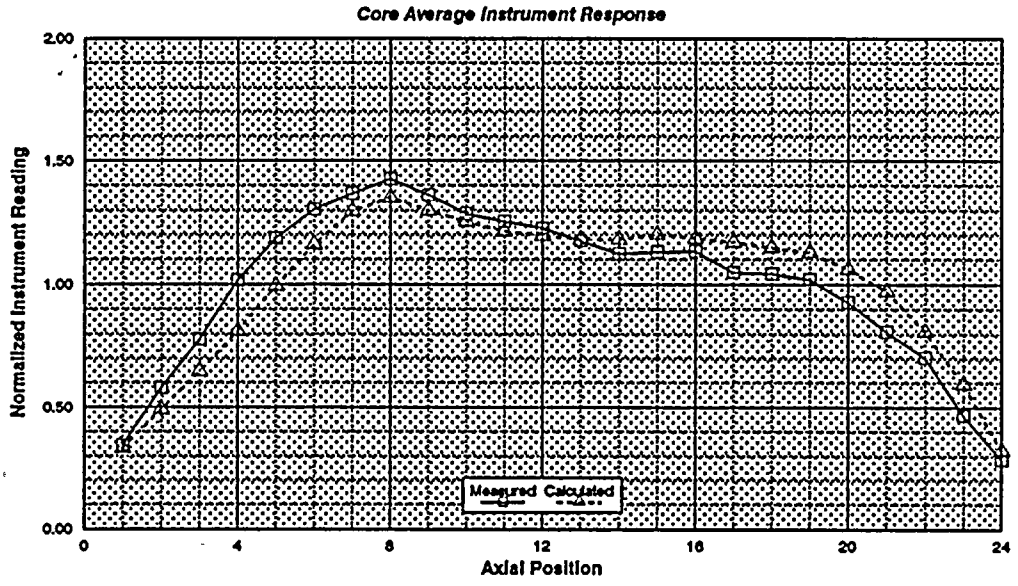

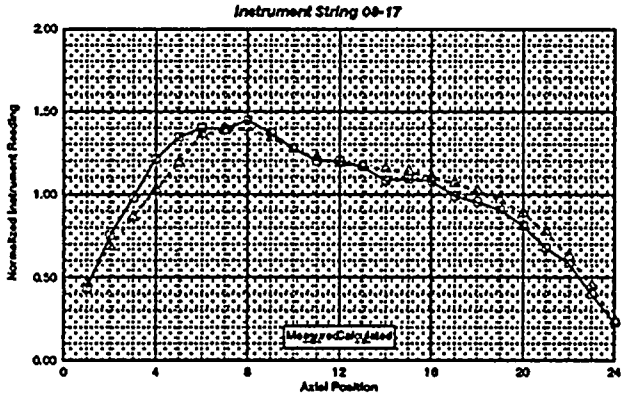

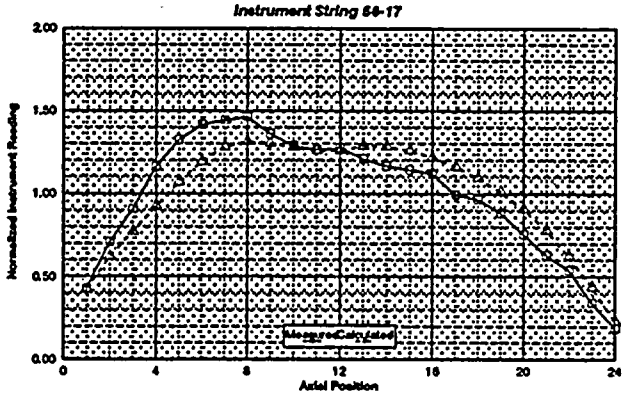

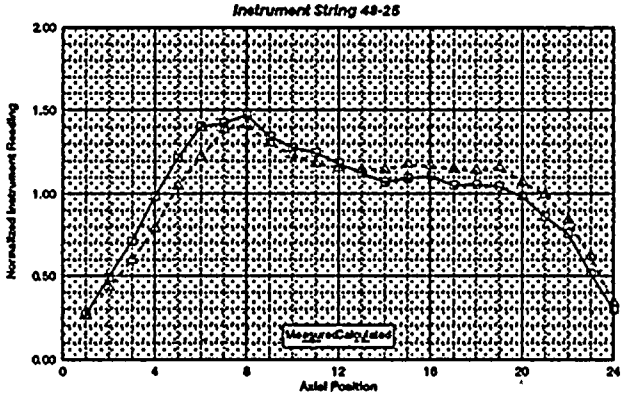

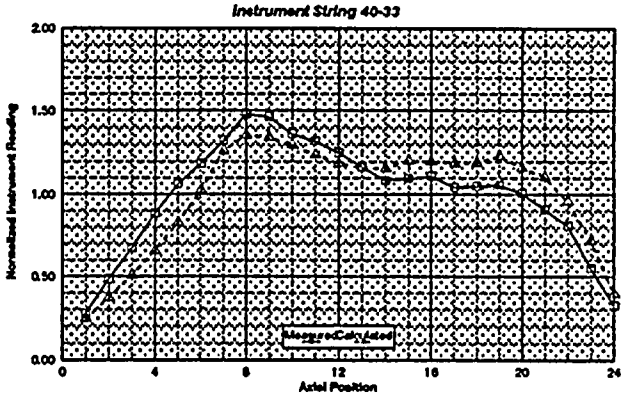

Figure 3.42

Peach Bottom 2 Cycle 1 TIP Predictions, 5800 MWd/MT

	16-57	24-57	32-57	40-57		
	0.654	0.768	0.793	0.827		
	0.692	0.862	0.870	0.860		
	5.890	12.294	9.751	4.000		
08-49	16-49	24-49	32-49	40-49	48-49	
0.741	1.031	1.046	1.061	1.139	0.853	
0.796	1.045	1.069	1.062	1.057	0.934	
7.331	1.358	2.220	0.131	-7.186	9.468	
08-41	16-41	24-41	32-41	40-41	48-41	56-41
1.083	1.090	1.003	1.101	1.106	1.071	0.789
1.100	1.058	1.035	1.041	1.030	1.059	0.862
1.589	-2.914	3.133	-5.510	-6.819	-1.064	9.245.
08-33	16-33	24-33	32-33	40-33	48-33	56-33
1.078	1.039	1.062	1.111	1.104	1.110	0.797
1.102	1.069	1.029	1.030	1.044	1.065	0.876
2.232	2.926	-3.053	-7.273	-5.421	-4.036	9.808
08-25	16-25	24-25	32-25	40-25	48-25	56-25
1.139	1.080	1.146	1.123	1.120	1.101	0.839
1.118	1.070	1.024	1.027	1.036	1.072	0.866
-1.849	-0.944	-10.606	-8.522	-7.499	-2.640	3.293
08-17	16-17	24-17	32-17	40-17	48-17	56-17
0.989	1.045	1.114	1.102	1.122	1.062	0.689
1.023	1.059	1.067	1.066	1.057	1.046	0.694
3.463	1.363	-4.160	-3.211	-5.815	-1.495	0.815
	16-09	24-09	32-09	40-09	48-09	
	0.872	1.043	1.075	1.094	0.791	
	1.020	1.116	1.098	1.097	0.794	
	17.023	6.978	2.148	0.256	0.396	

xx-xx	String Identification
x.xxx	Measured Average Instrument Response
x.xxx	Calculated Average Instrument Response
x.xxx	Percent error

Figure 3.43
Peach Bottom 2 Cycle 1 TIP Predictions
5800 MWd/MT

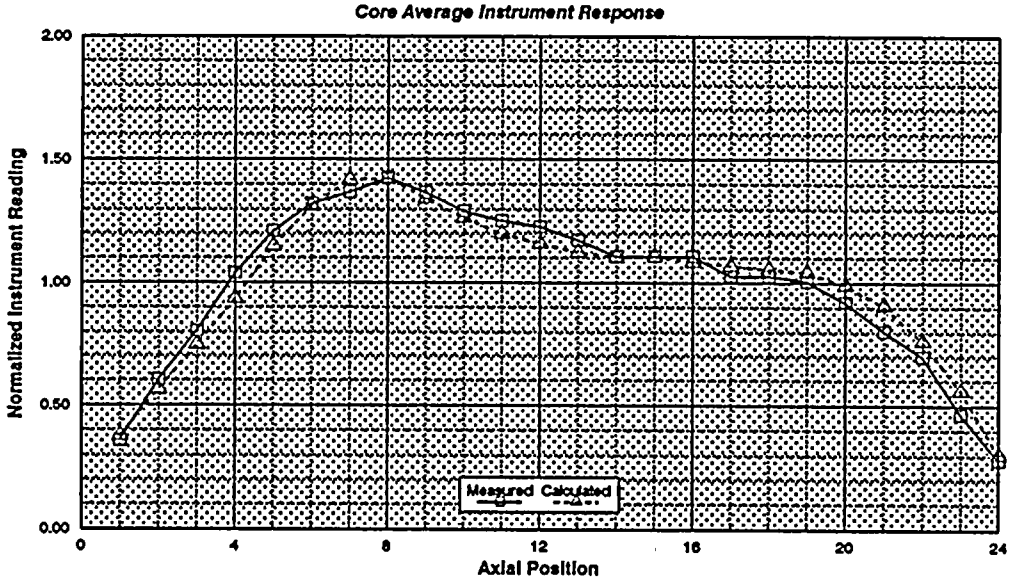

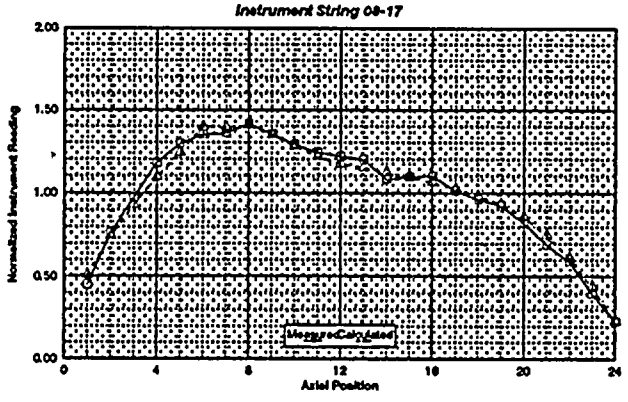

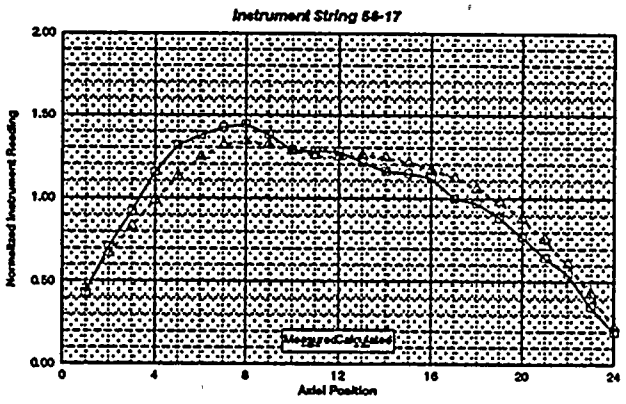

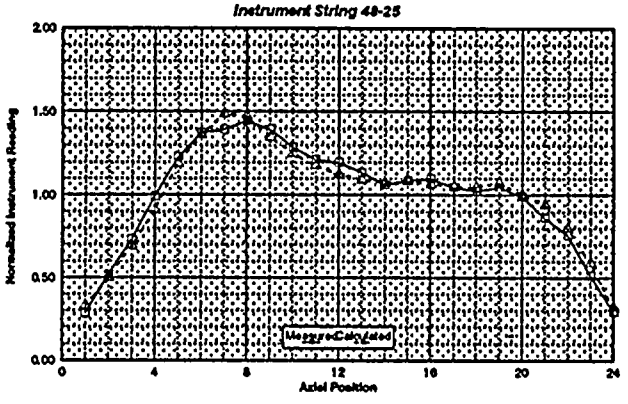

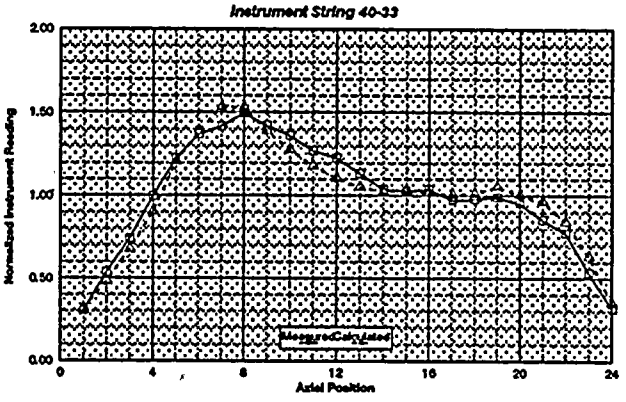

Figure 3.44

Peach Bottom 2 Cycle 1 TIP Predictions, 6731 MWd/MT

	16-57 0.667 0.710 6.571	24-57 0.802 0.880 9.779	32-57 0.842 0.905 7.521	40-57 0.880 0.894 1.564		
08-49 0.778 0.842 8.252	16-49 1.126 1.110 -1.405	24-49 1.085 1.077 -0.746	32-49 1.072 1.082 0.867	40-49 1.153 1.072 -7.024	48-49 0.938 1.025 9.307	
08-41 1.070 1.061 -0.882	16-41 1.080 1.035 -4.246	24-41 1.017 1.078 6.033	32-41 1.147 1.115 -2.757	40-41 1.097 1.046 -4.615	48-41 0.982 0.995 1.324	56-41 0.815 0.884 8.428
08-33 1.009 1.013 0.415	16-33 0.977 0.989 1.213	24-33 1.087 1.058 -2.727	32-33 1.127 1.084 -3.835	40-33 1.083 1.026 -5.257	48-33 0.941 0.905 -3.848	56-33 0.850 0.904 6.339
08-25 1.084 1.035 -4.492	16-25 1.040 1.006 -3.292	24-25 1.162 1.063 -8.522	32-25 1.166 1.089 -6.675	40-25 1.117 1.035 -7.366	48-25 0.958 0.939 -2.046	56-25 0.847 0.875 3.320
08-17 1.001 1.024 2.345	16-17 1.050 1.067 1.557	24-17 1.122 1.093 -2.618	32-17 1.164 1.132 -2.762	40-17 1.112 1.054 -5.219	48-17 1.081 1.063 -1.730	56-17 0.678 0.699 3.153
	16-09 0.878 1.031 17.438	24-09 0.996 1.064 6.793	32-09 1.027 1.049 2.084	40-09 1.087 1.072 -1.329	48-09 0.805 0.824 2.282	

xx-xx	String Identification
x.xxx	Measured Average Instrument Response
x.xxx	Calculated Average Instrument Response
x.xxx	Percent error

Figure 3.45
Peach Bottom 2 Cycle 1 TIP Predictions
6731 MWd/MT

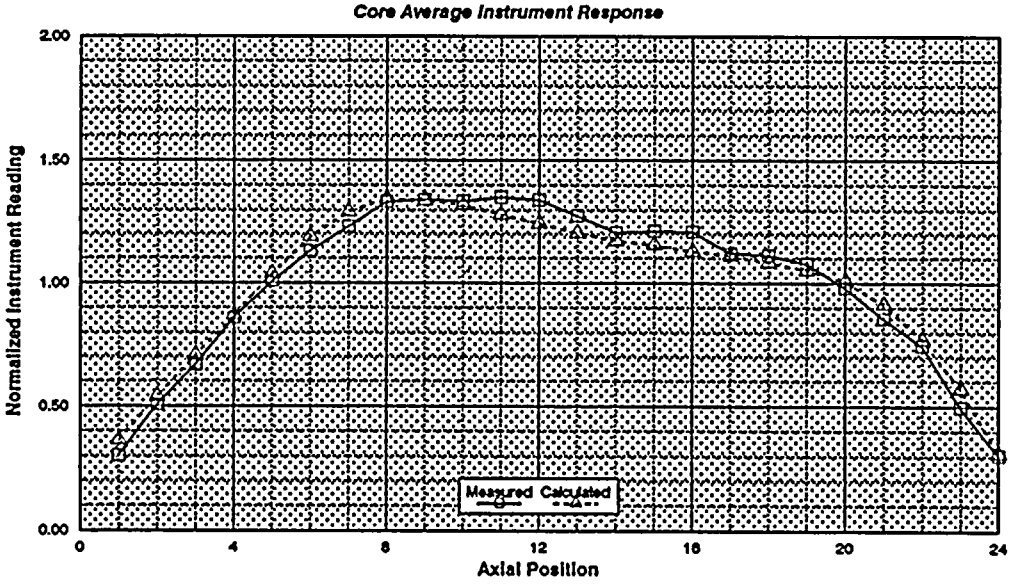

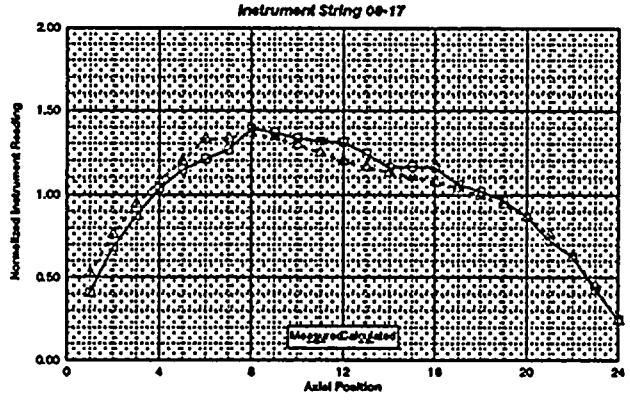

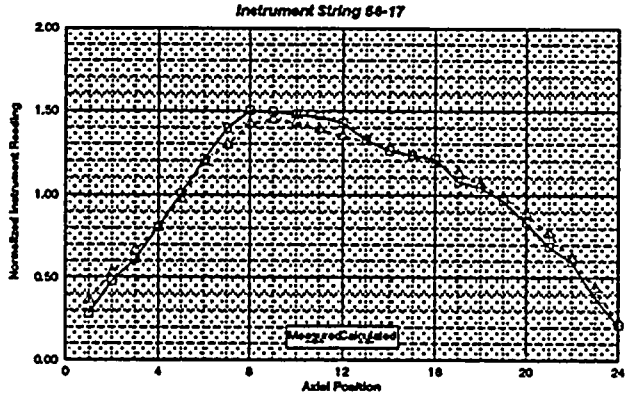

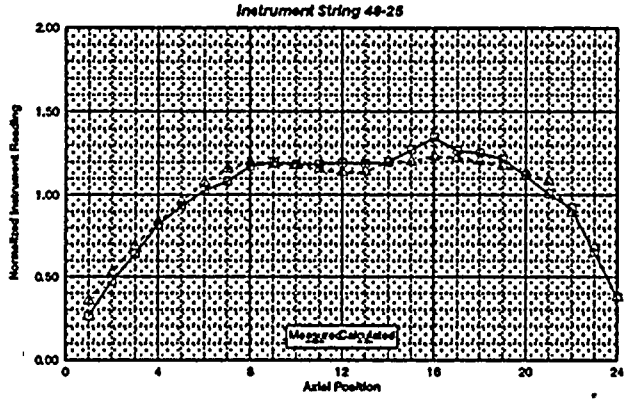

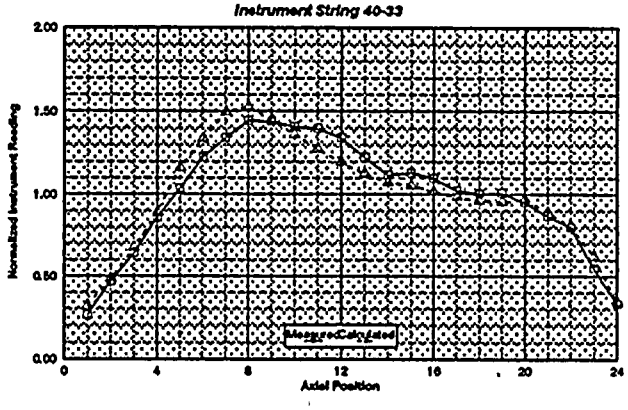

Figure 3.46

Peach Bottom 2 Cycle 1 TIP Predictions, 11133 MWd/MT

	16-57	24-57	32-57	40-57		
	0.661	0.808	0.826	0.855		
	0.588	0.796	0.840	0.773		
	-11.072	-1.413	1.739	-9.620		
08-49	16-49	24-49	32-49	40-49	48-49	
0.745	1.048	1.074	1.111	1.119	0.895	
0.679	1.007	1.083	1.106	1.059	0.883	
-8.811	-3.914	0.863	-0.446	-5.369	-1.315	
08-41	16-41	24-41	32-41	40-41	48-41	56-41
1.045	1.116	1.036	1.067	1.140	1.053	0.816
0.993	1.130	1.147	1.114	1.155	1.079	0.783
-4.994	1.268	10.707	4.429	1.326	2.556	-4.022
08-33	16-33	24-33	32-33	40-33	48-33	56-33
1.051	1.029	1.044	1.120	1.151	1.118	0.859
1.071	1.164	1.126	1.130	1.134	1.149	0.852
1.861	13.189	7.806	0.902	-1.437	2.770	-0.827
08-25	16-25	24-25	32-25	40-25	48-25	56-25
1.043	1.101	1.168	1.115	1.179	1.119	0.782
1.042	1.156	1.145	1.119	1.158	1.117	0.806
-0.150	5.000	-1.985	0.363	-1.763	-0.191	3.123
08-17	16-17	24-17	32-17	40-17	48-17	56-17
0.908	1.108	1.096	1.096	1.106	1.062	0.652
0.890	1.090	1.135	1.133	1.124	1.021	0.596
-1.980	-1.597	3.626	3.356	1.704	-3.921	-8.589
	16-09	24-09	32-09	40-09	48-09	
	0.861	1.012	1.051	0.989	0.766	
	0.882	1.028	1.053	0.983	0.679	
	2.362	1.565	0.153	-0.588	-11.310	

xx-xx	String Identification
x.xxx	Measured Average Instrument Response
x.xxx	Calculated Average Instrument Response
x.xxx	Percent error

Figure 3.47
Peach Bottom 2 Cycle 1 TIP Predictions
11133 MWd/MT

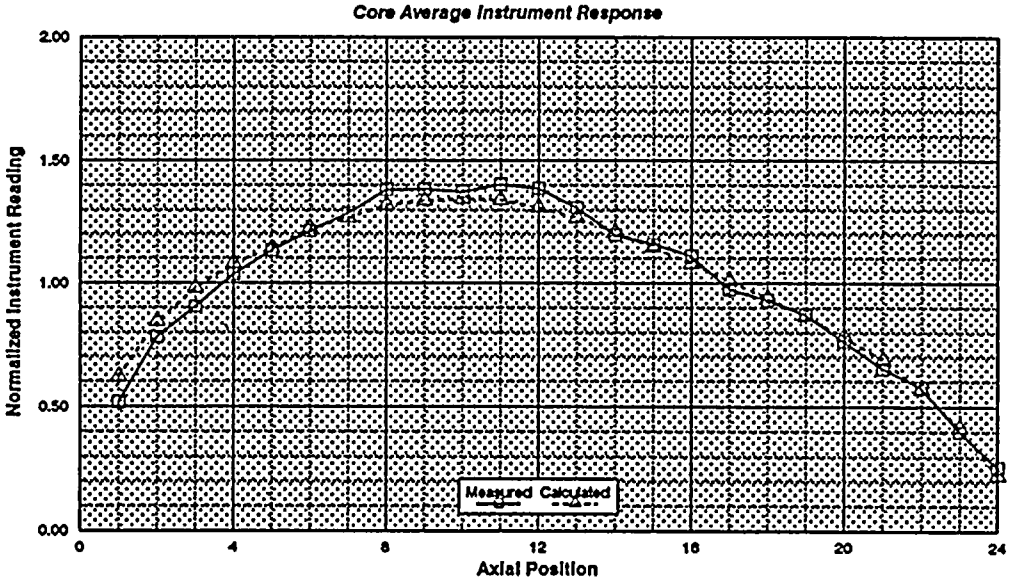

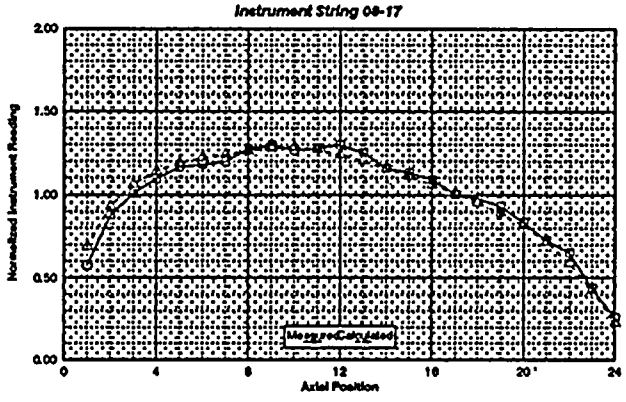

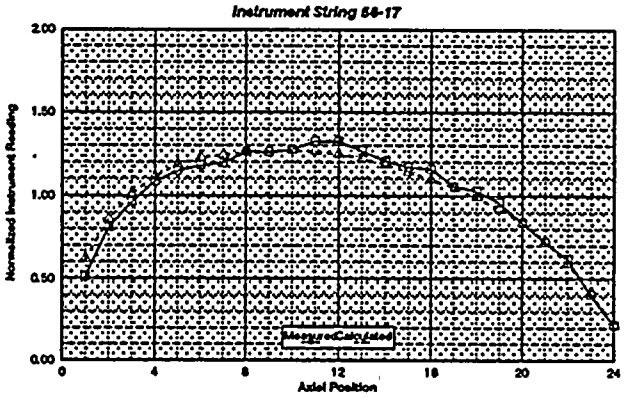

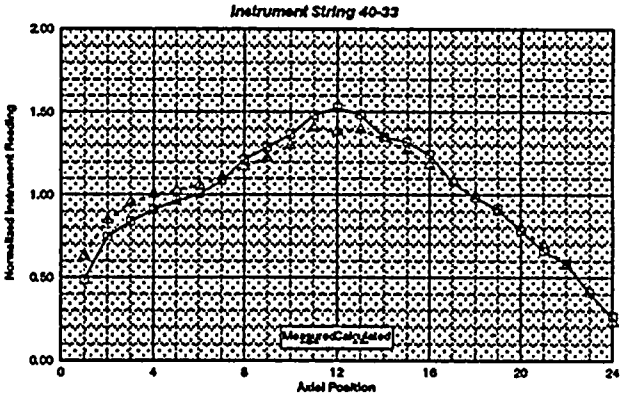

Figure 3.48

Peach Bottom 2 Cycle 2 TIP Predictions, 10726 MWd/MT

	16-57	24-57	32-57	40-57		
	0.770	0.934	0.906	1.022		
	0.721	0.966	0.967	0.908		
	-6.329	3.410	6.743	-11.189		
08-49	16-49	24-49	32-49	40-49	48-49	
0.909	1.010	1.012	1.043	1.051	0.982	
0.786	1.093	1.052	1.030	1.082	1.023	
-13.490	8.272	3.934	-1.178	2.959	4.087	
08-41	16-41	24-41	32-41	40-41	48-41	56-41
1.123	1.012	1.001	1.045	0.999	1.107	1.028
1.075	1.033	1.008	1.029	0.998	1.084	0.910
-4.335	2.119	0.673	-1.521	-0.086	-2.047	-11.464
08-33	16-33	24-33	32-33	40-33	48-33	56-33
1.024	0.923	0.981	1.084	1.063	0.991	0.916
1.056	1.007	1.025	1.056	1.030	1.046	0.970
3.213	9.066	4.503	-2.618	-3.044	5.590	5.920
08-25	16-25	24-25	32-25	40-25	48-25	56-25
1.071	1.028	1.005	1.057	0.970	1.072	0.977
1.070	1.018	1.022	1.029	1.007	1.054	0.969
-0.088	-0.896	-1.766	-2.631	3.730	-1.708	-0.832
08-17	16-17	24-17	32-17	40-17	48-17	56-17
0.982	1.044	1.026	1.022	1.015	1.128	0.771
0.983	1.063	1.018	1.005	1.038	1.093	0.728
0.139	1.897	-0.757	-1.674	2.258	-3.046	-5.658
	16-09	24-09	32-09	40-09	48-09	
	0.900	0.963	1.043	1.056	0.935	
	0.977	1.060	1.041	1.074	0.793	
	8.563	10.164	-0.197	1.703	-15.274	

xx-xx	String Identification
x.xxx	Measured Average Instrument Response
x.xxx	Calculated Average Instrument Response
x.xxx	Percent error

Figure 3.49
Peach Bottom 2 Cycle 2 TIP Predictions
10726 MWd/MT

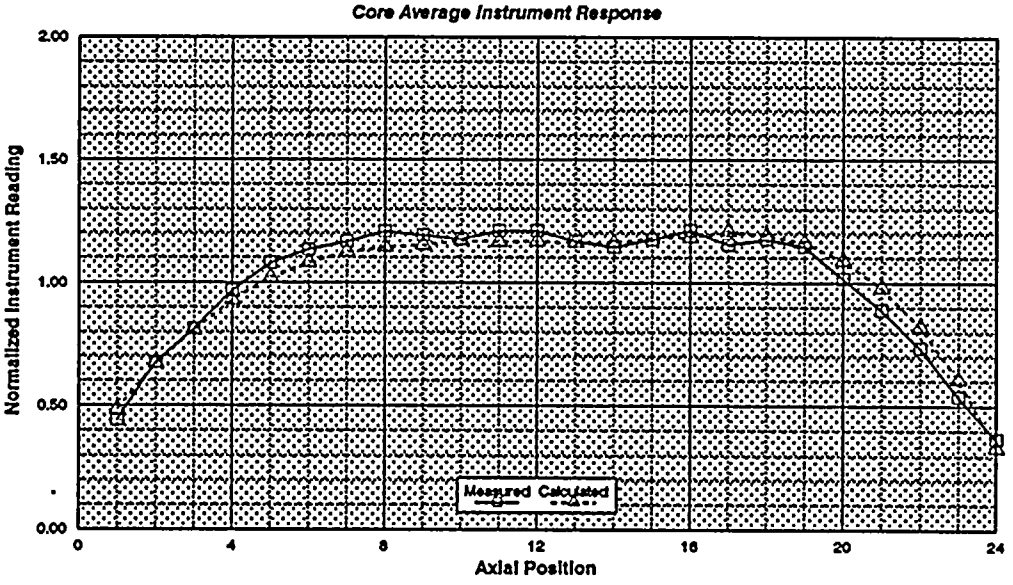

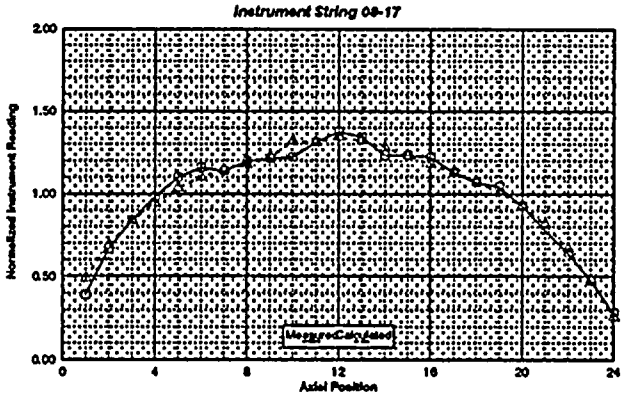

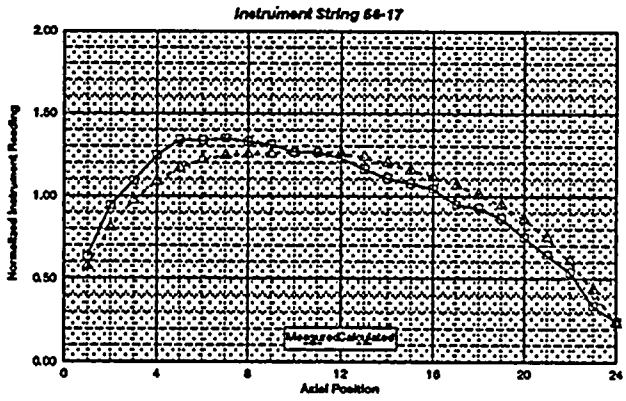

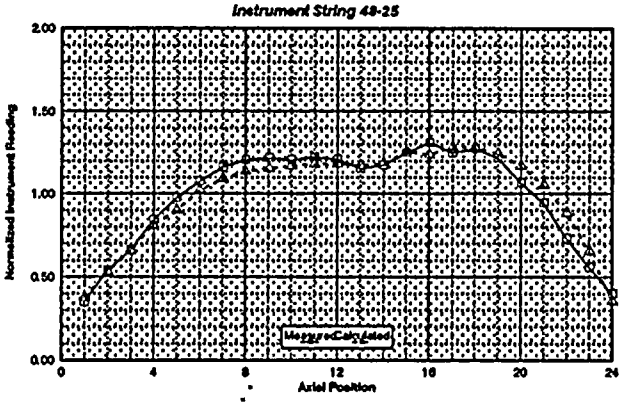

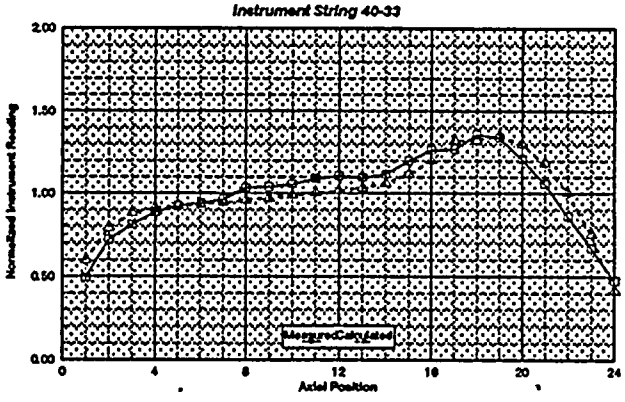

Figure 3.50

Peach Bottom 2 Cycle 2 TIP Predictions, 11078 MWd/MT

	16-57 0.766 0.709 -7.367	24-57 0.914 0.941 2.903	32-57 0.870 0.921 5.854	40-57 1.029 0.899 -12.622		
08-49 0.896 0.766 -14.495	16-49 1.033 1.096 6.146	24-49 1.043 1.065 2.104	32-49 1.042 1.039 -0.257	40-49 1.083 1.098 1.383	48-49 0.952 0.997 4.720	
08-41 1.145 1.064 -7.080	16-41 1.022 1.038 1.569	24-41 0.995 1.037 4.202	32-41 1.089 1.089 0.037	40-41 1.024 1.031 0.705	48-41 1.061 1.055 -0.533	56-41 1.001 0.892 -10.868
08-33 1.056 1.065 0.887	16-33 0.915 1.000 9.261	24-33 1.018 1.064 4.567	32-33 1.042 1.047 0.528	40-33 1.104 1.081 -2.124	48-33 0.975 1.028 5.455	56-33 0.883 0.949 7.480
08-25 1.100 1.074 -2.437	16-25 1.016 1.018 0.165	24-25 1.017 1.062 4.398	32-25 1.033 1.031 -0.177	40-25 1.007 1.045 3.780	48-25 1.041 1.020 -2.024	56-25 0.950 0.947 -0.316
08-17 0.995 0.968 -2.663	16-17 1.076 1.082 0.543	24-17 1.055 1.056 0.098	32-17 1.082 1.067 -1.445	40-17 1.042 1.058 1.478	48-17 1.086 1.062 -2.255	56-17 0.749 0.704 -6.074
	16-09 0.913 0.970 6.136	24-09 0.966 1.049 8.624	32-09 0.977 0.989 1.259	40-09 1.055 1.067 1.189	48-09 0.881 0.759 -13.846	

xx-xx	String Identification
x.xxx	Measured Average Instrument Response
x.xxx	Calculated Average Instrument Response
x.xxx	Percent error

Figure 3.51
Peach Bottom 2 Cycle 2 TIP Predictions
11078 MWd/MT

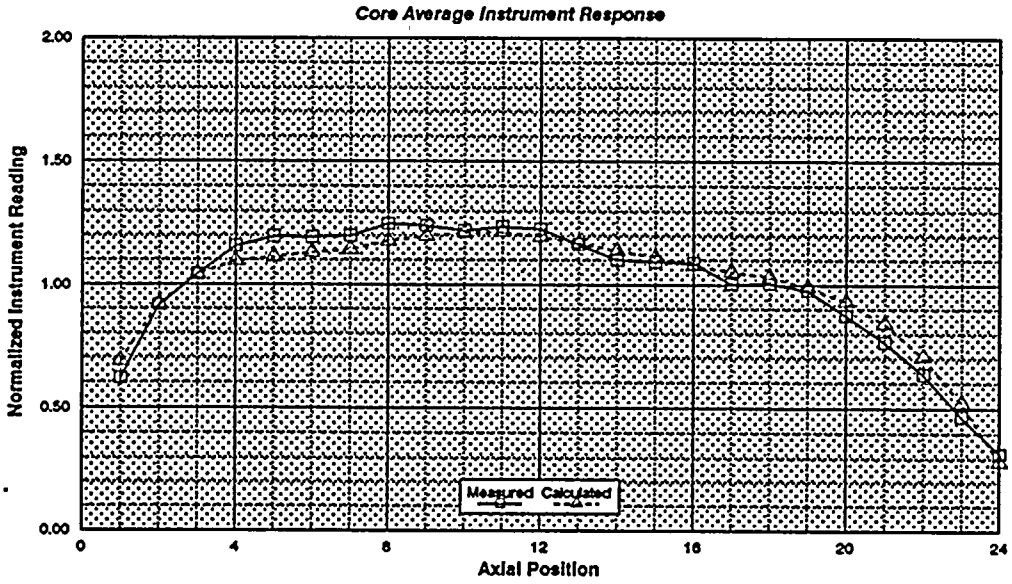

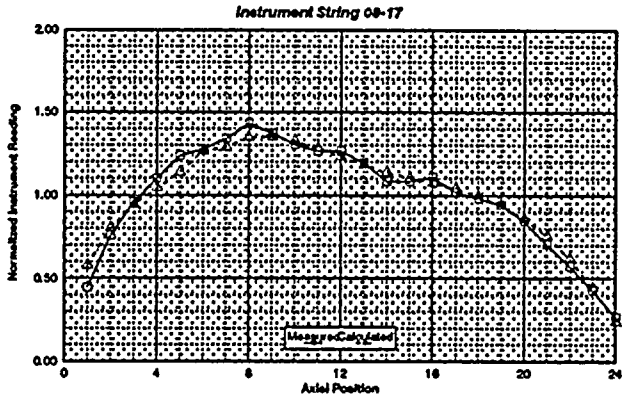

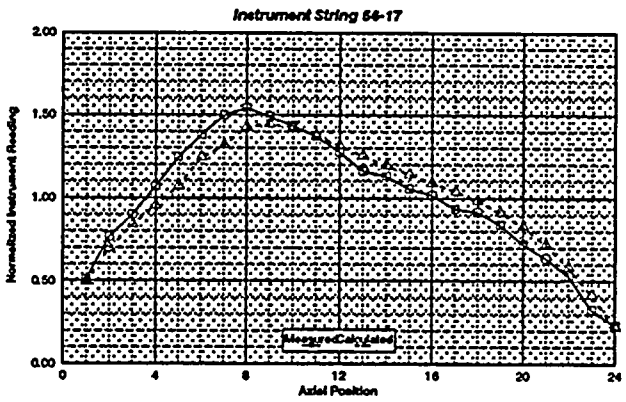

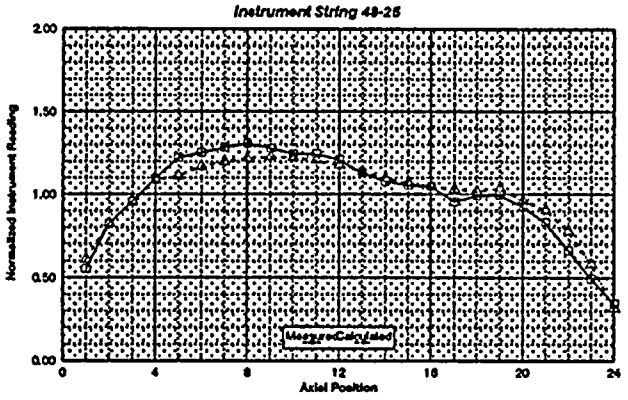

Figure 3.52

Peach Bottom 2 Cycle 2 TIP Predictions, 12754 MWd/MT

	16-57 0.744 0.701 -5.785	24-57 0.926 0.970 4.799	32-57 0.902 0.976 8.122	40-57 1.017 0.907 -10.743		
08-49 0.858 0.756 -11.896	16-49 0.959 1.035 7.887	24-49 1.071 1.087 1.470	32-49 1.108 1.098 -0.955	40-49 1.023 1.062 3.740	48-49 0.944 0.987 4.517	
08-41 1.116 1.061 -4.945	16-41 0.989 0.994 0.462	24-41 1.064 1.047 -1.567	32-41 1.102 1.105 0.231	40-41 0.982 0.986 0.420	48-41 1.090 1.069 -1.968	56-41 1.017 0.913 -10.263
08-33 1.041 1.074 3.139	16-33 0.992 1.053 6.118	24-33 0.899 0.942 4.860	32-33 0.963 0.954 -0.949	40-33 1.064 1.026 -3.630	48-33 1.025 1.094 6.743	56-33 0.928 0.980 5.667
08-25 1.089 1.081 -0.773	16-25 1.027 1.011 -1.622	24-25 0.990 1.017 2.733	32-25 1.061 1.037 -2.261	40-25 0.935 0.980 4.769	48-25 1.086 1.066 -1.863	56-25 0.971 0.976 0.581
08-17 0.991 0.970 -2.151	16-17 1.035 1.030 -0.529	24-17 1.089 1.073 -1.486	32-17 1.079 1.088 0.831	40-17 1.001 1.026 2.529	48-17 1.104 1.068 -3.254	56-17 0.752 0.718 -4.537
	16-09 0.899 0.956 6.310	24-09 1.025 1.099 7.219	32-09 1.092 1.092 -0.017	40-09 1.057 1.074 1.566	48-09 0.890 0.764 -14.155	

xx-xx	String Identification
x.xxx	Measured Average Instrument Response
x.xxx	Calculated Average Instrument Response
x.xxx	Percent error

Figure 3.53
Peach Bottom 2 Cycle 2 TIP Predictions
12754 MWd/MT

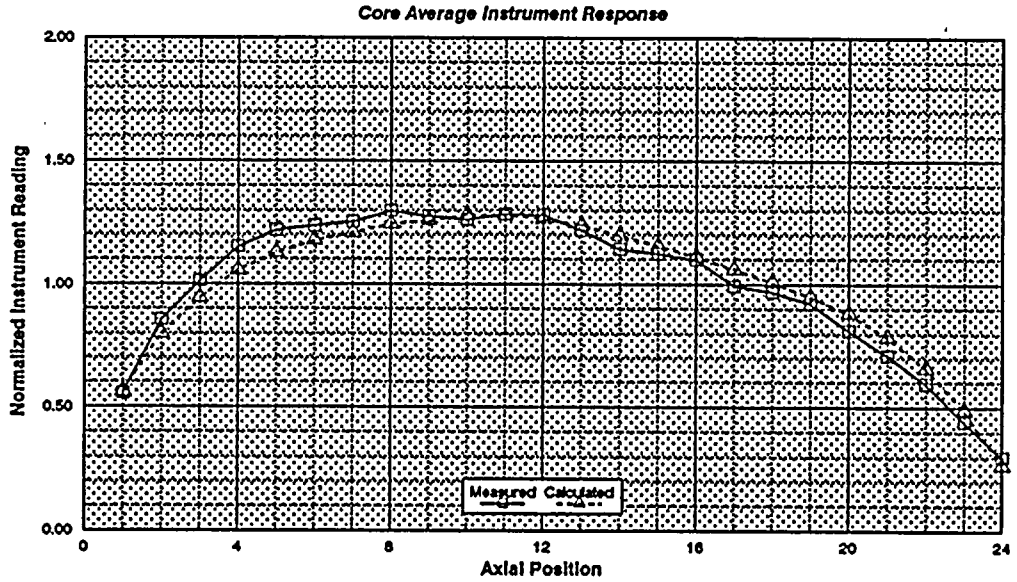

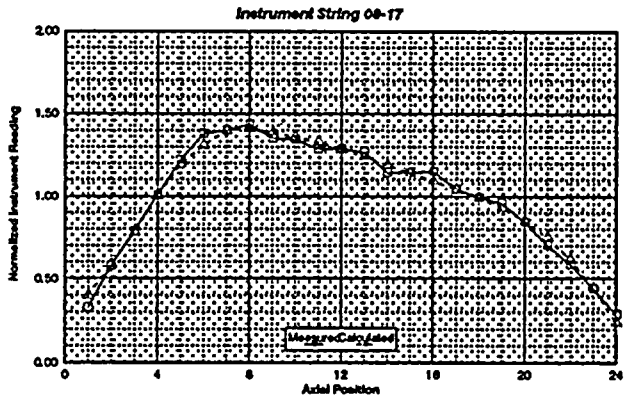

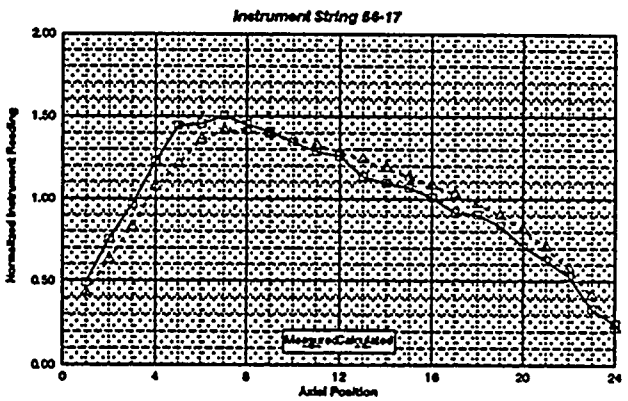

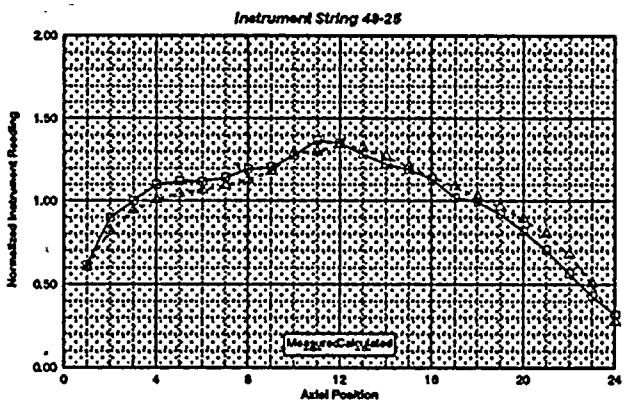

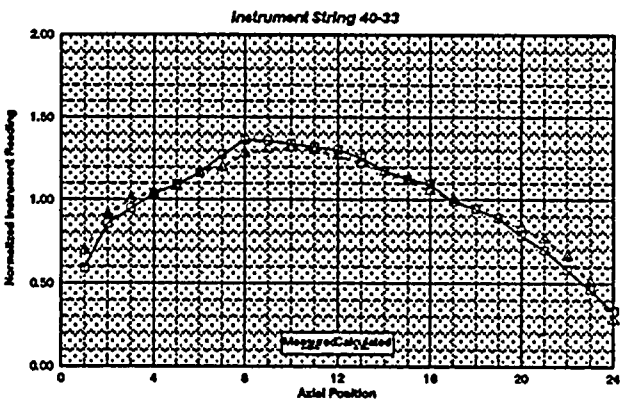

Figure 3.54

Peach Bottom 2 Cycle 2 TIP Predictions, 13812 MWd/MT

	16-57	24-57	32-57	40-57		
	0.741	0.905	0.884	0.985		
	0.690	0.931	0.934	0.870		
	-6.874	2.847	5.728	-11.649		
08-49	16-49	24-49	32-49	40-49	48-49	
0.844	0.997	1.052	1.078	1.049	0.936	
0.746	1.078	1.067	1.045	1.089	0.988	
-11.612	8.059	1.377	-3.055	3.775	5.599	
08-41	16-41	24-41	32-41	40-41	48-41	56-41
1.078	1.088	1.042	1.020	1.084	1.105	0.965
1.035	1.099	1.036	1.024	1.079	1.086	0.870
-4.015	1.006	-0.518	0.353	-0.492	-1.767	-9.805
08-33	16-33	24-33	32-33	40-33	48-33	56-33
1.028	0.925	1.020	1.126	1.058	1.024	0.896
1.053	1.011	1.066	1.123	1.027	1.065	0.941
2.501	9.323	4.424	-0.228	-2.905	4.009	5.009
08-25	16-25	24-25	32-25	40-25	48-25	56-25
1.048	1.033	1.024	1.097	1.002	1.109	0.945
1.053	1.047	1.059	1.069	1.038	1.071	0.933
0.478	1.424	3.425	-2.562	3.609	-3.393	-1.328
08-17	16-17	24-17	32-17	40-17	48-17	56-17
0.967	1.121	1.049	1.008	1.075	1.096	0.739
0.941	1.110	1.046	1.005	1.104	1.072	0.693
-2.656	-0.959	-0.290	-0.292	2.729	-2.126	-6.157
	16-09	24-09	32-09	40-09	48-09	
	0.881	0.964	1.036	1.003	0.877	
	0.941	1.044	1.036	1.035	0.752	
	6.783	8.329	-0.019	3.211	-14.330	

xx-xx	String Identification
x.xxx	Measured Average Instrument Response
x.xxx	Calculated Average Instrument Response
x.xxx	Percent error

Figure 3.55
Peach Bottom 2 Cycle 2 TIP Predictions
13812 MWd/MT

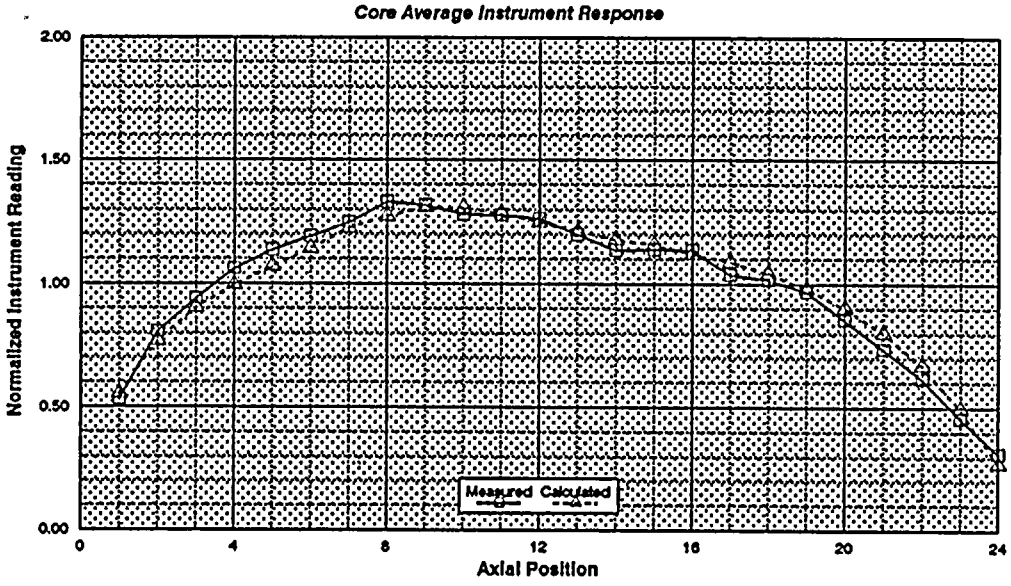

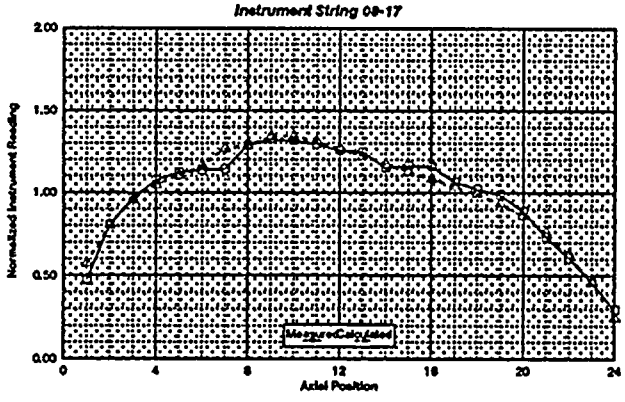

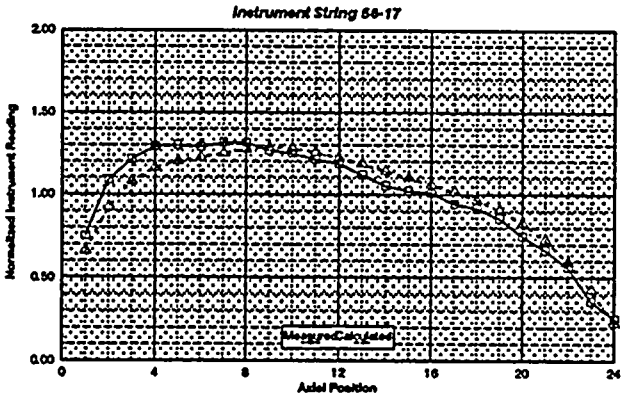

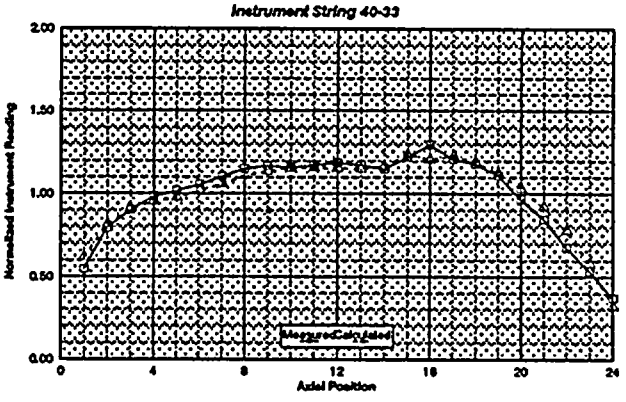

Figure 3.56
Quad Cities Critical Eigenvalue
Calculated by SIMULATE-E

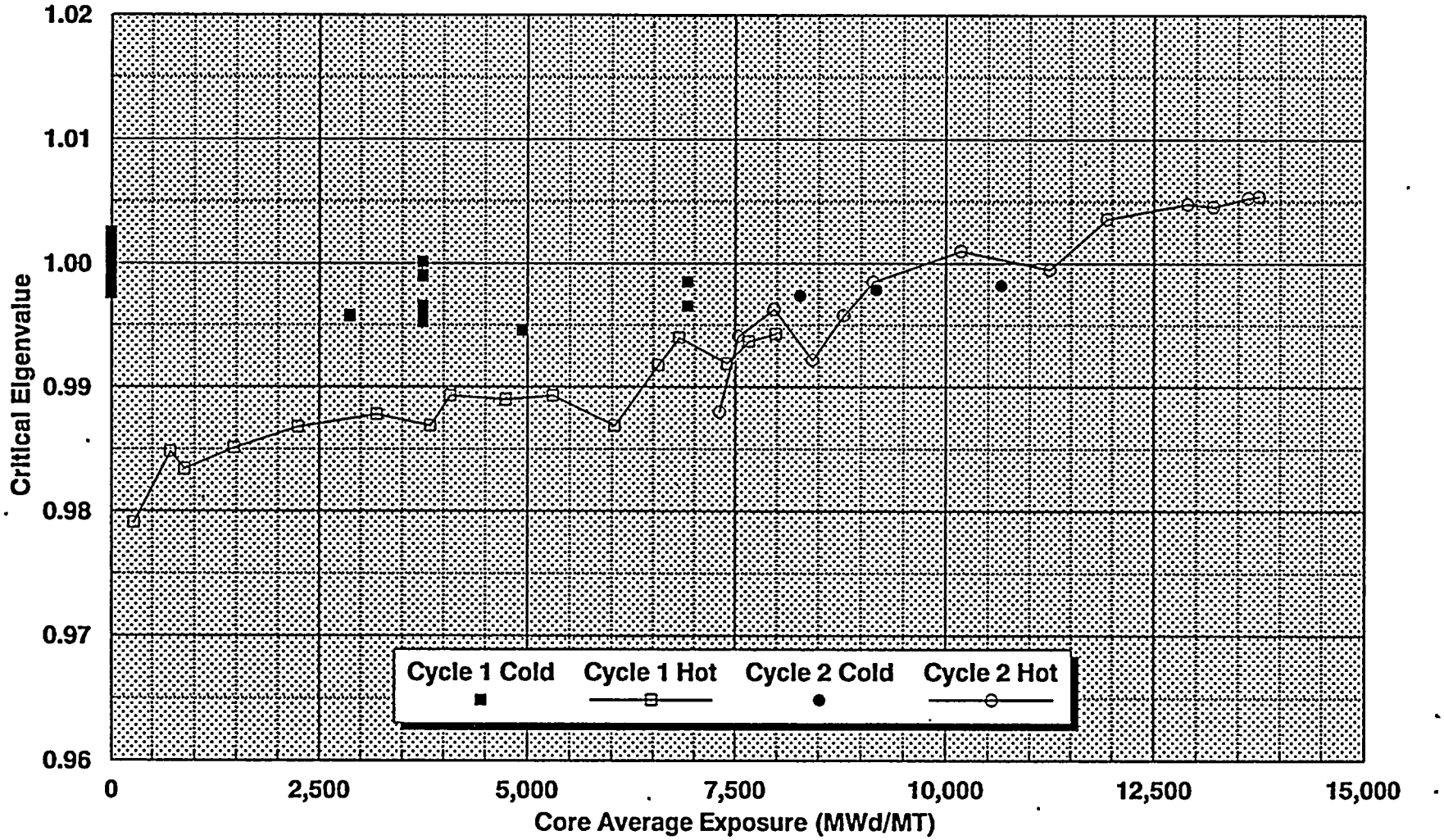

Figure 3.57
Summary of TIP Predictions
Quad Cities Benchmark

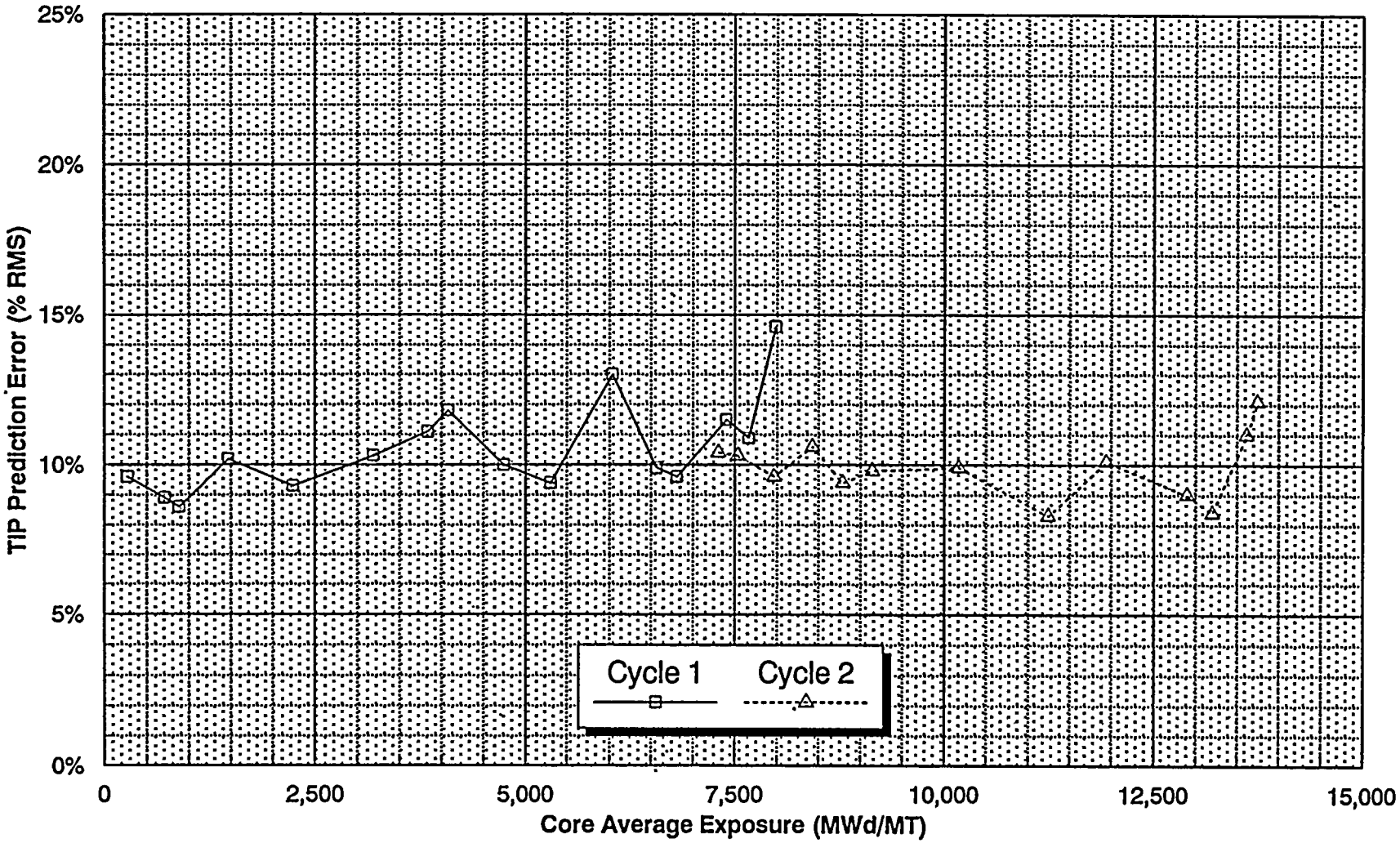

Figure 3.58

Quad Cities 1 Cycle 1 TIP Predictions, 712 MWd/MT

		24-57 0.988 0.954 -3.437	32-57 1.013 1.011 -0.216	40-57 0.749 0.731 -2.355		
08-49 0.771 0.701 -9.049	16-49 0.956 1.014 6.043	24-49 1.043 1.059 1.539	32-49 1.217 1.122 -7.815	40-49 0.966 1.013 4.796	48-49 0.957 0.999 4.383	
08-41 0.978 0.947 -3.206	16-41 1.036 1.044 0.767	24-41 1.125 1.060 -5.798	32-41 1.101 1.054 -4.303	40-41 1.024 1.071 4.542	48-41 0.900 1.011 12.252	56-41 0.643 0.730 13.631
08-33 1.027 1.092 6.332	16-33 1.080 1.108 2.535	24-33 1.034 1.032 -0.210	32-33 1.018 1.042 2.319	40-33 1.068 1.053 -1.394	48-33 1.118 1.121 0.267	56-33 1.002 1.010 0.829
08-25 0.968 1.049 8.361	16-25 0.995 1.063 6.832	24-25 1.011 1.049 3.774	32-25 1.005 1.032 2.672	40-25 1.115 1.059 -5.018	48-25 1.082 1.058 -2.261	56-25 1.024 0.953 -6.964
08-17 0.779 0.843 8.173	16-17 1.041 1.050 0.826	24-17 1.096 1.063 -2.945	32-17 1.155 1.108 -3.997	40-17 1.105 1.044 -5.450	48-17 1.117 1.012 -9.349	
	16-09 0.824 0.845 2.611	24-09 1.176 1.050 -10.669	32-09 1.037 1.092 5.351	40-09 0.918 0.949 3.330	48-09 0.738 0.702 -4.843	

xx-xx	String Identification
x.xxx	Measured Average Instrument Response
x.xxx	Calculated Average Instrument Response
x.xxx	Percent error

Figure 3.59
Quad Cities 1 Cycle 1 TIP Predictions
712 MWd/MT

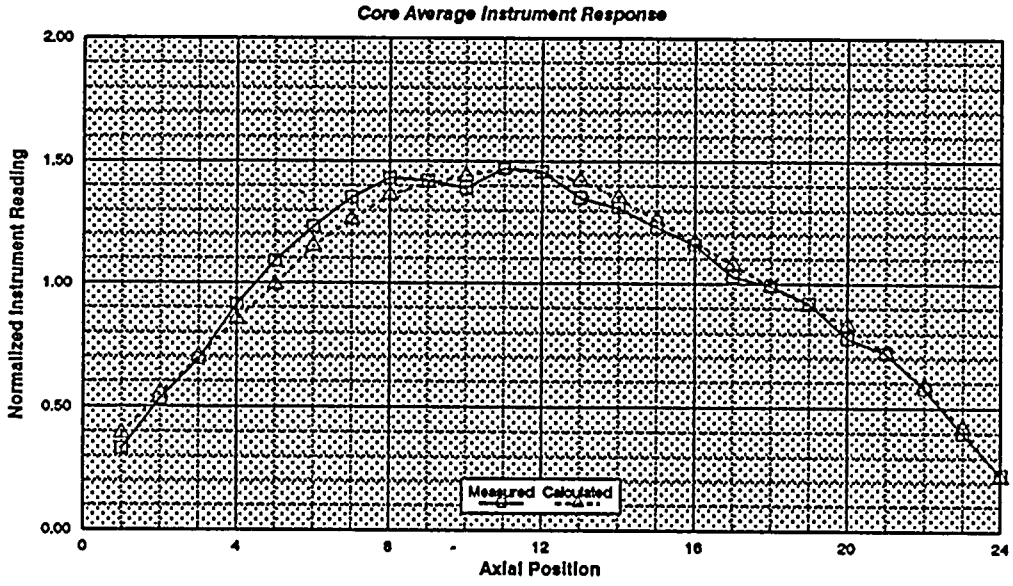

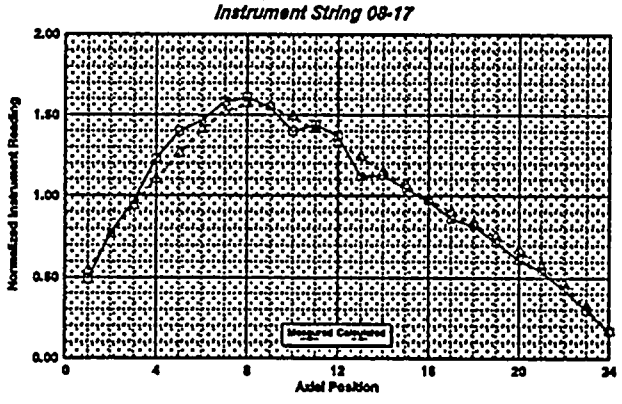

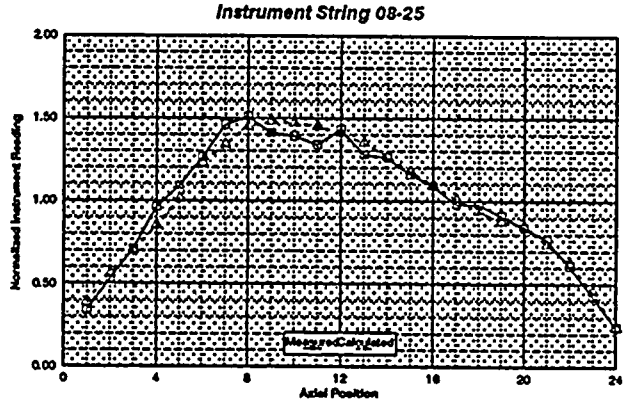

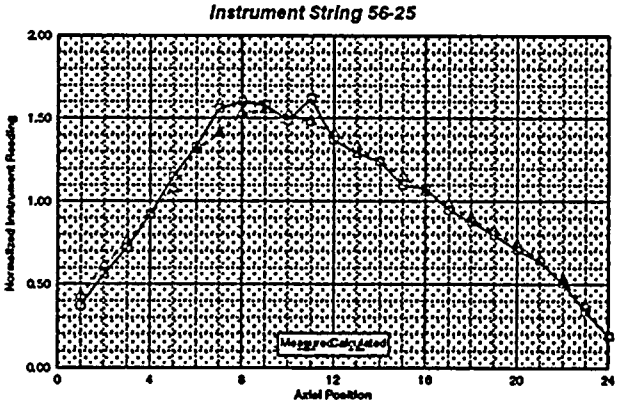

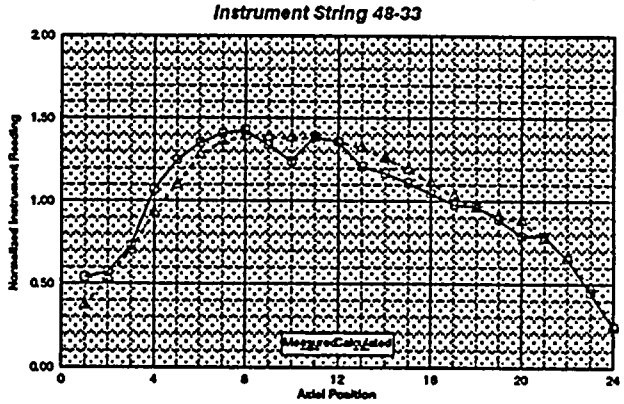

Figure 3.60

Quad Cities 1 Cycle 1 TIP Predictions, 2239 MWd/MT

		24-57 0.895 0.871 -2.706	32-57 0.906 0.912 0.733	40-57 0.767 0.737 -3.884		
08-49 0.784 0.745 -4.942	16-49 0.963 1.029 6.916	24-49 1.042 1.026 -1.610	32-49 1.168 1.051 -10.047	40-49 0.928 0.982 5.757	48-49 0.964 1.008 4.581	
08-41 1.095 1.023 -6.560	16-41 1.108 1.109 0.079	24-41 1.106 1.071 -3.152	32-41 1.089 1.043 -4.206	40-41 1.095 1.119 2.220	48-41 0.917 1.058 15.445	56-41 0.644 0.727 12.859
08-33 0.883 0.920 4.232	16-33 1.089 1.125 3.298	24-33 1.194 1.206 1.038	32-33 1.148 1.199 4.426	40-33 1.169 1.174 0.458	48-33 0.999 1.018 1.844	56-33 0.749 0.761 1.518
08-25 0.871 0.948 8.818	16-25 1.120 1.159 3.419	24-25 1.069 1.127 5.386	32-25 1.021 1.088 6.639	40-25 1.236 1.177 -4.779	48-25 1.051 1.039 -1.178	56-25 0.817 0.767 -6.107
08-17 0.947 0.981 3.538	16-17 1.012 1.019 0.682	24-17 1.108 1.055 -4.829	32-17 1.127 1.075 -4.633	40-17 1.055 1.005 -4.755	48-17 1.153 1.053 -8.687	
	16-09 0.962 0.936 -2.656	24-09 1.096 0.977 -10.874	32-09 0.937 0.993 5.997	40-09 0.973 0.967 -0.649	48-09 0.742 0.721 -2.864	

xx-xx	String Identification
x.xxx	Measured Average Instrument Response
x.xxx	Calculated Average Instrument Response
x.xxx	Percent error

Figure 3.61
Quad Cities 1 Cycle 1 TIP Predictions
2239 MWd/MT

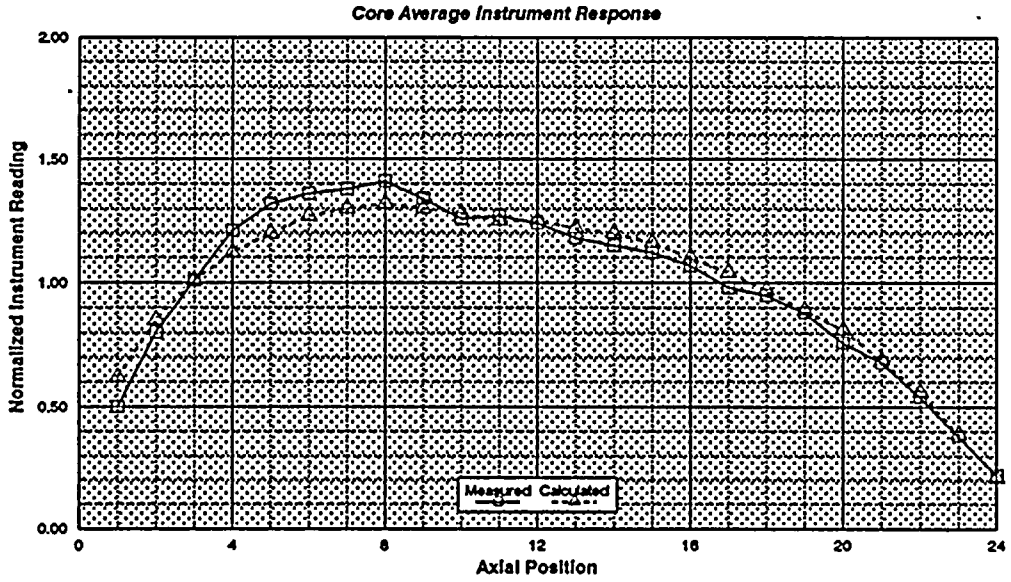

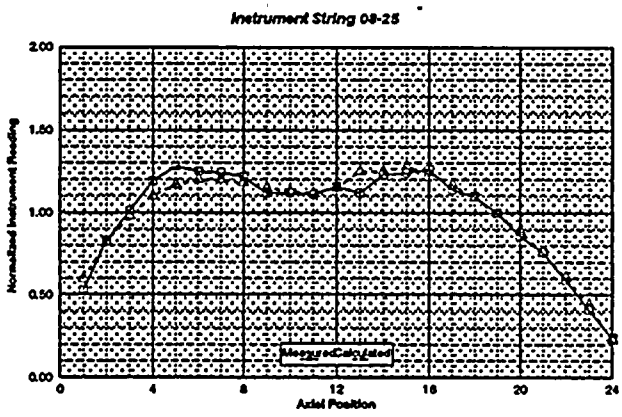

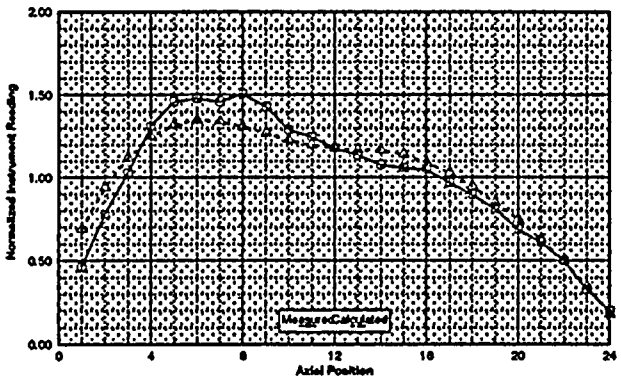

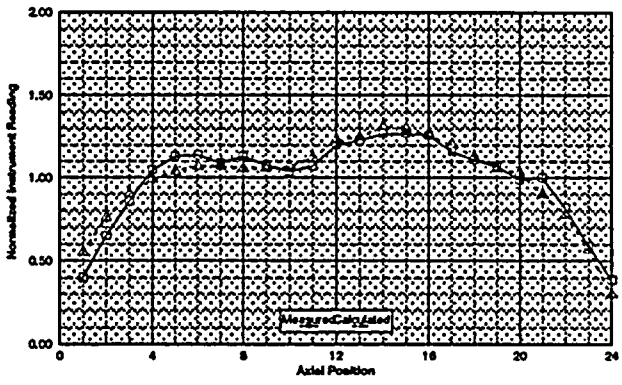

Figure 3.62

Quad Cities 1 Cycle 1 TIP Predictions, 4737 MWd/MT

		24-57 0.778 0.732 -5.984	32-57 0.824 0.805 -2.299	40-57 0.603 0.571 -5.263		
08-49 0.600 0.559 -6.755	16-49 0.921 0.959 4.112	24-49 1.038 1.045 0.666	32-49 1.187 1.073 -9.569	40-49 0.996 1.012 1.657	48-49 0.825 0.849 2.917	
08-41 1.049 0.986 -6.047	16-41 1.053 1.107 5.118	24-41 1.213 1.175 -3.082	32-41 1.179 1.144 -2.930	40-41 1.146 1.168 1.920	48-41 0.944 1.061 12.310	56-41 0.688 0.741 7.746
08-33 1.025 1.073 4.718	16-33 1.132 1.207 6.632	24-33 1.090 1.141 4.722	32-33 1.080 1.180 9.209	40-33 1.127 1.160 2.898	48-33 1.191 1.176 -1.238	56-33 0.896 0.876 -2.227
08-25 0.996 1.065 6.954	16-25 1.135 1.188 4.617	24-25 1.057 1.160 9.715	32-25 1.073 1.179 9.863	40-25 1.155 1.169 1.213	48-25 1.162 1.149 -1.071	56-25 0.980 0.890 -9.196
08-17 0.793 0.825 4.110	16-17 1.085 1.039 -4.215	24-17 1.183 1.151 -2.715	32-17 1.137 1.121 -1.393	40-17 1.197 1.119 -6.451	48-17 1.080 0.965 -10.615	
	16-09 0.811 0.784 -3.268	24-09 1.053 0.930 -11.670	32-09 0.966 0.994 2.881	40-09 0.889 0.872 -1.973	48-09 0.666 0.600 -9.936	

xx-xx	String Identification
x.xxx	Measured Average Instrument Response
x.xxx	Calculated Average Instrument Response
x.xxx	Percent error

Figure 3.63
Quad Cities 1 Cycle 1 TIP Predictions
4737 MWd/MT

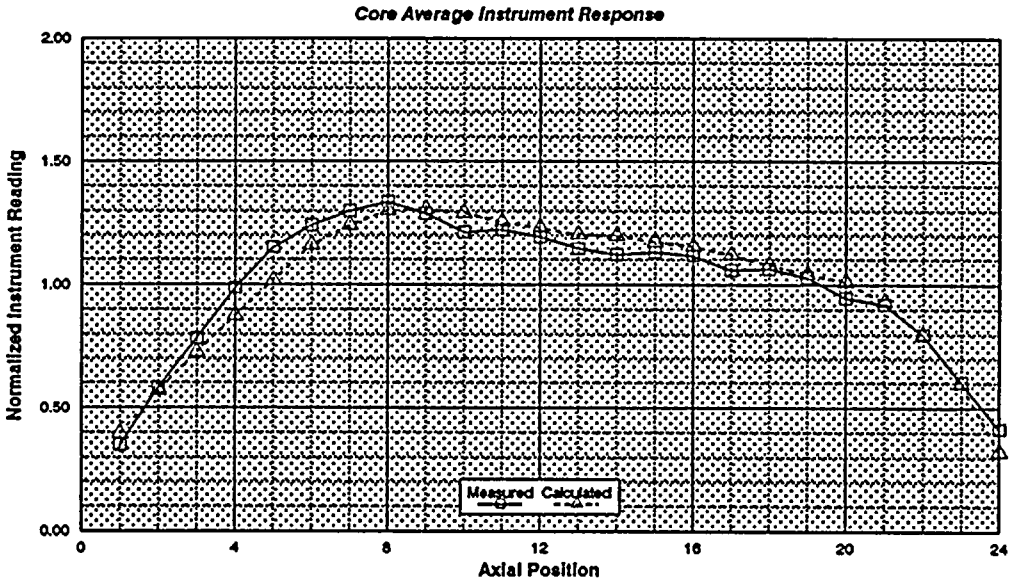

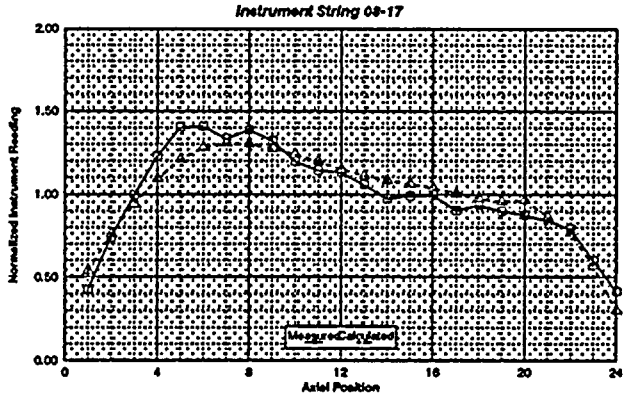

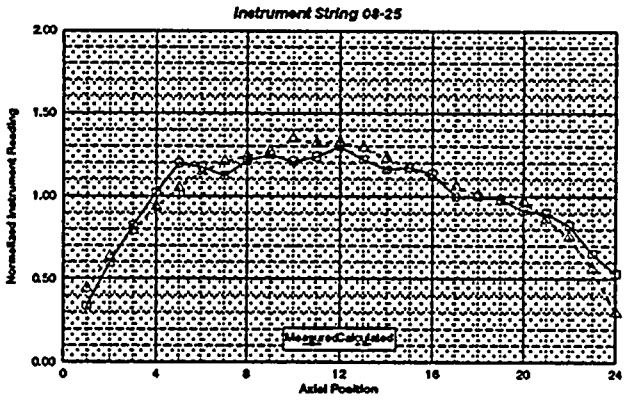

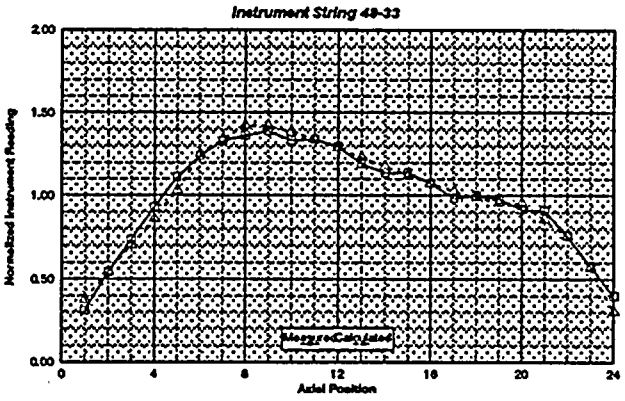

Figure 3.64

Quad Cities 1 Cycle 1 TIP Predictions, 6807 MWd/MT

		24-57 0.988 0.938 -5.047	32-57 0.956 0.962 0.586	40-57 0.797 0.763 -4.225		
08-49 0.825 0.754 -8.641	16-49 1.020 1.096 7.530	24-49 1.014 1.037 2.294	32-49 1.156 1.041 -9.887	40-49 1.026 1.077 4.903	48-49 1.055 1.058 0.286	
08-41 1.041 1.006 -3.376	16-41 0.986 1.058 7.360	24-41 1.077 1.048 -2.681	32-41 1.054 1.024 -2.776	40-41 1.035 1.063 2.738	48-41 0.976 1.069 9.503	56-41 0.690 0.752 8.931
08-33 0.976 1.021 4.635	16-33 1.006 1.045 3.811	24-33 0.955 1.001 4.813	32-33 0.983 1.014 3.204	40-33 0.995 1.017 2.179	48-33 1.042 1.033 -0.927	56-33 1.012 0.967 -4.500
08-25 0.965 1.028 6.548	16-25 0.988 1.037 5.005	24-25 0.983 1.032 5.054	32-25 0.914 1.001 9.510	40-25 1.041 1.045 0.391	48-25 1.010 1.028 1.776	56-25 1.014 0.932 -8.030
08-17 0.899 0.929 3.362	16-17 1.184 1.101 -7.016	24-17 1.033 1.045 1.176	32-17 1.074 1.059 -1.382	40-17 1.095 1.064 -2.895	48-17 1.212 1.097 -9.445	
	16-09 0.950 0.932 -1.918	24-09 1.155 1.035 -10.388	32-09 0.974 1.022 4.919	40-09 1.038 1.019 -1.855	48-09 0.807 0.749 -7.194	

xx-xx	String Identification
x.xxx	Measured Average Instrument Response
x.xxx	Calculated Average Instrument Response
x.xxx	Percent error

Figure 3.65
Quad Cities 1 Cycle 1 TIP Predictions
6807 MWd/MT

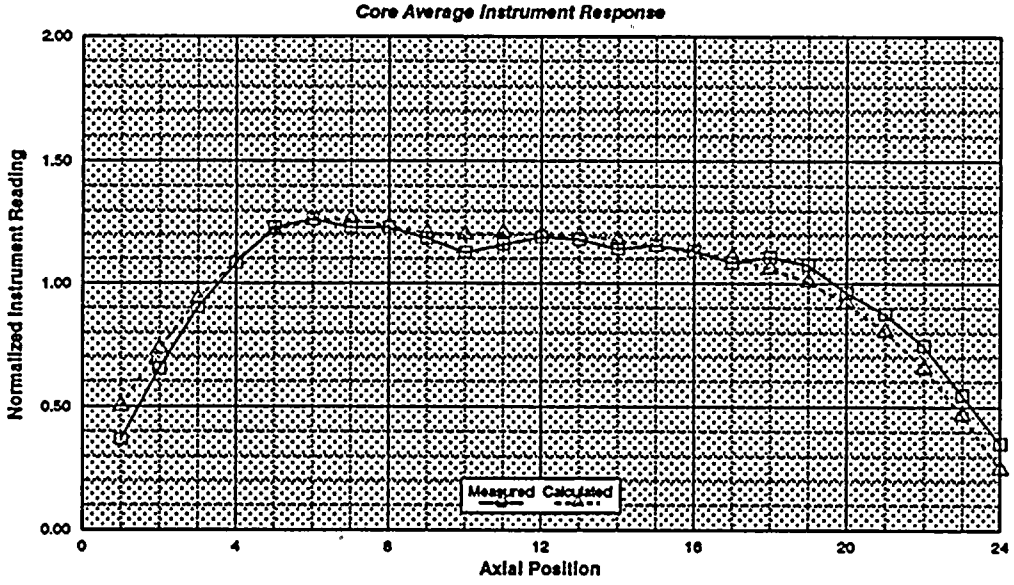

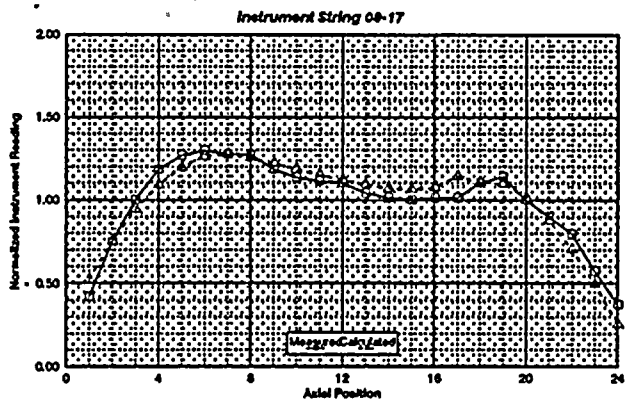

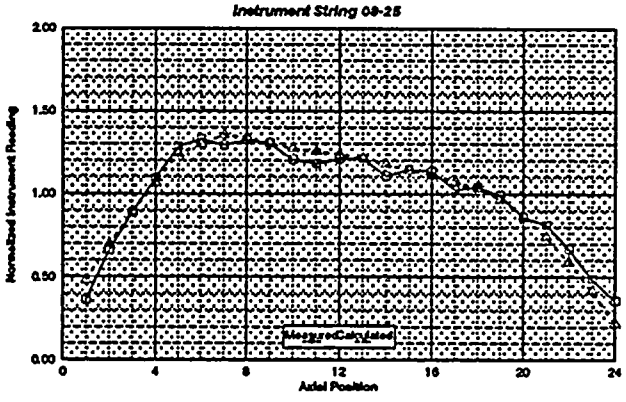

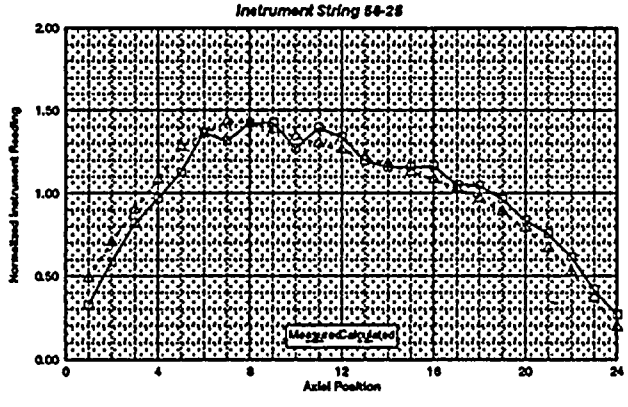

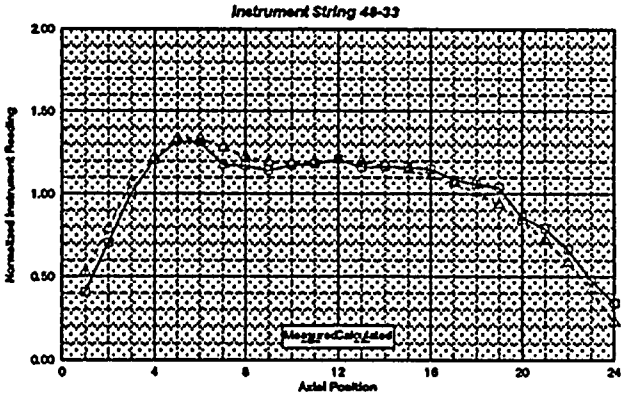

Figure 3.66

Quad Cities 1 Cycle 1 TIP Predictions, 8068 MWd/MT

		24-57 0.975 0.916 -6.055	32-57 0.950 0.945 -0.521	40-57 0.770 0.743 -3.417		
08-49 0.804 0.720 -10.472	16-49 0.965 1.060 9.769	24-49 1.023 1.063 3.913	32-49 1.168 1.069 -8.478	40-49 1.026 1.073 4.515	48-49 0.999 1.008 0.920	
08-41 1.009 0.985 -2.357	16-41 0.994 1.052 5.872	24-41 1.085 1.062 -2.105	32-41 1.089 1.056 -3.050	40-41 1.022 1.059 3.673	48-41 0.983 1.061 7.944	56-41 0.678 0.730 7.635
08-33 0.962 1.028 6.882	16-33 1.004 1.063 5.836	24-33 1.013 1.052 3.852	32-33 0.998 1.071 7.364	40-33 1.033 1.045 1.119	48-33 1.099 1.054 -4.093	56-33 1.010 0.948 -6.052
08-25 0.979 1.025 4.681	16-25 0.997 1.053 5.600	24-25 1.025 1.064 3.777	32-25 0.942 1.054 11.969	40-25 1.039 1.056 1.651	48-25 1.045 1.048 0.270	56-25 1.003 0.909 -9.315
08-17 0.867 0.897 3.439	16-17 1.154 1.070 -7.239	24-17 1.065 1.066 0.067	32-17 1.086 1.081 -0.407	40-17 1.093 1.061 -2.926	48-17 1.177 1.058 -10.095	
	16-09 0.946 0.903 -4.601	24-09 1.175 1.038 -11.727	32-09 0.966 1.036 7.256	40-09 0.986 1.002 1.561	48-09 0.797 0.717 -10.099	

xx-xx	String Identification
x.xxx	Measured Average Instrument Response
x.xxx	Calculated Average Instrument Response
x.xxx	Percent error

Figure 3.67
Quad Cities 1 Cycle 1 TIP Predictions
8068 MWd/MT

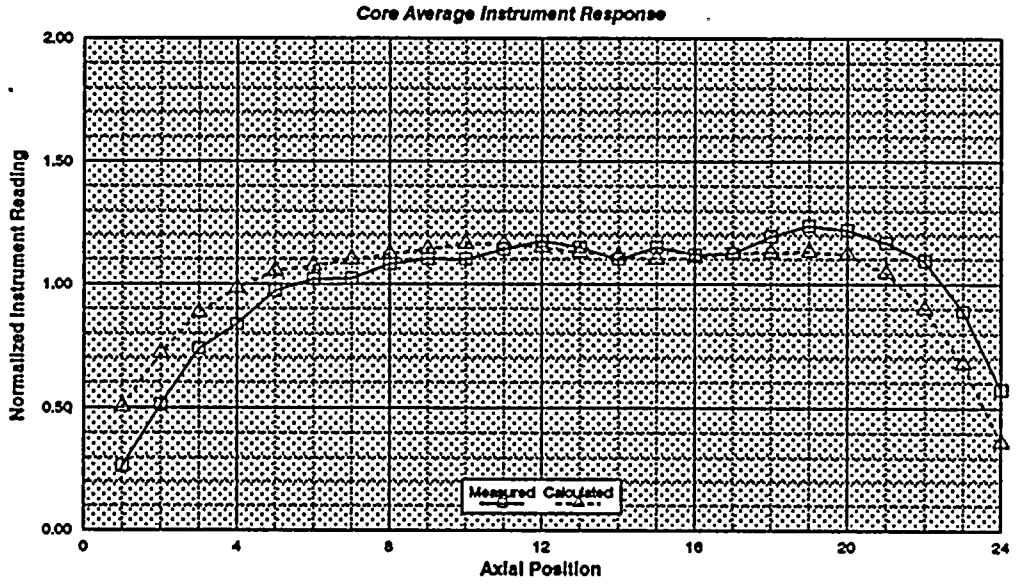

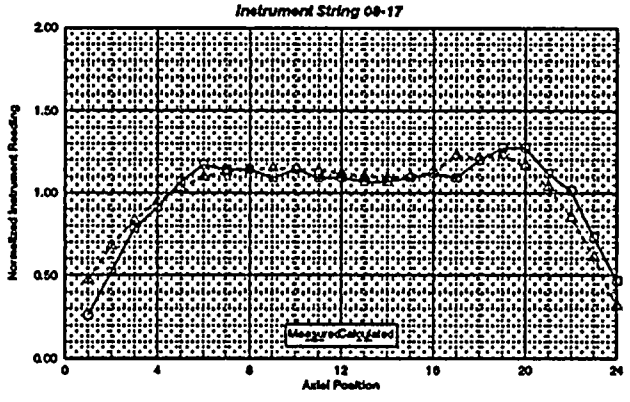

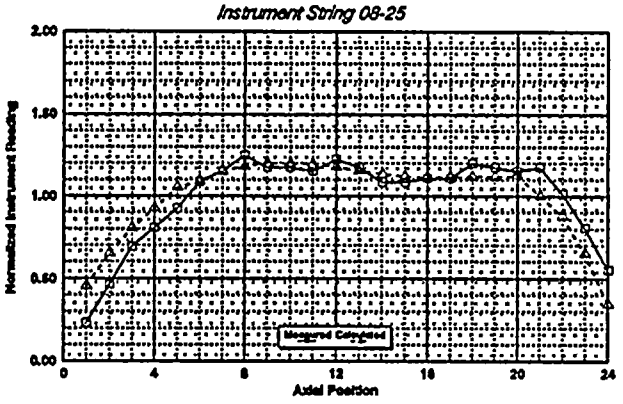

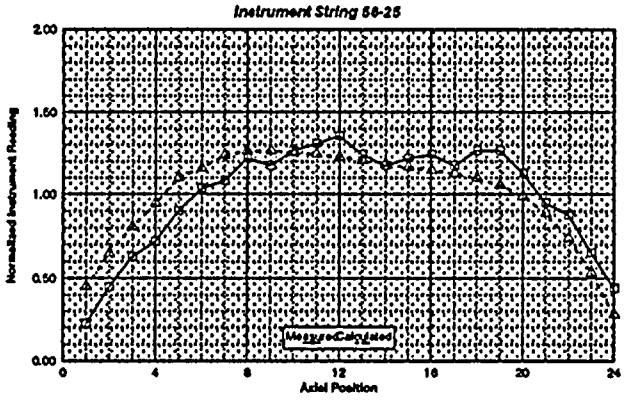

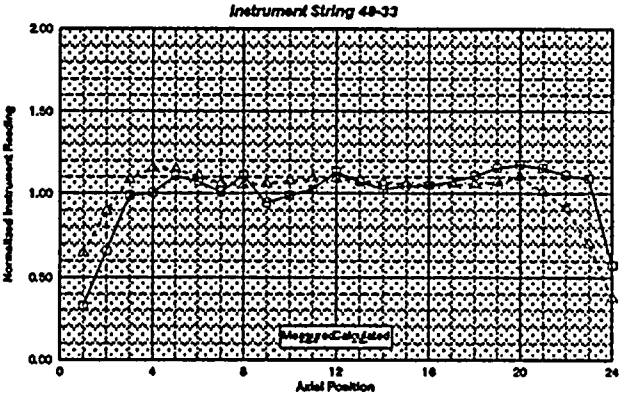

Figure 3.68

Quad Cities 1 Cycle 2 TIP Predictions, 7964 MWd/MT

		24-57 0.928 0.872 -5.990	32-57 0.915 0.883 -3.526	40-57 0.803 0.735 -8.412		
08-49 0.793 0.723 -8.785	16-49 1.040 1.096 5.358	24-49 0.969 1.018 5.105	32-49 1.068 0.995 -6.852	40-49	48-49 1.021 1.024 0.300	
08-41 1.098 0.998 -9.115	16-41 1.060 1.035 -2.349	24-41 1.050 1.083 3.091	32-41 1.124 1.107 -1.531	40-41 0.995 1.046 5.170	48-41 1.041 1.081 3.868	56-41 0.700 0.722 3.098
08-33 0.912 0.962 5.385	16-33 1.021 1.025 0.409	24-33 1.139 1.227 7.751	32-33 1.210 1.240 2.467	40-33 1.051 1.104 5.018	48-33 0.999 0.984 -1.426	56-33 0.964 0.894 -7.323
08-25 0.969 0.985 1.622	16-25 1.012 1.029 1.689	24-25 1.122 1.190 6.070	32-25 1.173 1.230 4.911	40-25	48-25 1.025 1.011 -1.367	56-25
08-17 0.922 0.924 0.175	16-17 1.121 1.086 -3.174	24-17 0.989 1.033 4.453	32-17	40-17 1.083 1.035 -4.401	48-17	
	16-09 0.959 0.930 -3.035	24-09	32-09 0.938 0.962 2.536	40-09 1.013 1.012 -0.108	48-09 0.775 0.722 -6.843	

xx-xx	String Identification
x.xxx	Measured Average Instrument Response
x.xxx	Calculated Average Instrument Response
x.xxx	Percent error

Figure 3.69
Quad Cities 1 Cycle 2 TIP Predictions
7964 MWd/MT

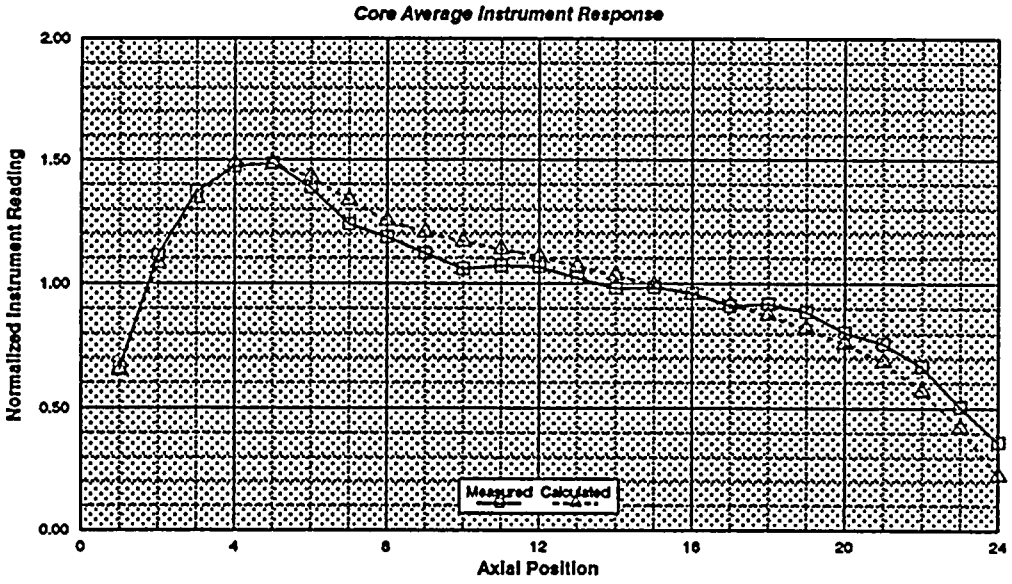

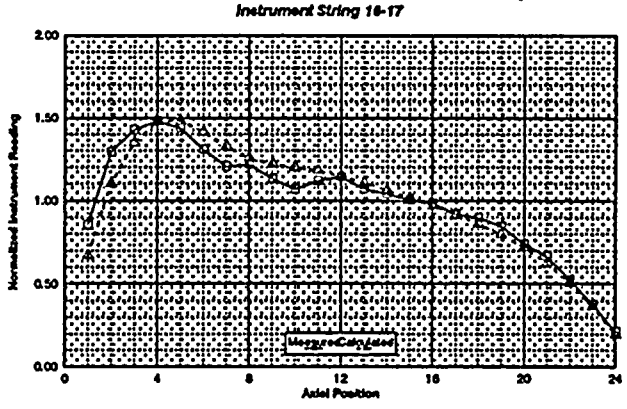

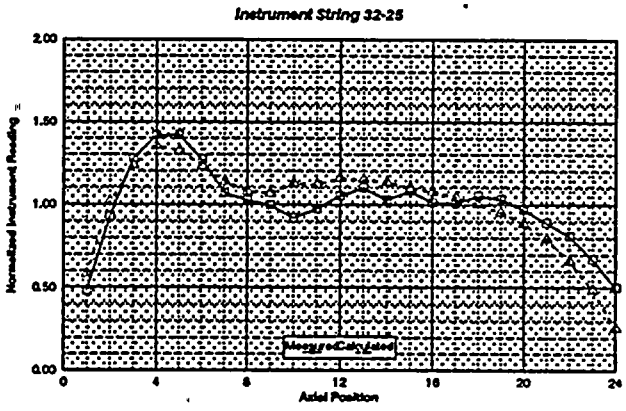

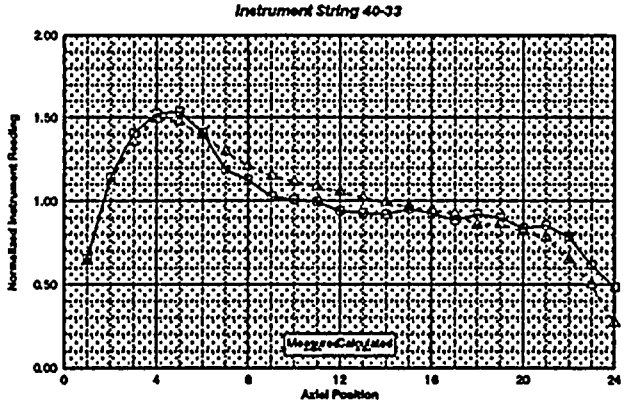

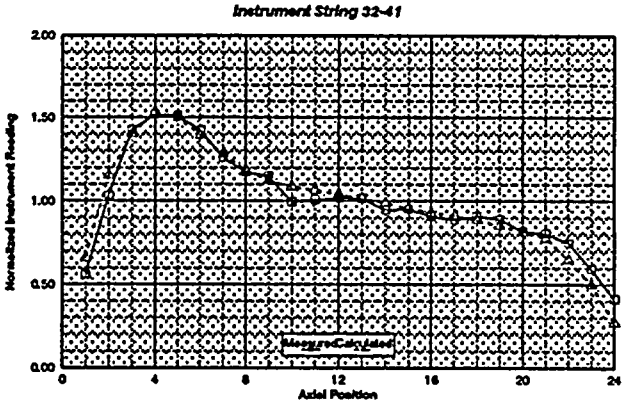

Figure 3.70

Quad Cities 1 Cycle 2 TIP Predictions, 9141 MWd/MT

		24-57	32-57	40-57		
		0.926	0.972	0.736		
		0.854	0.924	0.668		
		-7.715	-4.944	-9.159		
08-49	16-49	24-49	32-49	40-49	48-49	
0.715	1.020	1.084	1.232		0.910	
0.621	1.038	1.134	1.155		0.895	
-13.199	1.780	4.608	-6.255		-1.682	
08-41	16-41	24-41	32-41	40-41	48-41	56-41
1.045	1.139	1.161	1.138	1.163	0.987	0.582
0.928	1.099	1.205	1.131	1.199	1.028	0.596
-11.195	-3.594	3.790	-0.532	3.075	4.100	2.376
08-33	16-33	24-33	32-33	40-33	48-33	56-33
0.867	1.159	1.016	1.108	1.047	1.118	0.680
0.922	1.172	1.112	1.130	1.118	1.110	0.655
6.299	1.180	9.443	1.913	6.787	-0.683	-3.651
08-25	16-25	24-25	32-25	40-25	48-25	56-25
0.940	1.154	1.030	1.081		1.118	
0.945	1.169	1.151	1.159		1.110	
0.522	1.283	11.725	7.230		-0.735	
08-17	16-17	24-17	32-17	40-17	48-17	
0.857	1.102	1.144		1.262		
0.822	1.082	1.215		1.177		
-4.131	-1.884	6.220		-6.734		
	16-09	24-09	32-09	40-09	48-09	
	0.885		1.048	0.906	0.666	
	0.835		1.099	0.935	0.607	
	-5.623		4.802	3.243	-8.846	

xx-xx	String Identification
x.xxx	Measured Average Instrument Response
x.xxx	Calculated Average Instrument Response
x.xxx	Percent error

Figure 3.71
Quad Cities 1 Cycle 2 TIP Predictions
9141 MWd/MT

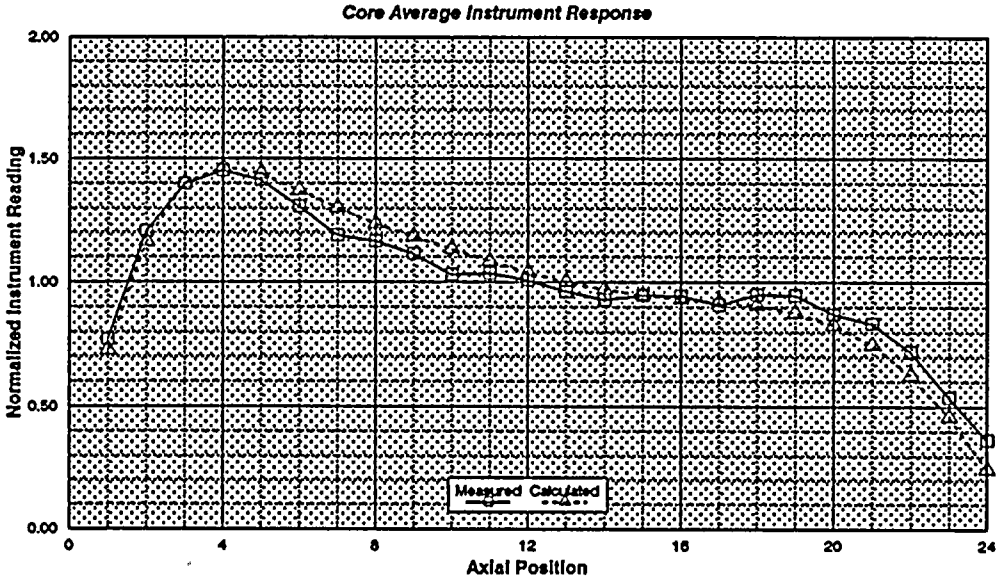

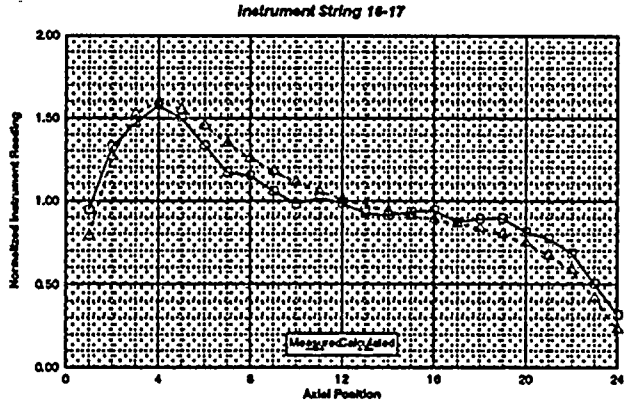

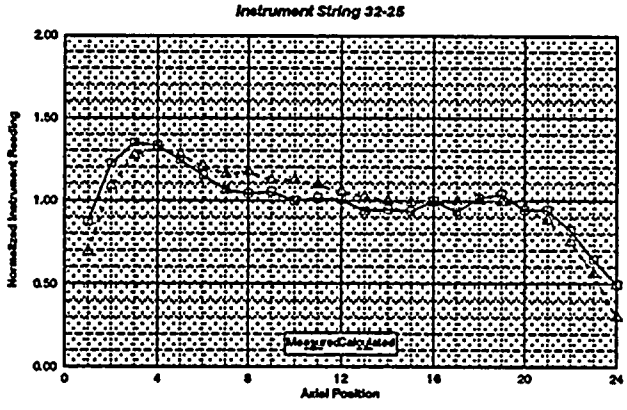

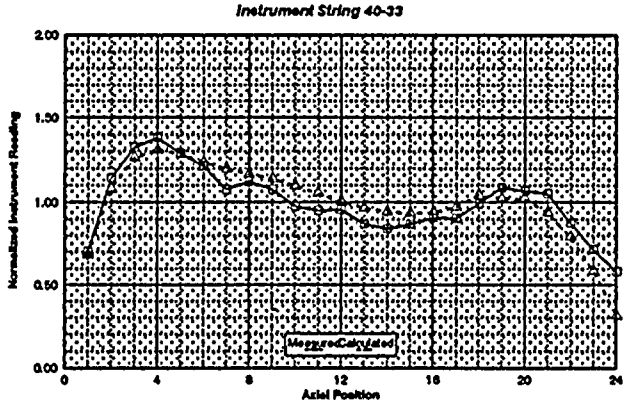

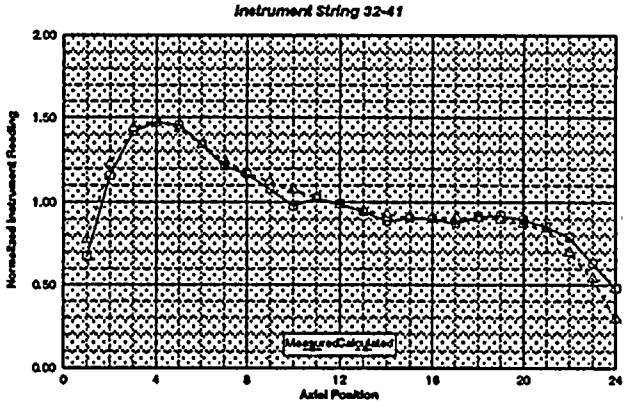

Figure 3.72

Quad Cities 1 Cycle 2 TIP Predictions, 13198 MWd/MT

		24-57 0.825 0.801 -2.954	32-57 0.821 0.817 -0.481	40-57 0.682 0.646 -5.353		
08-49 0.673 0.601 -10.700	16-49 1.006 1.089 8.268	24-49 1.054 1.146 8.787	32-49 1.153 1.101 -4.452	40-49	48-49 0.925 0.924 -0.045	
08-41 1.053 0.963 -8.491	16-41 1.187 1.157 -2.531	24-41 1.094 1.137 3.938	32-41 1.128 1.102 -2.311	40-41 1.102 1.160 5.254	48-41 1.128 1.112 -1.446	56-41 0.626 0.617 -1.477
08-33 0.968 1.006 3.946	16-33 1.094 1.117 2.115	24-33 1.035 1.097 5.930	32-33 1.089 1.099 0.908	40-33 1.040 1.103 6.070	48-33 1.123 1.081 -3.686	56-33 0.882 0.801 -9.166
08-25 1.045 1.026 -1.793	16-25 1.153 1.152 -0.092	24-25 1.024 1.116 9.012	32-25 1.036 1.097 5.882	40-25	48-25 1.163 1.125 -3.300	56-25
08-17 0.869 0.830 -4.524	16-17 1.239 1.178 -4.906	24-17 1.096 1.158 5.648	32-17	40-17 1.231 1.166 -5.330	48-17	
	16-09 0.870 0.850 -2.315	24-09	32-09 0.999 1.023 2.402	40-09 0.955 0.998 4.425	48-09 0.633 0.605 -4.386	

xx-xx	String Identification
x.xxx	Measured Average Instrument Response
x.xxx	Calculated Average Instrument Response
x.xxx	Percent error

Figure 3.73
Quad Cities 1 Cycle 2 TIP Predictions
13198 MWd/MT

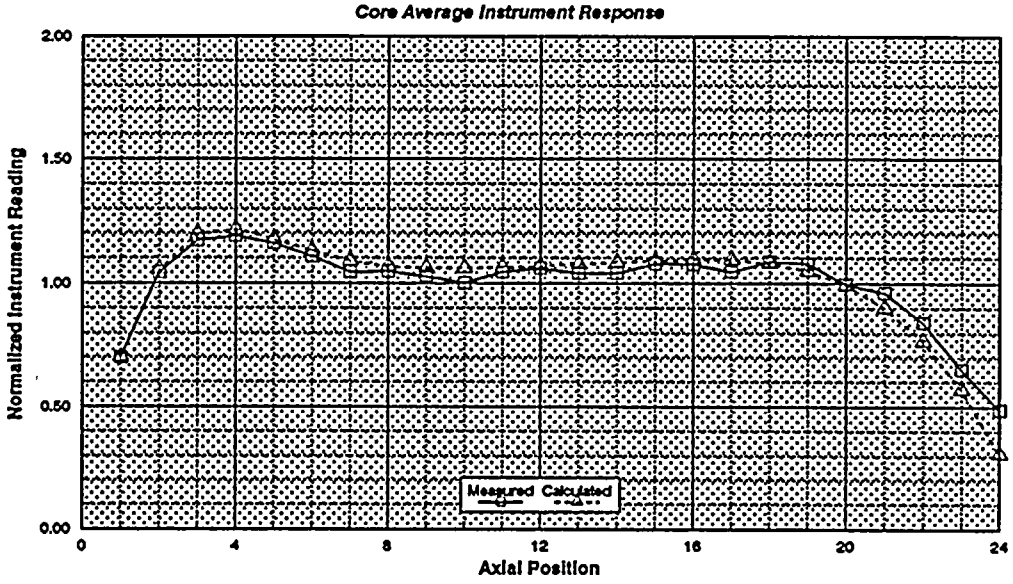

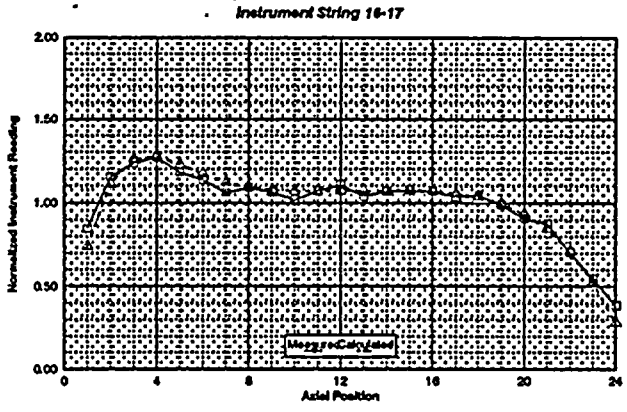

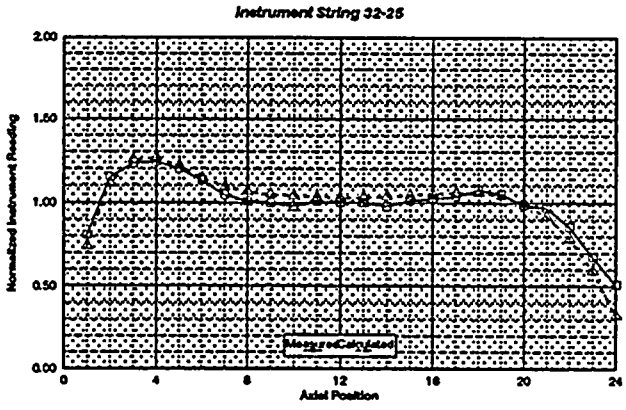

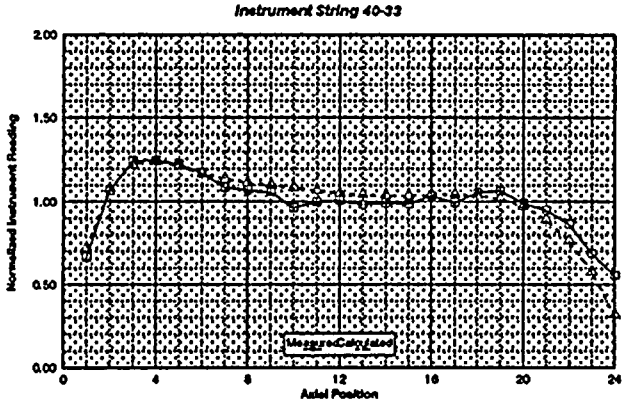

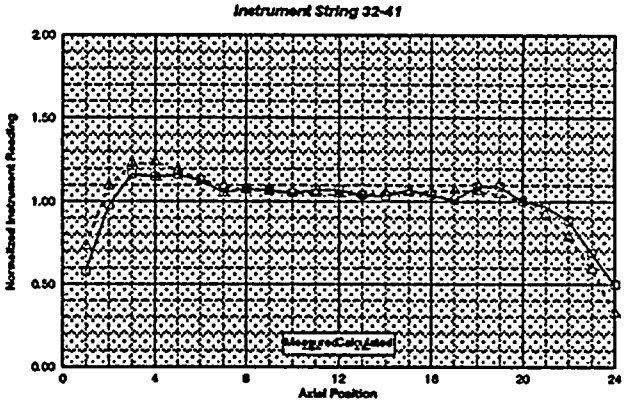

Figure 3.74

Quad Cities 1 Cycle 2 TIP Predictions, 13741 MWd/MT

		24-57 0.818 0.803 -1.882	32-57 0.835 0.817 -2.121	40-57 0.709 0.645 -8.945		
08-49 0.693 0.602 -13.172	16-49 1.024 1.095 6.916	24-49 1.064 1.149 8.052	32-49 1.146 1.102 -3.807	40-49	48-49 0.927 0.929 0.228	
08-41 1.027 0.967 -5.854	16-41 1.173 1.160 -1.068	24-41 1.087 1.132 4.164	32-41 1.123 1.095 -2.466	40-41 1.119 1.160 3.611	48-41 1.148 1.116 -2.840	56-41 0.647 0.615 -4.910
08-33 0.964 1.007 4.469	16-33 1.103 1.112 0.859	24-33 1.039 1.089 4.847	32-33 1.103 1.100 -0.337	40-33 1.028 1.094 6.436	48-33 1.104 1.081 -2.148	56-33 0.893 0.800 -10.464
08-25 1.070 1.030 -3.737	16-25 1.184 1.150 -2.855	24-25 1.031 1.109 7.559	32-25 1.025 1.089 6.223	40-25	48-25 1.025 1.126 9.873	56-25
08-17 0.874 0.833 -4.731	16-17 1.256 1.185 -5.693	24-17 1.091 1.157 6.040	32-17	40-17 1.221 1.167 -4.375	48-17	
	16-09 0.870 0.851 -2.202	24-09	32-09 0.968 1.025 5.939	40-09 0.967 1.002 3.650	48-09 0.643 0.604 -6.014	

xx-xx	String Identification
x.xxx	Measured Average Instrument Response
x.xxx	Calculated Average Instrument Response
x.xxx	Percent error

Figure 3.75
Quad Cities 1 Cycle 2 TIP Predictions
13741 MWd/MT

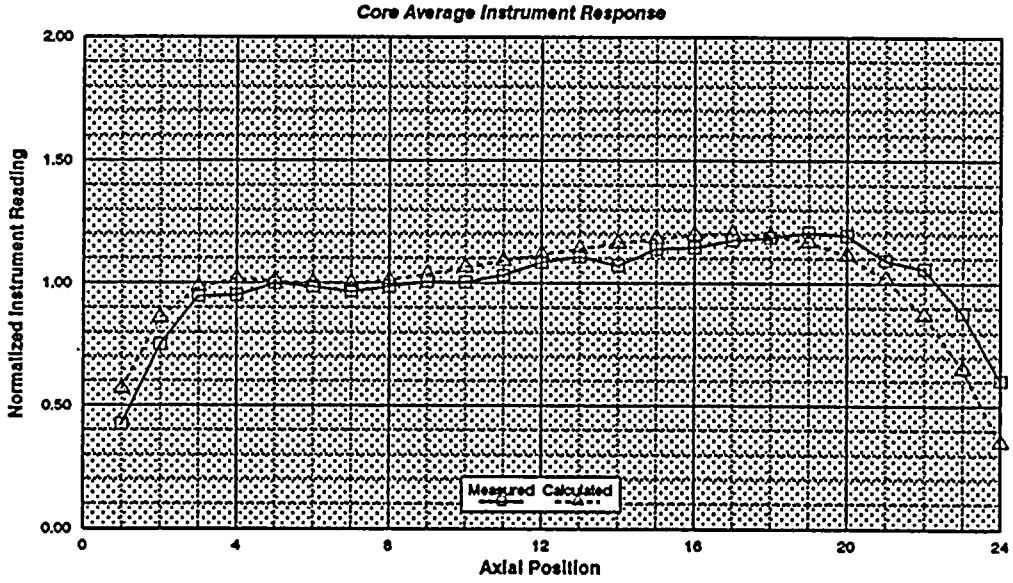

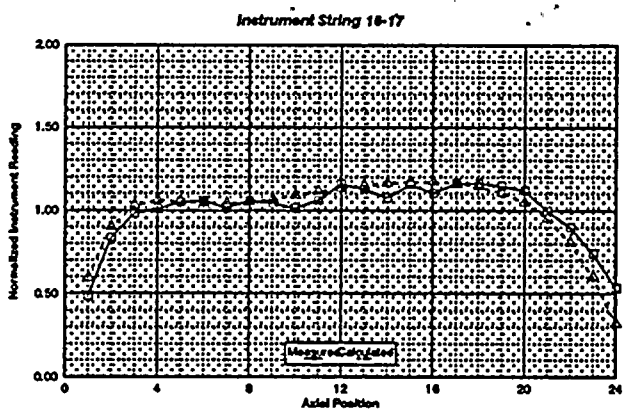

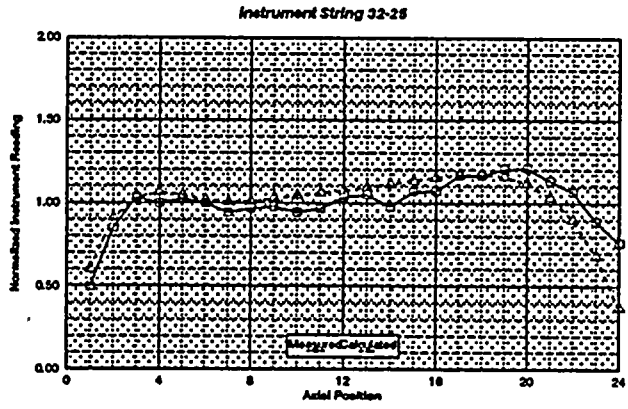

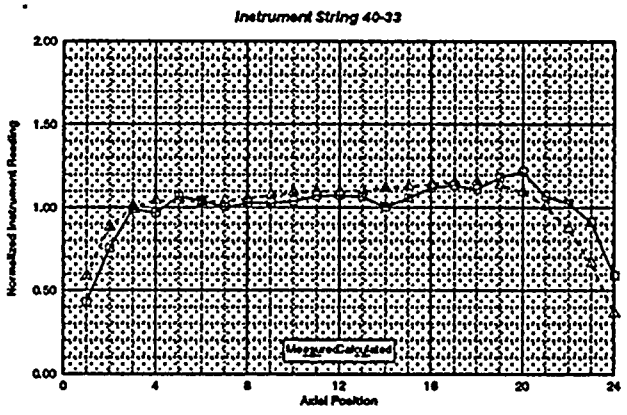

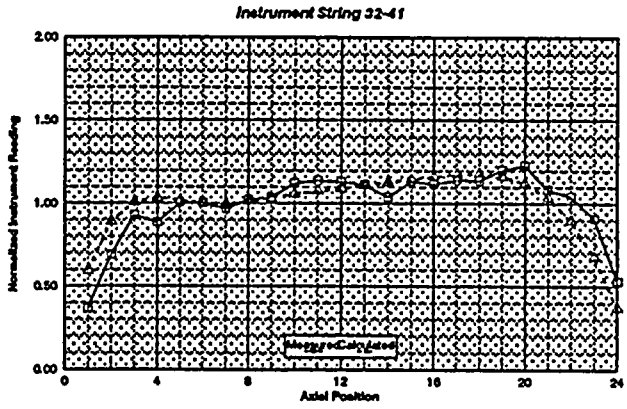

Figure 3.76
Quad Cities Radial Power Benchmark
Assembly Averaged Activity Levels

				0.624												
				0.622												
				-0.30												
			* * *	0.822	1.023											
			* *	0.817	1.034											
			* * *	-0.62	1.09											
		0.582	0.779	0.997	* * *	1.584										
		0.610	0.775	1.021	* *	1.556										
		4.80	-0.51	2.41	* * *	-1.81										
		0.634	0.909	1.103	* * *	1.372	1.426									
		0.675	0.927	1.139	* *	1.441	1.484									
		6.48	2.04	3.27	* * *	5.07	4.07									
		0.758	* * *	* * *	1.350	1.740	* * *	1.717								
		0.804	* * *	*	1.396	1.708	* *	1.747								
		5.99	* * *	* * *	3.41	-1.84	* * *	1.77								
	0.629	* * *	1.120	1.282	* * *	* * *	1.475	1.508	1.474							
	0.627	* *	1.121	1.325	* * * *		1.515	1.543	1.489							
	-0.29	* * *	0.09	3.37	* * *	* * *	2.71	2.31	1.03							
0.503	0.774	* * *	1.203	1.639	1.444	1.429	1.435	1.542	* * *	1.663						
0.502	0.754	* *	1.217	1.565	1.435	1.452	1.476	1.543	* *	1.639						
-0.19	-2.53	* * *	1.19	-4.52	-0.66	1.60	2.86	0.07	* * *	-1.47						
* * *	* * *	1.092	* * *	1.409	* * *	1.416	1.435	* * *	1.430	* * *	1.386					
* * * *		1.078	* *	1.405	* *	1.457	1.433	* *	1.427	* *	1.388					
* * *	* * *	-1.22	* * *	-0.32	* * *	2.90	-0.13	* * *	-0.22	* * *	0.14					
* * *	0.919	1.136	* * *	1.717	1.447	1.730	1.457	1.711	1.431	1.407	* * *	1.650				
* *	0.914	1.128	* *	1.616	1.463	1.684	1.456	1.651	1.436	1.407	* *	1.586				
* * *	-0.52	-0.70	* * *	-5.89	1.14	-2.61	-0.12	-3.55	0.33	0.05	* * *	-3.93				
0.651	* * *	* * *	1.274	1.372	* * *	1.420	1.440	1.424	* * *	* * *	1.383	1.399	1.404	* * *	1.414	1.398
0.693	* * * *		1.285	1.381	* *	1.428	1.411	1.427	* * * *		1.376	1.384	1.384	* *	1.400	1.384
6.52	* * *	* * *	0.84	0.71	* * *	0.60	-2.02	0.24	* * *	* * *	-0.52	-1.07	-1.43	* * *	-1.05	-0.98
0.664	0.952	1.124	1.224	1.315	1.365	1.373	1.408	1.411	1.387	1.359	1.354	1.391	1.442	1.744	1.731	1.396
0.708	0.950	1.129	1.258	1.335	1.367	1.385	1.407	1.387	1.376	1.348	1.342	1.359	1.398	1.703	1.703	1.398
6.60	-0.22	0.44	2.77	1.51	0.14	0.90	-0.04	-1.70	-0.80	-0.82	-0.83	-2.29	-3.01	-2.36	-1.63	0.14

MEAS	Normalization:	Sum of 77 bundles	1.748	1.722
CALC		set to 100.00.	1.703	1.703
%DIF			-2.58	-1.11

Figure 3.77
Quad Cities Radial Power Benchmark
Radial La140 Distribution at Axial Plane 7

				0.542												
				0.559												
				3.25												
				***	0.717	0.929										
				* *	0.750	0.962										
				***	4.48	3.48										
			0.537	0.687	0.875	***	1.654									
			0.573	0.708	0.941	* *	1.623									
			6.66	3.06	7.45	***	-1.83									
			0.560	0.800	0.996	***	1.384	1.427								
			0.620	0.848	1.067	* *	1.441	1.478								
			10.79	6.00	7.18	***	4.10	3.58								
			0.665	***	***	1.323	1.858	***	1.875							
			0.736	* *	* *	1.408	1.819	* *	1.871							
			10.69	***	***	6.43	-2.11	***	-0.21							
		0.523	***	0.974	1.222	***	***	1.491	1.510	1.457						
		0.548	* *	1.047	1.315	* *	* *	1.540	1.548	1.460						
		4.72	***	7.50	7.62	***	***	3.28	2.49	0.18						
	0.420	0.638	***	1.098	1.660	1.405	1.388	1.385	1.565	***	1.753					
	0.441	0.673	* *	1.173	1.601	1.435	1.454	1.448	1.550	* *	1.704					
	4.82	5.58	***	6.81	-3.60	2.15	4.80	4.57	-0.95	***	-2.80					
***	***	0.944	***	1.303	***	1.398	1.411	***	1.428	***	1.383					
*	* *	0.990	* *	1.385	* *	1.453	1.424	* *	1.418	* *	1.373					
***	***	4.81	***	6.34	***	3.91	0.93	***	-0.67	***	-0.71					
***	0.797	1.044	***	1.770	1.437	1.875	1.444	1.839	1.454	1.443	***	1.778				
*	0.832	1.071	* *	1.656	1.448	1.763	1.457	1.777	1.480	1.444	* *	1.663				
***	4.44	2.55	***	-6.46	0.75	-5.98	0.86	-3.37	1.74	0.07	***	-6.43				
0.605	***	***	1.241	1.322	***	1.405	1.468	1.458	***	***	1.421	1.415	1.441	***	1.463	1.441
0.635	*	* *	1.255	1.348	* *	1.392	1.418	1.471	* *	* *	1.409	1.380	1.363	* *	1.399	1.363
5.00	***	***	1.15	1.96	***	-0.91	-3.36	0.91	***	***	-0.87	-2.51	-5.38	***	-4.36	-5.42
0.619	0.879	1.079	1.194	1.293	1.341	1.337	1.420	1.453	1.461	1.411	1.404	1.422	1.493	2.003	1.973	1.474
0.653	0.879	1.078	1.218	1.283	1.311	1.338	1.422	1.433	1.440	1.397	1.370	1.357	1.412	1.897	1.897	1.412
5.51	0.03	-0.12	1.99	-0.74	-2.27	0.04	0.16	-1.34	-1.44	-0.96	-2.44	-4.60	-5.37	-5.31	-3.89	-4.17
MEAS			Normalization:		Sum of 77 bundles									2.003	1.992	
CALC					at this elevation									1.897	1.897	
%DIF					set to 100.00									-5.33	-4.80	

Figure 3.78
Quad Cities Radial Power Benchmark
Radial La140 Distribution at Axial Plane 15

				0.658												
				0.681												
				3.42												
				* * *	0.876	1.071										
				* *	0.881	1.096										
				* * *	0.64	2.36										
			0.638	0.848	1.061	* * *	1.610									
			0.673	0.844	1.091	* *	1.587									
			5.39	-0.48	2.90	* * *	-1.43									
			0.678	0.987	1.156	* * *	1.397	1.438								
			0.739	0.997	1.201	* *	1.471	1.501								
			8.96	1.03	3.85	* * *	5.27	4.36								
			0.795	* * *	* * *	1.382	1.758	* * *	1.705							
			0.868	* * * *		1.413	1.704	* *	1.749							
			9.12	* * *	* * *	2.25	-3.07	* * *	2.54							
		0.667	* * *	1.167	1.307	* * *	* * *	1.467	1.543	1.481						
		0.686	* *	1.170	1.346	* * * *		1.499	1.552	1.508						
		2.86	* * *	0.25	3.00	* * *	* * *	2.17	0.59	1.83						
0.543	0.837	* * *	1.253	1.674	1.439	1.424	1.441	1.551	* * *	1.657						
0.557	0.814	* *	1.238	1.563	1.414	1.427	1.475	1.551	* *	1.637						
2.42	-2.69	* * *	-1.25	-6.63	-1.75	0.22	2.39	0.02	* * *	-1.24						
* * *	* * *	1.155	* * *	1.409	* * *	1.397	1.430	* * *	1.410	* * *	1.370					
* * * *		1.127	* *	1.397	* *	1.428	1.412	* *	1.421	* *	1.359					
* * *	* * *	-2.44	* * *	-0.91	* * *	2.23	-1.30	* * *	0.77	* * *	-0.82					
* * *	0.985	1.159	* * *	1.745	1.436	1.720	1.439	1.687	1.377	1.354	* * *	1.595				
* *	0.975	1.167	* *	1.611	1.454	1.650	1.425	1.604	1.389	1.353	* *	1.527				
* * *	-1.01	0.70	* * *	-7.67	1.21	-4.03	-0.99	-4.91	0.85	-0.04	* * *	-4.27				
0.678	* * *	* * *	1.281	1.379	* * *	1.398	1.417	1.371	* * *	* * *	1.332	1.345	1.350	* * *	1.366	1.358
0.753	* * * *		1.303	1.393	* *	1.419	1.380	1.372	* * * *		1.311	1.337	1.344	* *	1.353	1.344
11.17	* * *	* * *	1.67	1.04	* * *	1.50	-2.57	0.01	* * *	* * *	-1.54	-0.60	-0.50	* * *	-0.97	-1.09
0.693	0.985	1.146	1.220	1.321	1.356	1.359	1.371	1.349	1.300	1.284	1.292	1.343	1.408	1.698	1.694	1.348
0.769	1.008	1.156	1.271	1.351	1.382	1.384	1.375	1.324	1.296	1.272	1.280	1.324	1.366	1.635	1.635	1.366
11.06	2.26	0.90	4.18	2.30	1.93	1.82	0.26	-1.88	-0.28	-0.88	-0.95	-1.44	-2.99	-3.72	-3.50	1.34
MEAS			Normalization:		Sum of 77 bundles									1.705	1.675	
CALC					at this elevation									1.635	1.635	
%DIF					set to 100.00.									-4.13	-2.40	

Figure 3.79
Quad Cities Radial Power Benchmark
Radial La140 Distribution at Axial Plane 18

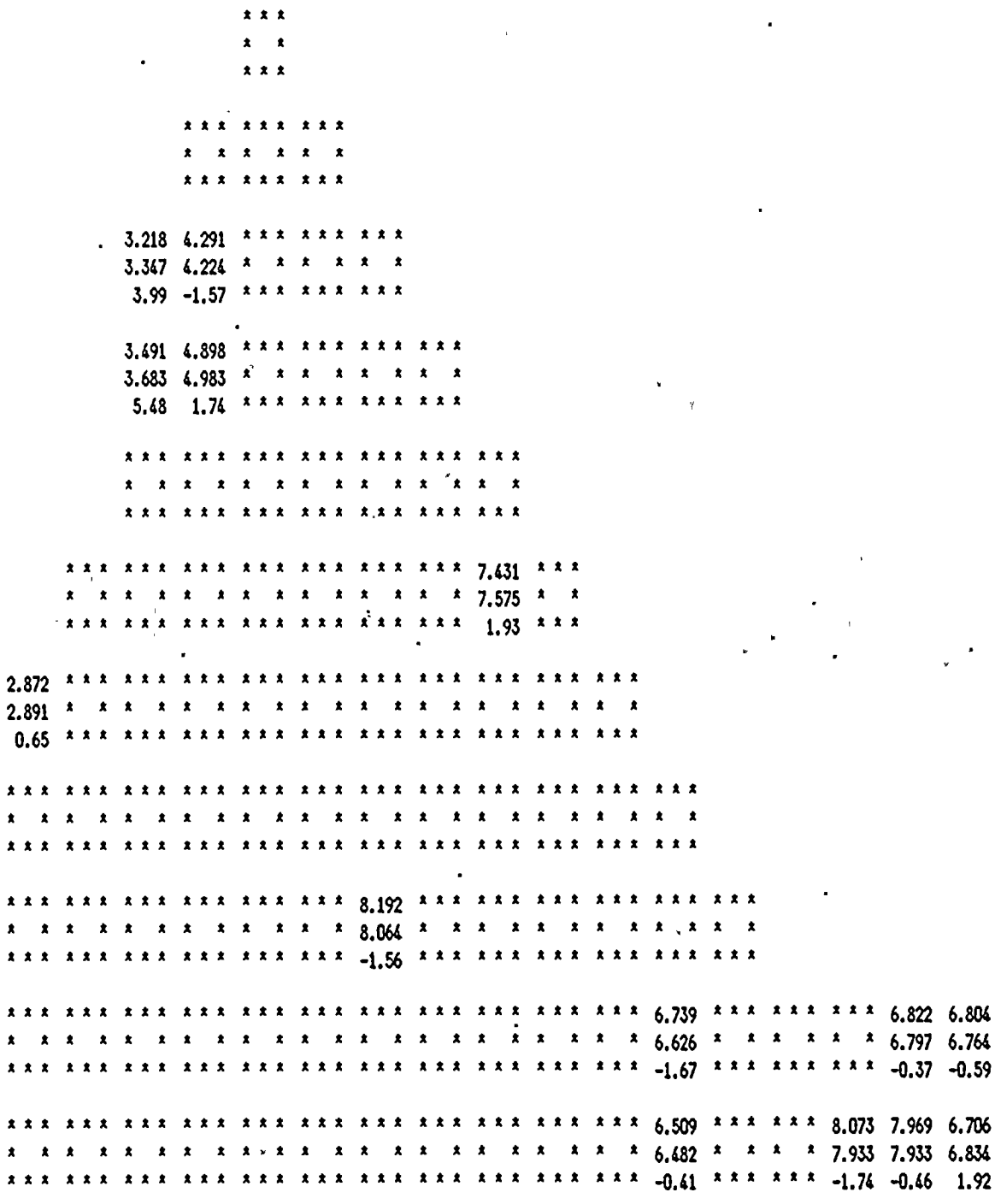

MEAS	Normalization:	Sum of 16 bundles	8.023	7.961
CALC		at this elevation	7.933	7.933
%DIF		set to 100.00.	-1.13	-0.35

Figure 3.80
Core Average Axial La-140 Distribution
Quad Cities Gamma Scan Benchmark

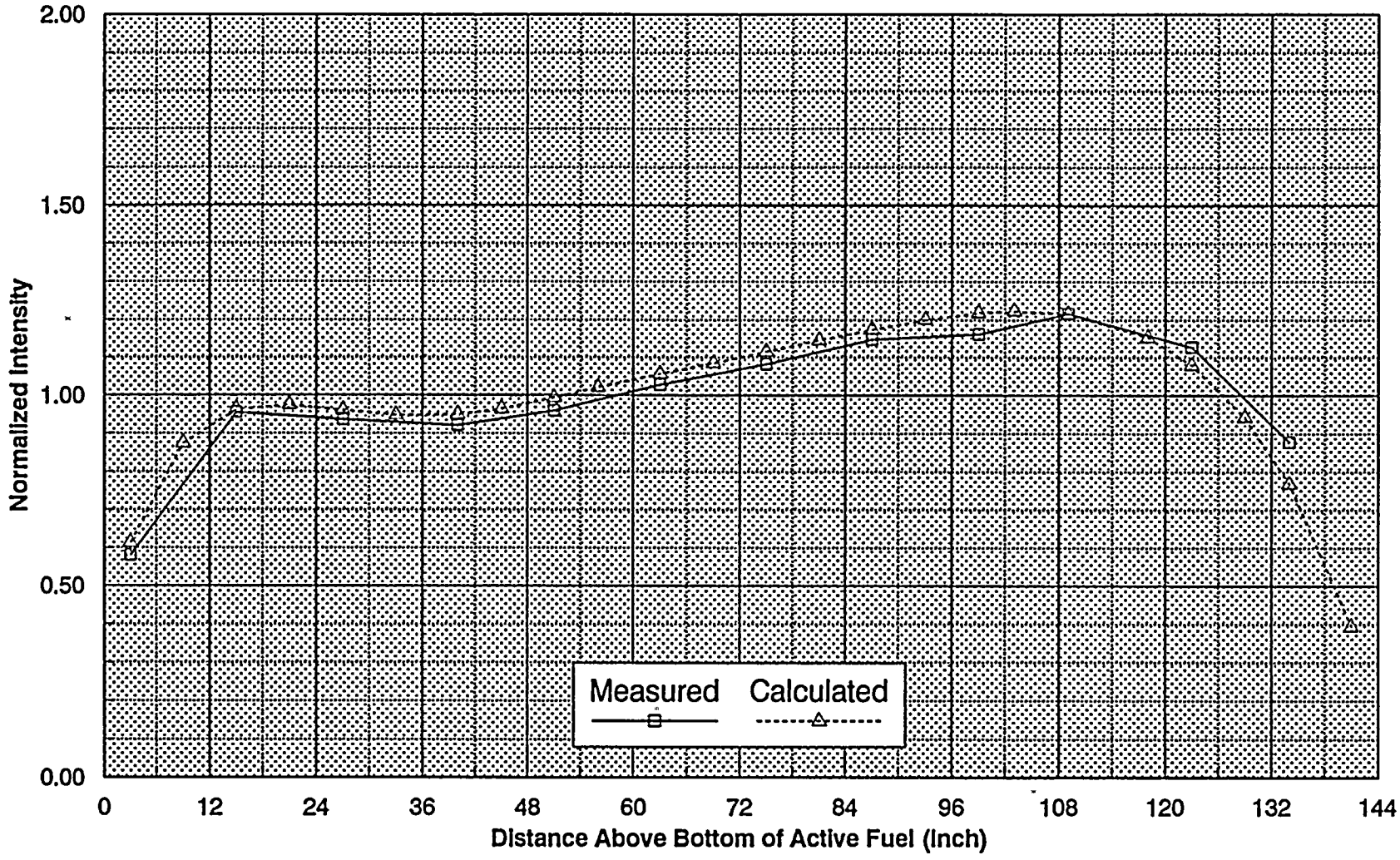

Figure 3.81
Axial La-140 Distribution for Assembly CX0553
Quad Cities Gamma Scan Benchmark

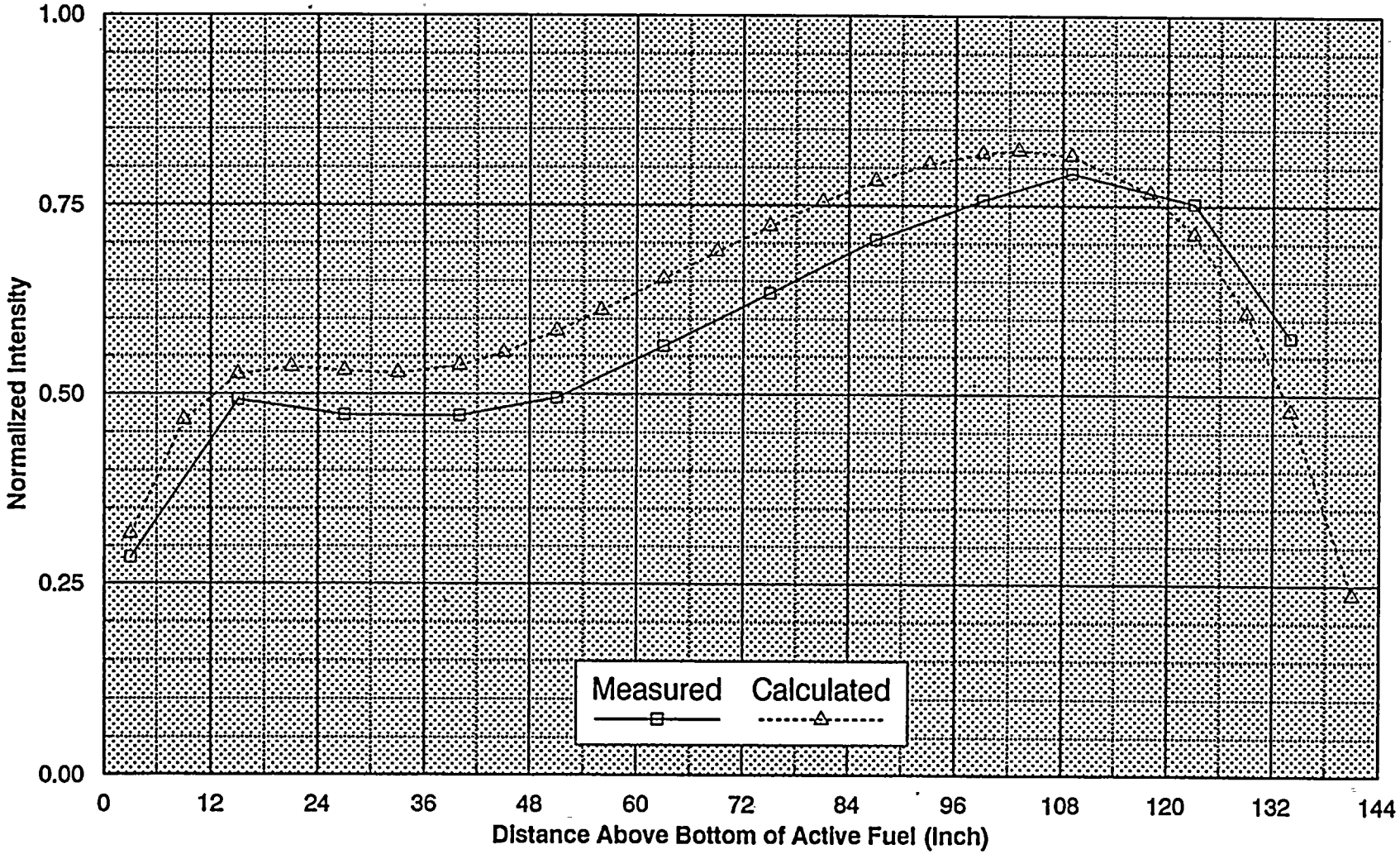

Figure 3.82
Axial La-140 Distribution for Assembly GEH023
Quad Cities Gamma Scan Benchmark

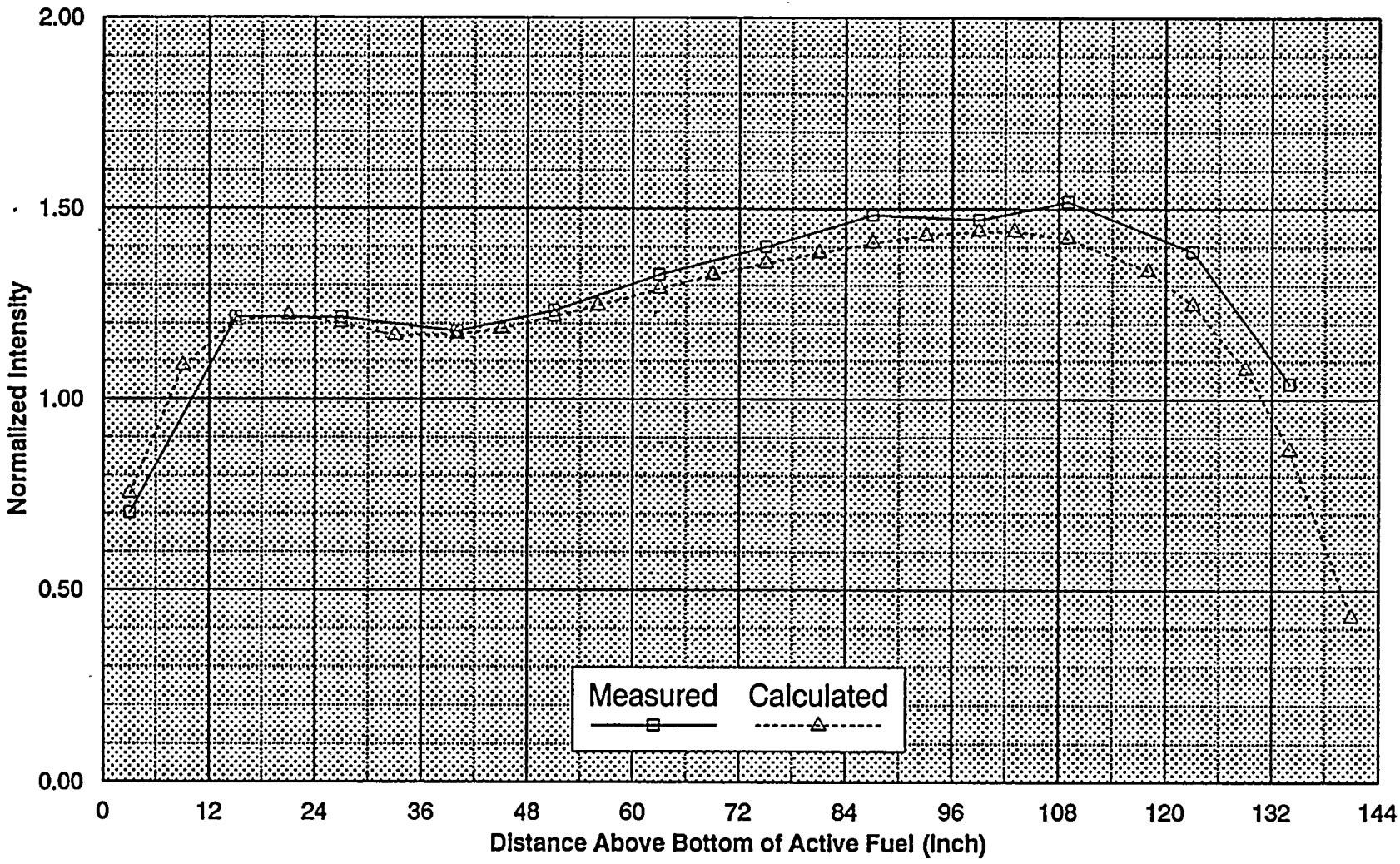

Figure 3.83
Axial La-140 Distribution for Assembly CX0214
Quad Cities Gamma Scan Benchmark

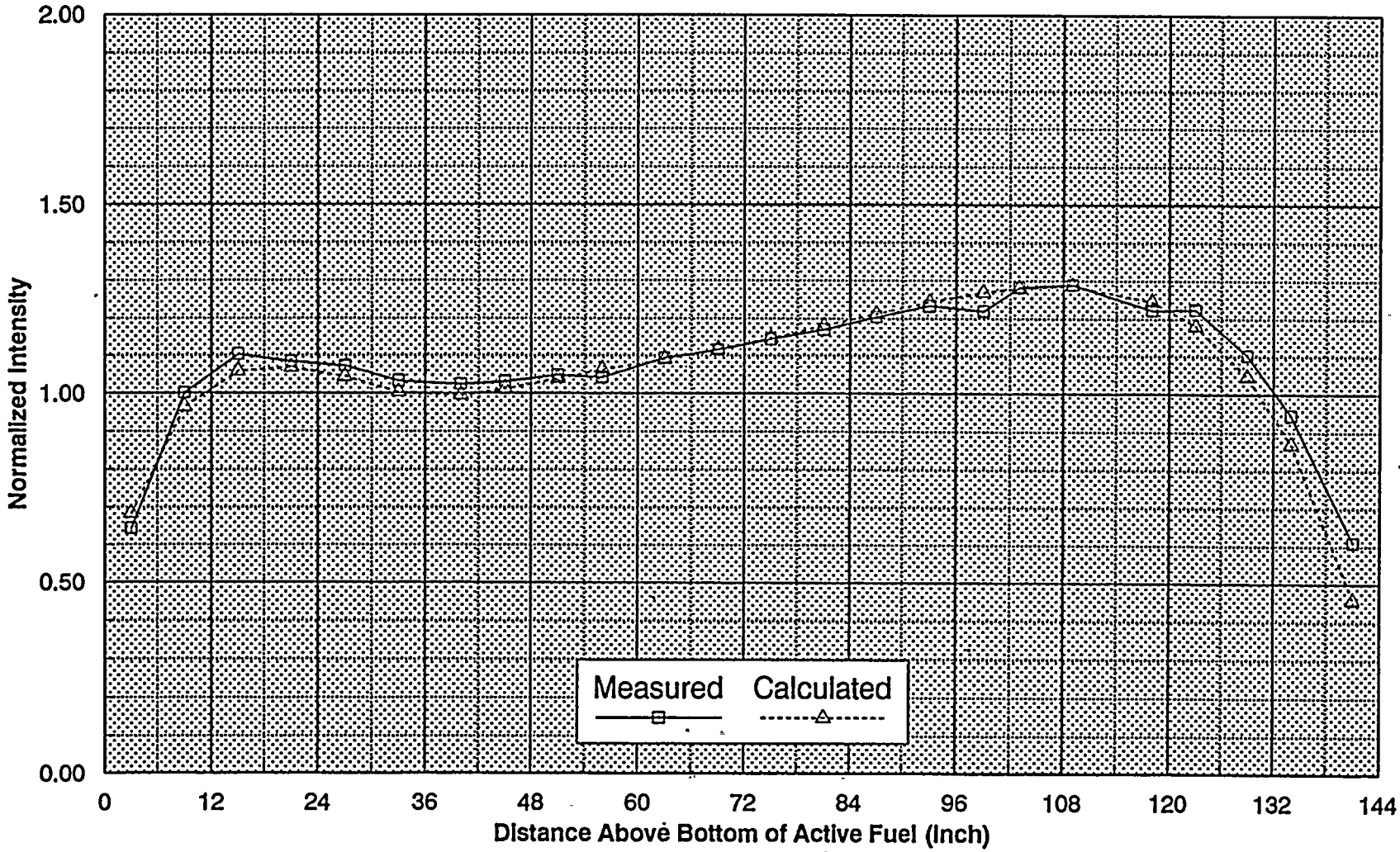

Figure 3.84
Axial La-140 Distribution for Assembly GEB161
Quad Cities Gamma Scan Benchmark

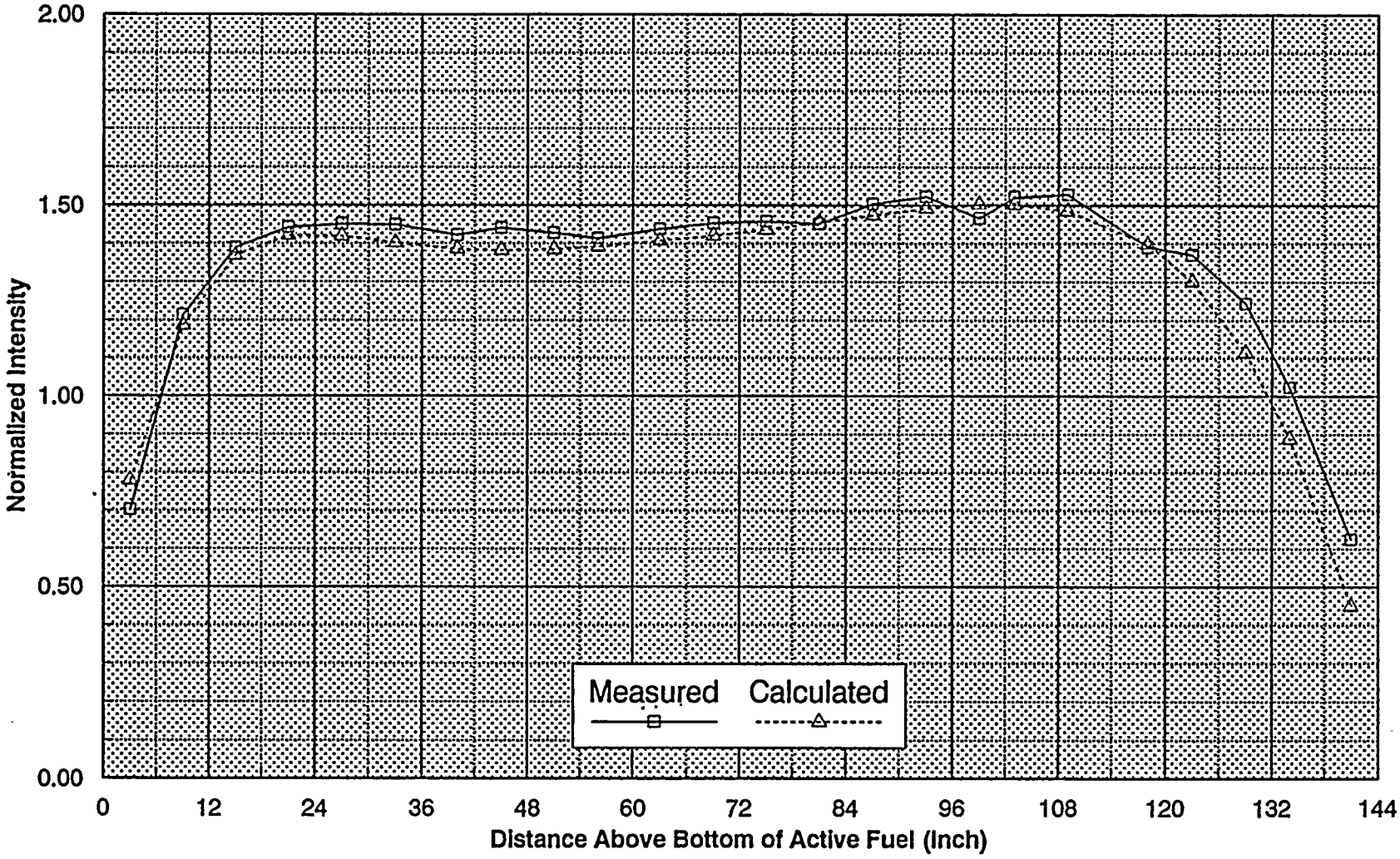

4.0 SUMMARY AND CONCLUSIONS

The benchmark comparisons presented in this topical report quantify the accuracy of the Supply System core physics model in steady state applications and demonstrate the qualifications of the Supply System engineering staff to perform steady state core physics calculations in support of the WNP-2 nuclear plant. An overall summary of the benchmarks presented in this report follows.

The lattice physics benchmarks include uniform lattice criticals and assembly local power distributions. Fifteen uniform lattice criticals, consisting of eight TRX UO_2 criticals and seven ESADA mixed oxide criticals, were analyzed. The eight TRX UO_2 criticals yielded a mean k-effective of 0.99616 with a standard deviation of 0.00184. The seven ESADA mixed oxide criticals yielded a mean k-effective of 1.00872 with a standard deviation of 0.00782. The local power distribution benchmark was based on gamma scans of individual fuel pins at the end of Cycle 2 at Quad Cities 1. Comparisons of local powers of pins from five scanned assemblies yielded an overall standard deviation of 3.20%. The published measurement uncertainty is 1.7%, indicating that calculational and measurement uncertainties are comparable. Comparisons of maximum local peaking factors yielded an overall standard deviation of 2.14% which is even closer to the measurement uncertainty of 1.7%

The core simulation benchmarks are based on data from WNP-2, Peach Bottom 2, and Quad Cities 1. They include hot and cold criticals, TIP comparisons, and nodal gamma scan comparisons.

The overall performance of the calculated k-effectives is shown in Figure 3.1 (WNP-2), Figure 3.34 (PB-2), and Figure 3.56 (QC-1). As observed by other licensees, the CASMO-2/SIMULATE-E analysis produces k-effectives which show a general increase with increasing exposure, and which exhibit a small bias between hot and cold criticals. The overall performance of the TIP comparisons is shown in Table 3.3 and Figures 3.2-3.33 (WNP-2), Table 3.5 and Figures 3.35-3.55 (PB-2), and Table 3.8 and Figures 3.57-3.75 (QC-1). The overall TIP rms for WNP-2 (4 cycles) is 8.08%. The corresponding results for PB-2 and QC-1 (two cycles) are 10.18% and 10.65%, respectively. Analysis of asymmetries suggests that these uncertainties contain approximately equal contributions from experimental and calculational uncertainties. An additional benchmark of the nodal power distribution is provided by the nodal gamma scan data from Quad Cities 1. The comparisons of calculated and measured activities are shown in Figures 3.76-3.84 and in Table 3.10. Comparisons of calculated and measured peak-to-average activities for each assembly are shown in Table 3.11, which shows an average difference of 0.59% with an rms of 1.53%.

In summary, the results presented here demonstrate the ability of the Supply System staff to set up and run detailed steady state core physics calculations in support of the WNP-2 plant. The validity of the Supply System methodology and accuracy of the numerical results is demonstrated by extensive comparisons to measured data from WNP-2, Peach Bottom 2, and Quad Cities 1.

Supply System management has a strong commitment to maintain and improve in-house core physics capabilities. The initial development of these capabilities and their enhancement is part of the overall Supply System's objective of self sufficient design capability with respect to the ownership of WNP-2. Ongoing core follow analysis and TIP comparisons performed in support of WNP-2 plant operations provide continuing opportunities to benchmark Supply System core physics methods.

5.0 REFERENCES

1. "Licensee Qualification for Performing Safety Analyses in Support of Licensing Actions," Generic Letter 83-11, Office of Nuclear Reactor Regulation, U.S. Nuclear Regulatory Commission, dated February 8, 1983.

2. "Qualification of Steady State Core Physics Methods for BWR Design and Analysis," PL-NF-87-001, Pennsylvania Power & Light Company (1987).

3. "Methods for the Analysis of Boiling Water Reactors, Steady State Core Physics," YAEC-1238, Yankee Atomic Electric Company (1981).

4. M. Edenius and A. Ahlin, "MICBURN, Microscopic Burnup in Gadolinia Fuel Pins," EPRI CCM-3, Part II, Chapter 7, Electric Power Research Institute (1975).

5. M. Edenius, A. Ahlin, and H. Haggblom, "CASMO-2, A Fuel Assembly Burnup Program, User's Manual," STUDSVIK/NR-81/3, Studsvik Energiteknik AB (March 1981).

6. A. Ahlin and M. Edenius, "The Collision Probability Module EPRI-CPM," EPRI CCM-3, Part II, Chapter 6, Electric Power Research Institute (1975).

7. J.R. Brown et al., "Kinetic and Buckling Measurements on Lattices of Slightly Enriched Uranium or UO_2 Rods in Light Water," WAPD-176, Westinghouse Electric Corporation (1958).

8. R.D. Leamer et al., "PuO_2-UO_2 Fueled Critical Experiments," WCAP-3726-1, Westinghouse Electric Corporation (1967).

9. M.B. Cutrone and G.F. Valby, "Gamma Scan Measurements at Quad Cities Nuclear Power Station Unit 1 Following Cycle 2," EPRI NP-214, Electric Power Research Institute (1976).

10. N.H. Larsen, G.R. Parkos, and O. Raza, "Core Design and Operating Data for Cycles 1 and 2 of Quad Cities 1," EPRI NP-240, Electric Power Research Institute (1976).

11. S. Borreson, "A Simplified, Coarse-Mesh, Three-Dimensional Diffusion Scheme for Calculating the Gross Power Distribution in a Boiling Water Reactor," Nuclear Science and Engineering, Vol. 44, pp. 37-43 (1971).

12. W.R. Cobb, B.S. Singer, and B.L. Darnell, "NORGE-B: A Nodal Representation Generator for Boiling Water Reactors - Computer Code User's Manual," EPRI Research Project 976-3, Science Applications, Inc. (1984).

13. B.L. Darnell, B. Morris, and M.L. Zerkle, "ABLE - An Albedo and Boundary Leakage Evaluation Program for Light Water Reactors - Computer Code User's Manual," Science Applications Inc. (1984).

14. D.M. Ver Planck, W.R. Cobb, R.S. Borland, B.L. Darnell and P.L. Versteegen, "SIMULATE-E (Mod. 3) Computer Code Manual," EPRI NP-4574-CCM, Part II, Ch. 8, Electric Power Research Institute (September 1987).

15. B.J. Gitnick, R.R. Gay, R.S. Borland, and A.F. Ansari, "FIBWR: A Steady-State Core Flow Distribution Code for Boiling Water Reactors; Computer Code User's Manual," EPRI NP-1924-CCM, Electric Power Research Institute (1981).

16. A.F. Ansari, R.R. Gay, and B.J. Gitnick, "FIBWR: A Steady-State Core Flow Distribution Code for Boiling Water Reactors; Code Verification and Qualification Report," EPRI NP-1923, Electric Power Research Institute (1981).

17. D.M. Ver Planck, "Development of a Nodal Core Analysis Program Research Project RP710-1, Manual for the Reactor Analysis Program SIMULATE," Electric Power Research Institute (1978).

18. D.M. Ver Planck, "SIMULATE-2: A Nodal Core Analysis Program for Light Water Reactors, Computer Code User's Manual," Research Project 710-1, Computer Code Manual, Electric Power Research Institute (1982).

19. L.A. Carmichael and R.O. Niemi, "Transient and Stability Tests at Peach Bottom Atomic Power Station Unit 2 at End of Cycle 2," EPRI NP-564, Electric Power Research Institute (1978).

20. N.H. Larsen, "Core Design and Operating Data for Cycles 1 and 2 of Peach Bottom-2," EPRI NP-563, Electric Power Research Institute (1978).